Weighted reduced basis methods for parabolic PDEs with random input data

Vom Fachbereich Mathematik
der Technischen Universität Darmstadt
zur Erlangung des Grades
Doktor rerum naturalium
(Dr. rer. nat.)

Dissertation
von
Dipl.-Ing. Christopher Spannring

TECHNISCHE
UNIVERSITÄT
DARMSTADT

Erstgutachter: Prof. Dr. Jens Lang
Zweitgutachter: Prof. Dr. Sebastian Schöps

Darmstadt 2018

Abstract

This work focuses on model order reduction for parabolic partial differential equations with parametrized random input data. The input data enter the model via model coefficients, external sources or boundary conditions, for instance. The outcome of the model problem is not only the solution, but also a quantity of interest (or output). The output is determined by a functional which maps the solution to a real number. Random data cause randomness of the outcomes of the model problem and, hence, statistical quantities are of interest. In particular, this work studies the expected value of the solution and the output. In order to approximate the expectation, a Monte Carlo estimator is utilized. For high accuracy Monte Carlo requires many evaluations of the underlying problem and, hence, it can become computationally infeasible. In order to overcome this computational issue, a reduced basis method (RBM) is considered. The RBM is a Galerkin projection onto a low-dimensional space (reduced basis space). The construction of the reduced basis space combines a proper orthogonal decomposition (POD) with a greedy approach, called POD-greedy algorithm, which is state of the art for the RBM for parabolic problems. The POD-greedy uses computationally cheap error estimators in order to build a reduced basis.

This thesis proposes efficient reduced order models regarding the expected value of the errors resulting from the model order reduction. To this end, the probability density function of the random input data is used as a weight for the reduced space construction of the RBM, called weighted RBM. In the past, a weighted RBM has been successfully applied to elliptic partial differential equations with parametrized random input data. This work combines the ideas of a RBM for parabolic partial differential equations Grepl and Patera (2005) and a weighted RBM for elliptic problems Chen et al. (2013) in order to extend the weighted approach also for the RBM for parabolic problems.

The performance of a non-weighted and a weighted approach are compared numerically with respect to the expected solution error and the expected output error. Furthermore, this work provides a numerical comparison of a non-weighted RBM and a weighted RBM regarding an optimum reference. The reference is obtained by an orthogonal projection onto a POD space, which minimizes the expected squared solution error.

Zusammenfassung

In dieser Arbeit wird die Modellreduktion von parabolischen partiellen Differentialgleichungen mit parametrisierten zufälligen Eingangsdaten betrachtet. Die Eingangsdaten gehen zum Beispiel durch physikalische Koeffizienten im Modell, externe Quellen oder Randbedingungen in die partielle Differentialgleichung ein. Die gesuchte Variable des Problems ist nicht nur die Lösung, sondern auch ein Output. Dieser Output wird durch ein Funktional, welches die Lösung auf eine reelle Zahl abbildet, berechnet. Durch die Zufälligkeit der Eingangsdaten sind auch die gesuchten Variablen des Problems Zufallsgrößen. Aus diesem Grund sind statistische Größen von Interesse, wobei diese Arbeit den Erwartungswert der Lösung und des Outputs untersucht. Um den Erwartungswert zu approximieren, wird ein Monte Carlo Schätzer verwendet. Monte Carlo benötigt viele Auswertungen des zugehörigen Problems, um eine hohe Genauigkeit zu erzielen, und kann deshalb zu großem Rechenaufwand führen. Mit Hilfe der Reduzierte-Basis-Methode (RBM) wird der Rechenaufwand reduziert. Die RBM ist eine Galerkin-Projektion auf einen niedrigdimensionalen Raum. Die Konstruktion dieses reduzierten Raumes erfolgt durch eine Kombination einer Proper Orthogonal Decomposition (POD) und eines Greedy Verfahrens (POD-greedy Algorithmus). Der POD-greedy Algorithmus ist Stand der Technik im Kontext der RBM für parabolische Probleme. Für die Konstruktion des reduzierten Raumes werden Fehlerschätzer verwendet, welche unter einem geringen Rechenaufwand bestimmt werden können. Die Fehlerschätzer werden als Kriterium für die Wahl der Basis des reduzierten Raumes verwendet.

Diese Arbeit entwickelt effiziente reduzierte Modelle hinsichtlich des Erwartungswertes der Fehler, welche aus der Modellreduktion resultieren. Dazu wird die Wahrscheinlichkeitsdichtefunktion der zufälligen Eingangsdaten als Gewichtsfunktion für Konstruktion des reduzierten Raumes verwendet (gewichtete RBM). In der Literatur wurde die gewichtete RBM erfolgreich für elliptische partielle Differentialgleichungen mit parametrisierten zufälligen Eingangsdaten angewendet. Diese Arbeit kombiniert die Ideen einer RBM für parabolische partielle Differentialgleichungen Grepl and Patera (2005) und einer gewichteten RBM für elliptische Probleme Chen et al. (2013), um die gewichtete RBM auf parabolische Probleme zu erweitern.

Numerische Tests vergleichen eine nicht-gewichtete RBM und eine gewichtete RBM bezüglich des erwarteten Fehlers der Lösung und des erwarteten Fehlers des Outputs. Darüber hinaus liefert diese Arbeit einen numerischen Vergleich der nicht-gewichteten RBM und der gewichteten RBM hinsichtlich eines Optimums. Das Optimum wird durch eine Orthogonalprojektion auf einen POD Raum bestimmt und minimiert den Erwartungswert des quadratischen Fehlers der Lösung.

Acknowledgements

I truly thank my supervisors Professor Jens Lang and Professor Sebastian Schöps for enabling this thesis and the pleasant guidance in the last years.

My deep thanks go to Sebastian Ullmann for the friendly atmosphere and for many inspiring discussions. I very much appreciated that you always lend me a sympathetic ear.

I gratefully acknowledge the willingness of Professor Reinhard Farwig and Professor Martin Kiehl to participate in my examination committee.

I thank David Frenzel, Bogdan Radu and Iryna Kulchytska-Ruchka for proofreading parts of this thesis.

I like to express my appreciation to my colleagues at the Graduate School Computational Engineering, who made my time as a PhD student enjoyable at and apart from work. Especially I wish to thank Christopher Müller, who became not only an office colleague. Beside enthusiastic mathematical discussions you also extended my culinary focus. Beyond your inspiration in the kitchen, you also increased my consciousness for waste sorting. I also want to thank Max Bucher for teaching me cultural and geographical aspects of Germany.

I would like to thank the Deutsche Forschungsgemeinschaft and the Forschungsdezernat of Technische Universität Darmstadt for the financial support. I want to thank the administration and the system administration of the Graduate School Computational Engineering for the willingness to help in the past years.

Finally, I want to share my deepest thanks to my parents, Roswitha and Martin Spannring, for all their thoughtful support in my life. I am grateful that you enabled me this educational path and that you always encouraged me and my ideas.

viii

Contents

Notations

Acronyms

KL	Karhunen-Loève
MC	Monte Carlo
MOR	model order reduction
RB	reduced basis
RBM	reduced basis method
ROM	reduced order model
PDE	partial differential equation
PPDE	parametrized partial differential equation
pdf	probability density function
POD	proper orthogonal decomposition

Variables

a	bilinear form of weak formulation
a_q	affine decomposition of a
α	coercivity constant
$\overline{\alpha}$	lower bound of coercivity constant
b	right hand side functional of weak formulation
b_q	affine decomposition of b
c	eigenfunction of KL expansion
d	space dimension
Δ	Laplace operator
Δt	time step size
Δ_N	error estimator for N-dimensional reduced solution
$\Delta_{\tilde{N}}^{\psi}$	dual solution error estimator
$\Delta_{\tilde{N}}^{\psi,k}$	dual solution error estimator for time index k

$\Delta_{\tilde{N}}^{\psi,\rho}$	weighted dual solution error estimator
Δ_N^u	primal solution error estimator
$\Delta_N^{u,k}$	primal solution error estimator for time index k
$\Delta_N^{u,\rho}$	weighted primal solution error estimator
$\Delta_{N,\tilde{N}}^s$	output error estimator
$\Delta_{N,\tilde{N}}^{s,\rho}$	weighted output error estimator
Δ_N	error estimator for N-dimensional reduced solution
e_h^k	detailed primal solution error for time index k
$\tilde{e}_h^k$	detailed dual solution error for time index k
e_N^k	reduced primal solution error for time index k
$\tilde{e}_{\tilde{N}}^k$	reduced dual solution error for time index k
$\mathbb{E}$	expectation
$\mathbb{E}_{\mathrm{MC}}$	MC estimator
$\mathbb{E}_{\mathrm{MC}}^{\mathcal{U}}$	MC estimator using uniformly distributed samples
f	external heat force
$\mathcal{F}$	sigma algebra that contains set of events
g	function on boundary condition
h	mesh size of finite element discretization
γ_a	continuity constant of the bilinear form a
γ_b	continuity constant of the functional b
γ_l	continuity constant of the functional l
$\overline{\gamma}_a$	upper bound of γ_a
$\overline{\gamma}_b$	upper bound of γ_b
$\overline{\gamma}_l$	upper bound of γ_l
Γ	parameter domain
H^1	Sobolev space
I	time interval
k	time index
κ	random field modeled by KL expansion
K	final time index
l	output functional
λ	eigenvalue of KL expansion
l_q	affine decomposition of l
L^2	set of square integrable functions
$\mathcal{M}_h^K$	solution manifold
N	reduced dimension regarding primal problem
$\tilde{N}$	reduced dimension regarding dual problem

$\mathcal{N}$	number of discretization points in space
N_{MC}	number of MC samples
∇	gradient
Ω	spatial domain
p	parameter dimension
$\frac{\partial}{\partial n}$	normal derivative
$\partial\Omega$	boundary of spatial domain
∂_t	partial derivative w.r.t. time
ϕ	finite element basis function
φ	reduced basis function regarding primal problem
ψ	dual solution
ψ_h	finite element dual solution
ψ_h^k	ψ_h approximated at t^k
$\psi_{\tilde{N}}$	reduced dual solution
$\psi_{\tilde{N}}^k$	$\psi_{\tilde{N}}$ approximated at t^k
$\mathbb{P}$	probability measure
Φ_N	N-dimensional reduced basis
q	affine decomposition index
Q_a	number of affine decomposition regarding a
Q_b	number of affine decomposition regarding b
Q_l	number of affine decomposition regarding l
ρ	pdf
$\rho_{\mathcal{B}}$	pdf of beta distribution
$\rho_{\mathcal{U}}$	pdf of uniform distribution
r_h^k	detailed primal residual for time index k
$\tilde{r}_h^k$	detailed dual residual for time index k
r_N^k	reduced primal residual for time index k
$\tilde{r}_{\tilde{N}}^k$	reduced dual residual for time index k
$\mathbb{R}$	set of real numbers
$\mathbb{R}^+$	set of positive real numbers
s	quantity of interest or output
σ	eigenvalues obtained by POD
s_h	output approximated by finite element method
$s_{N,\tilde{N}}$	output approximated by RBM
t	time variable
t^k	point in time at index k

θ	random sample
θ_q^a	affine parameter decomposition of a
θ_q^b	affine parameter decomposition of b
θ_q^l	affine parameter decomposition of l
T	end point in time
Θ	sample space
u	primal solution
u_h	finite element primal solution
u_h^k	u_h approximated at t^k
u_N	reduced primal solution
u_N^k	u_N approximated at t^k
$u_{\mathrm{POD},N}^k$	reduced solution obtained by a POD for time index k
w	POD basis function
x	space variable
ξ	random parameter vector
X	solution space
X'	dual space of X
X_h	finite element space
X_h^K	K-dimensional finite element space
X_N	reduced basis space regarding primal problem
X_N^K	K-dimensional X_N
$\tilde{X}_{\tilde{N}}$	reduced basis space regarding dual problem
$\tilde{X}_{\tilde{N}}^K$	K-dimensional $\tilde{X}_{\tilde{N}}$
$X_{\mathrm{POD},N}$	reduced basis space obtained by POD
ζ	reduced basis function regarding dual problem
$\|\cdot\|_\xi$	parameter dependent norm induced by symmetric a
$\interleave\cdot\interleave_\xi^{\mathrm{du}}$	dual parameter-dependent energy norm
$\interleave\cdot\interleave_\xi^{\mathrm{pr}}$	primal parameter-dependent energy norm

Chapter 1

Introduction

Mathematical models can describe many different physical phenomena in applied sciences such as, for instance, heat conduction in mechanical devices, velocity of a liquid through a pipe or pressure in a blood vessel. These phenomena can be approximated by numerical simulations of partial differential equations (PDEs). Numerous applications require many degrees of freedom in order to obtain accurate computational results and thus lead to high-dimensional problems. Solving these high-fidelity models demands powerful hardware and entails time consuming computations. In practice the interest might not only be in the solution itself, but also in a quantity of interest (or output). The output is evaluated by an output functional that maps the solution of the underlying problem to a real number. It can model heat loss over a boundary of the domain or lift and drag in computational fluid dynamics, for instance.

Specific applications demand solutions for different input parameters, for instance changing model coefficients, various boundary conditions or varying geometry. Such problems are described by parametrized partial differential equations (PPDEs). The parametrization of the PDEs entails parametrized solutions and parametrized outputs.

Usually the input data is not known exactly and, hence, the input parameters are random variables. A broad overview on such problems can be found in LeMaître and Knio (2010); Xiu (2010); Lord et al. (2014); Gunzburger et al. (2014). These uncertainties are modeled as random variables or random vectors that are fully characterized by a given probability density function (pdf). The input uncertainties are passed on the unknowns of the PPDE and hence statistical quantities are of interest. In particular, this work studies the expectation of the solution and the output of the underlying problem. The expectation is estimated by the well-known Monte Carlo (MC) method, which averages the evaluations of the PPDE (snapshots) for randomly sampled parameters. However, due to the moderate error convergence rate of MC, the method requires solutions for a large number of parameter realizations. Especially for an accurate statistical approximation the computation becomes infeasible.

To reduce the computational effort, a low-dimensional surrogate of the high-fidelity model is obtained by means of model order reduction (MOR) techniques. A reduced order model (ROM) yields approximations for the high-fidelity solution and the output for any element of the parameter domain. This work utilizes the reduced basis method (RBM), introduced in Almroth et al. (1978); Noor and

Peters (1980) for nonlinear structural analysis. A recent overview of the RBM can be found in Quarteroni et al. (2016); Hesthaven et al. (2016); Haasdonk (2017). The RBM is a Galerkin projection onto a low-dimensional space, called reduced basis space. In order to construct the reduced space, a greedy algorithm, introduced in Veroy et al. (2003) for the RBM, is the method of choice for elliptic PPDEs. However, focusing on parabolic PPDEs, the space construction combines a proper orthogonal decomposition (POD) with a greedy procedure, called POD-greedy. The POD-greedy algorithm was introduced in Haasdonk and Ohlberger (2008) and is state of the art for the reduced space construction for parabolic problems in an RBM framework. This work uses computationally cheap error estimators, derived in Grepl and Patera (2005), in order to build a reduced basis.

The idea of a weighted RBM method was introduced in Chen et al. (2013) for elliptic PPDEs. It assigns different weights to the parameters in the stage of the reduced space construction. In the stochastic framework the pdf is utilized as the weight, which gives more probable parameters higher priority. Numerical results (Chen et al., 2013, section 5) have shown that the weighted RBM for elliptic problems needs less basis functions than the non-weighted RBM in order to obtain the same accuracy of the expected output error.

This thesis develops efficient reduced spaces regarding the expected value of the solution error and the output error. To this end, the thesis combines the ideas of the RBM for parabolic problems Grepl and Patera (2005) and the weighted RBM for elliptic problems Chen et al. (2013) and, hence, extends the weighted RBM to parabolic PPDEs.

The work compares the performance of a non-weighted RBM and a weighted RBM for a two dimensional heat conduction test example. Therefore, the expected value of the squared solution error and the expected value of the absolute output error are demonstrated. Furthermore, this thesis compares the non-weighted and the weighted approach to an optimum. The optimum can be accomplished by a POD in terms of the MC approximation of the root mean square error. The MC snapshots are projected onto the reduced POD space and, hence, the expected squared solution error becomes minimal. It is assessed whether the solution obtained by a weighted approach is significantly closer to the optimum than the solution obtained by a non-weighted equivalent.

The thesis is structured as follows: In chapter 2 the strong formulation of a linear parabolic PDE is introduced. A linear output functional is defined, which maps the solution to the quantity of interest. The un-parametrized weak formulation is stated in section 2.1, followed by the parametrized weak formulation in section 2.2. The stochastic framework is set up, which characterizes the random input data. Conditions for existence and uniqueness of a solution for the parametrized problem are stated. In order so solve the model problem, in sections 2.2.1 and 2.2.2 the PPDE is discretized at first in time and then in space. The time discretization is achieved by an implicit Euler method and a linear finite element method is used as a space discretization method. The error quantities, e.g. the residual in each time step, regarding the discretization are introduced. The resulting system of linear algebraic equations are defined in section 2.2.3. In section 2.3, by means of a standard primal-dual approach, the dual problem of the PPDE is derived. It allows higher accuracy for the output computation and yields sharper error bounds. The dual problem is discretized in time and space in sections 2.3.2 and 2.3.3, respectively, using the same discretization methods

as the primal problem. Analogously to the primal problem, error quantities for the dual problem are defined. The corresponding algebraic equations of the dual problem are stated in section 2.3.4.

Chapter 3 starts with a short overview of previous and recent work on the RBM. In section 3.1 the reduced primal problem and the reduced dual problem are introduced. An adjoint-corrected reduced output computation, which uses the solution of the reduced dual problem, is described. In order to guarantee an efficient computation of the reduced quantities independently of the high-fidelity dimension, the property of an affine parameter dependence is assumed. The algebraic equations of the reduced primal and the reduced dual problem are stated in section 3.1.1. In section 3.2 the discretization error between the high-fidelity model and the reduced model is considered. In particular, section 3.2.1 states rigorous error bounds for the solution error measured in a parameter dependent norm and the absolute output error. Weighted error estimators, utilizing the probability density function, are defined in section 3.2.2. Furthermore, in section 3.2.1 it has been shown that the error estimators can be extended to the time continuous setting as well. The error bounds require the dual norm of the primal and the dual residuals. The corresponding computations are explained in section 3.2.3. In section 3.3 the reduced space construction is discussed. The space construction is based on a POD-greedy algorithm utilizing an error estimator of section 3.2 as a selection criterion for the reduced basis functions. If the algorithm utilizes a non-weighted error estimator of section 3.2.1 the (non-weighted) POD-greedy results whereas the use of a weighted error estimator of section 3.2.2 yields the weighted POD-greedy. The differences between these two approaches regarding the reduced space construction are described in sections 3.3.1 and 3.3.2, respectively. Results on the error convergence rates of a greedy approximation are briefly summarized in section 3.3.3. Scenarios are discussed where the non-weighted approach and the weighted approach coincide.

Chapter 4 considers a reduced space construction by means of a POD in order to assess the reduced spaces obtained from the non-weighted and the weighted RBM regarding the expected value of the solution error. The expected value is approximated by the MC method. A short overview of this method is given in section 4.1. The reduced space construction utilizing the POD is explained in section 4.2. The reduced POD solution is represented by the orthogonal projection of a snapshot onto the POD space, such that the error becomes minimal in a root mean square sense.

In chapter 5 numerical results of a two dimensional heat conduction with Robin boundary conditions and random input data are shown. Section 5.1 describes the mathematical model and states the governing equations. The input data enter the problem via the boundary conditions and is characterized by a random field acting as a heat inflow and a random coefficient which acts as a cooling parameter. The random field is approximated by a truncated Karhunen-Loève (KL) expansion. The random cooling coefficient follows a beta distribution. The quantity of interest is determined by the average temperature in the domain at the end point in time. In section 5.2, by means of a linear finite element method, the plots of numerical simulations show the heat conduction in the domain for different time steps and varying parameters. The set up of the different ROMs is described in section 5.3. The reduced solutions for different parameters are visualized and compared to a reference solution obtained by the finite element method. The non-weighted and the weighted error bounds of

the solution and the output, stated in section 3.2, are illustrated over a finite parameter set. Furthermore, the error convergence between the high-fidelity and the reduced solution for increasing the reduced space dimension is shown. The performance of the non-weighted and the weighted RBM regarding the root mean square error is assessed by an optimal reduced POD space. To this end, the expected squared solution error is compared between these three MOR techniques. In addition, the expected absolute output error of the non-weighted approach and the weighted approach is compared for increasing dimension. The different parameter selection of these two methods are illustrated. The thesis is concluded in chapter 6.

Chapter 2

Linear parabolic PDE

The thesis considers model order reduction (MOR) for a second-order linear parabolic model problem. In order to reduce the dimension of the underlying parabolic problem, the reduced basis method (RBM) is applied. The RBM for parabolic partial differential equations (PDEs) has been studied in, e.g. Grepl and Patera (2005); Rovas et al. (2006); Nguyen et al. (2009, 2010). Further investigations on the RBM, where time was treated in a space-time framework, were done in Yano (2014); Urban and Patera (2014). In this work data uncertainties enter the parabolic problem, which emerge from lack of knowledge or imprecise input data. Once the parabolic PDE is solved, the solution of the PDE is mapped to a quantity of interest. In order to obtain sharper error bounds for the quantity of interest, a standard dual problem is derived. For the discretization of the parabolic problem, a linear finite element method in space and an implicit Euler method in time is used.

At first, in this chapter the time dependent parabolic PDE is stated. The time interval $I := [0, T]$ is determined by the finite final time $T > 0$. In the following the spatial domain $\Omega \subset \mathbb{R}^d$ is bounded and its boundary $\partial\Omega$ is Lipschitz continuous. Here $\Delta := \sum_{i=1}^{d} \frac{\partial^2}{\partial^2 x_i}$ denotes the Laplace operator and ∂_t the partial derivative with respect to the time variable t. The right hand side $f \colon \Omega \times I \to \mathbb{R}$ models a source term. Further, $\frac{\partial}{\partial n}$ denotes the normal derivative with respect to the outer normal to the boundary. On the boundary a time independent function $g \colon \partial\Omega \to \mathbb{R}$ is defined. The solution $u \colon \Omega \times I \to \mathbb{R}$ satisfies

$$\partial_t u - \Delta u = f, \quad \text{in } \Omega \times (0, T], \tag{2.1a}$$

$$\frac{\partial u}{\partial n} = g, \quad \text{on } \partial\Omega \times (0, T], \tag{2.1b}$$

$$u = 0, \quad \text{on } \Omega \times \{0\}, \tag{2.1c}$$

where (2.1a) models instationary heat conduction, (2.1b) is an inhomogeneous Neumann boundary condition modeling heat exchange at the boundary, and (2.1c) is the initial condition. In case of an inhomogeneous initial condition $u(0) = u_0 \in C^2\left(\overline{\Omega}\right)$, the condition can be homogenized, see appendix A.2. Here, the space C^2 contains the functions with 2 continuous derivatives and $\overline{\Omega}$ denotes the closure of the domain Ω. The solution field $u(x, t)$ of (2.1) describes the heat distribution for spatial points $x \in \Omega$ and points in time $t \in I$. This work considers the solution pointwise in time, meaning that for $t \in I$ the solution

$u(t)\colon \Omega \to \mathbb{R}$ is sought for a certain point in time.

In practical applications the objective is not only the solution, but rather an output (or quantity of interest) $s \in \mathbb{R}$, e.g. the average temperature in the domain, the loss of temperature over the boundary etc. It maps the solution to a real number, such that

$$s = l(u(\cdot, T)), \tag{2.2}$$

where a linear output functional l evaluates the solution at the end time T.

2.1   Weak formulation

In this section the weak formulation of problem (2.1) is stated. However, first standard spaces are introduced.

Definition 2.1 ($L^2(\Omega)$ space). The space of square integrable functions on a bounded domain $\Omega \subset \mathbb{R}^d$ is defined by

$$L^2(\Omega) = \left\{ f\colon \Omega \to \mathbb{R} \quad : f \text{ measurable}, \int_\Omega f(x)^2 \mathrm{d}x < \infty \right\}.$$

It is a Hilbert space, see definition A.1, with the inner product

$$(f, g)_{L^2(\Omega)} = \int_\Omega f(x)g(x)\, \mathrm{d}x \tag{2.3}$$

and the induced norm

$$\|f\|_{L^2(\Omega)} = \sqrt{(f, f)_{L^2(\Omega)}}.$$

Definition 2.2 (dual space). Let V be a normed vector space. The dual space of V is defined by

$$V' = \{ f\colon V \to \mathbb{R} \quad : f \text{ is continuous and linear} \}.$$

Definition 2.3 (dual norm). Let V' denote the dual space of V and $g \in V'$. Then the dual norm of g is defined by

$$\|g\|_{V'} := \sup_{v \in V} \frac{|g(v)|}{\|v\|_V}. \tag{2.4}$$

Proposition 2.4. Let $g \in V'$ and $w \in V$, then it holds

$$g(w) \leq \|g\|_{V'} \|w\|_V. \tag{2.5}$$

Proof. Equation (2.5) simply follows from

$$g(w) = \frac{g(w)}{\|w\|_V} \|w\|_V \leq \sup_{v \in V} \frac{|g(v)|}{\|v\|_V} \|w\|_V = \|g\|_{V'} \|w\|_V.$$

$\square$

Definition 2.5 ($H^1(\Omega)$ space). Let $\Omega \subset \mathbb{R}^d$ be a bounded domain. The Sobolev space $H^1(\Omega) \subset L^2(\Omega)$ is defined by

$$H^1(\Omega) = \{ v \in L^2(\Omega) \colon v' \in L^2(\Omega) \}.$$

The derivative v' is understood in the weak sense, i.e. $\int_\Omega v'w = -\int_\Omega vw'$ and w is infinitely differentiable function with compact support. The inner product

$$(f,g)_{H^1} = (f,g)_{L^2(\Omega)} + (\nabla f, \nabla g)_{L^2(\Omega)}$$

induces the norm

$$\|f\|_{H^1} = \sqrt{\|f\|_{L^2(\Omega)}^2 + \|\nabla f\|_{L^2(\Omega)}^2}.$$

In order to derive the weak formulation, (2.1a) and (2.1c) are multiplied by a test function of the Sobolev space $X := H^1(\Omega)$, see definition 2.5. The equations are integrated over the spatial domain Ω. Integration by parts for the Laplace term shifts the derivative to the test function and the Neumann boundary condition (2.1b) enters the equation. For the sake of notational convenience, the solution is written without the space dependence in the following. The weak formulation of (2.1) is stated.

Problem 2.6 (weak formulation)**.** Find the solution $u(t) \in X$, such that

$$\langle \partial_t u(t), v \rangle + a(u(t), v) = b(v), \quad \forall v \in X,\, t \in (0, T], \tag{2.6a}$$
$$(u(t), v)_{L^2(\Omega)} = 0, \quad \forall v \in X,\, t = 0. \tag{2.6b}$$

and evaluate the output

$$s = l(u(T)). \tag{2.6c}$$

Here, $\langle \cdot, \cdot \rangle$ denotes a duality pairing between X' and X. The time derivative of the solution needs to lie in the dual space, i.e. $\partial_t u(t) \in X'$. The initial condition (2.6b) contains the standard L^2 inner product given by (2.3). The bilinear form $a\colon X \times X \to \mathbb{R}$ and the linear functional $b\colon X \to \mathbb{R}$ in (2.6a) are defined by $a(w,v) := \int_\Omega \nabla w \cdot \nabla v$ and $b(v) := \int_\Omega fv + \int_{\partial\Omega} gv$, respectively. The space dependence of the functions are omitted, i.e., e.g., $f(x) = f$ and therefore also the integration variable, i.e. $\int_\Omega f(x)\mathrm{d}x = \int_\Omega f$. Equation (2.6b) results from the homogeneous initial condition. The solution of (2.6a) and (2.6b) determines the output (2.6c).

2.2 Parametrized weak formulation

Many applications demand evaluations of a PDE for various input data. The given data parameterizes the underlying PDE, which is called parametrized partial differential equation (PPDE). Lack of knowledge regarding the input data causes data uncertainties and hence the input parameters are modeled stochastically. In order to describe the stochastic quantities, a complete probability space $(\Theta, \mathcal{F}, \mathbb{P})$ is introduced. The sample space Θ contains all possible outcomes $\theta \in \Theta$. The sigma algebra $\mathcal{F}$ is given by a subset of all possible subsets of Θ, i.e. $\mathcal{F} \subset 2^\Theta$, and the probability measure $\mathbb{P}\colon \mathcal{F} \to [0,1]$ maps an event to its probability. Let $\xi\colon \Theta \to \Gamma$ denote a random parameter vector whose image is in a bounded parameter domain $\Gamma \subset \mathbb{R}^p$. The parameter domain is determined by the support of the random variables, such that $\Gamma := [a_1, b_1] \times \cdots \times [a_p, b_p]$, with $-\infty < a_n < b_n < \infty$, $n = 1, \ldots, p$. We assume that ξ has a joint probability density function (pdf) $\rho\colon \Gamma \to \mathbb{R}^+$ such that $\int_\Theta \mathrm{d}\mathbb{P}(\theta) = \int_\Gamma \rho(\xi)\mathrm{d}\xi = 1$.

Now the continuous parametrized problem is stated.

Problem 2.7 (parametrized weak formulation)**.** For given realization $\xi \in \Gamma$, find the solution $u(t;\xi) \in X$, such that

$$\langle \partial_t u(t;\xi), v \rangle + a(u(t;\xi), v;\xi) = b(v;\xi), \qquad \forall v \in X,\, t \in (0,T], \qquad (2.7\text{a})$$

$$(u(t;\xi), v)_{L^2(\Omega)} = 0, \qquad \forall v \in X,\, t = 0, \qquad (2.7\text{b})$$

and evaluate the output

$$s(\xi) = l(u(T;\xi);\xi). \qquad (2.7\text{c})$$

The parameter dependence can enter the problem by the parametrized bilinear form $a(\cdot, \cdot;\xi)$, the parametrized linear right hand side functional $b(\cdot;\xi) \in X'$ and the parametrized linear output functional $l(\cdot;\xi) \in X'$ for all $\xi \in \Gamma$. Linearity regarding the parameter domain Γ does not necessarily hold. However, the bilinear form and the functionals are bounded regarding Γ. The parameter dependence is transferred to the output (2.7c), such that $s \colon \Gamma \to \mathbb{R}$.

In order to guarantee existence and uniqueness of Problem 2.7 the following assumptions have to hold.

Assumption 2.8. The bilinear form is uniformly coercive and uniformly bounded and the functionals are uniformly bounded, i.e.

$$\overline{\alpha} \le \alpha(\xi) = \inf_{0 \neq v \in X} \frac{a(v,v;\xi)}{\|v\|_X^2}, \qquad \sup_{0 \neq u,v \in X} \frac{a(u,v;\xi)}{\|u\|_X \|v\|_X} = \gamma_a(\xi) \le \overline{\gamma}_a, \text{ and} \quad (2.8)$$

$$\sup_{0 \neq v \in X} \frac{|b(v;\xi)|}{\|v\|_X} = \gamma_b(\xi) \le \overline{\gamma}_b, \qquad \sup_{0 \neq v \in X} \frac{|l(v;\xi)|}{\|v\|_X} = \gamma_l(\xi) \le \overline{\gamma}_l, \qquad (2.9)$$

with $0 < \overline{\alpha}$ and $\overline{\gamma}_a, \overline{\gamma}_b, \overline{\gamma}_l < \infty$, for all $\xi \in \Gamma$.

Assumption 2.9. The bilinear form is assumed to be symmetric, i.e.

$$a(u,v;\cdot) = a(v,u;\cdot),\, \forall u,v \in X. \qquad (2.10)$$

Equation (2.10) defines a parameter-dependent energy norm, such that

$$\|v\|_\xi = \sqrt{(v,v)_\xi} = \sqrt{a(v,v;\xi)}, \quad \forall v \in X,\, \forall \xi \in \Gamma,. \qquad (2.11)$$

At this point Problem 2.7 is continuous in time and space. In order to get rid of the time derivative, a time discretization method is applied.

2.2.1   Semi-discretized model problem

First, Problem 2.7 is discretized in time, also known as Rothe's method. The implicit Euler method is used as a time discretization method. The time interval I is split into $K \in \mathbb{N}$ equidistant time intervals with step size $\Delta t := \frac{T}{K}$. The solution is approximated at points in time $\{t^k = k\Delta t \colon k = 0, \ldots, K\}$, such that $u(t^k;\xi) \approx u^k(\xi)$. The $(K+1)$th power of the ansatz space is introduced by $X^{K+1} := X \times \cdots \times X$. Due to the implicit Euler method the time derivative in (2.7a) is discretized.

Problem 2.10 (semi-discretized problem)**.** For given realization $\xi \in \Gamma$, find $\{u^k(\xi)\}_{k=0}^K \in X^{K+1}$, such that

$$(u^k(\xi), v)_{L^2(\Omega)} + \Delta t a(u^k(\xi), v; \xi)$$
$$= (u^{k-1}(\xi), v)_{L^2(\Omega)} + \Delta t b(v; \xi), \ \forall v \in X, \, k = 1, \ldots, K, \quad (2.12a)$$
$$(u^k(\xi), v)_{L^2(\Omega)} = 0, \qquad\qquad\qquad \forall v \in X, \, k = 0, \qquad (2.12b)$$

and evaluate the output

$$s(\xi) = l(u^K(\xi); \xi). \tag{2.12c}$$

The problem is solved iteratively, where the time index, starting with $k = 0$, is increasing. Since (2.12b) is zero for all $v \in X$ and due to the properties of the L^2 norm, the solution at the initial point in time is zero. For an inhomogeneous initial condition the right hand side of (2.12b) would be non-zero. The output in (2.12c) is computed by means of the solution at the end point in time $u^K(\xi) \approx u(T; \xi)$, which is obtained from the last iteration step $k = K$ solving (2.12a) and (2.12b).

Problem 2.10 is continuous in space. In order to obtain a finite dimensional problem, a space discretization method is used.

2.2.2 Fully discretized model problem

Problem 2.10 is discretized in space by a standard Galerkin method. Here, h denotes the spatial step size and the high dimensional space $X_h := \text{span}\{\phi_1, \ldots, \phi_{\mathcal{N}}\} \subset X$, with $\dim(X_h) = \mathcal{N}$, contains piecewise linear basis functions. Further, $X_h^{K+1} := X_h \times \cdots \times X_h$ denotes the $(K + 1)$th power of the discretized space.

Problem 2.11 (fully discretized problem)**.** For given realization $\xi \in \Gamma$, find the detailed solutions $\{u_h^k(\xi)\}_{k=0}^K \in X_h^{K+1}$, such that

$$(u_h^k(\xi), v)_{L^2(\Omega)} + \Delta t\, a(u_h^k(\xi), v; \xi)$$
$$= (u_h^{k-1}(\xi), v)_{L^2(\Omega)} + \Delta t\, b(v; \xi), \forall v \in X_h, k = 1, \ldots, K, \quad (2.13a)$$
$$(u_h^k(\xi), v)_{L^2(\Omega)} = 0, \qquad\qquad\qquad \forall v \in X_h, k = 0, \qquad (2.13b)$$

and evaluate the output

$$s_h(\xi) = l(u_h^K(\xi); \xi). \tag{2.13c}$$

The problem is solved iteratively with an increasing time index, starting with $k = 0$. The output in (2.13c) is computed by means of the detailed solution at the end point in time $u_h^K(\xi)$, which is obtained from the last iteration step $k = K$ solving (2.13b) and (2.13c). A finite element method entails an $\mathcal{N}$-dimensional system of linear algebraic equations. Many applications demand $\mathcal{N}$ to be rather large and hence the discretized primal problem becomes computationally expensive to solve. The local support of the detailed basis functions implies sparsity of the system matrix. Hence, for each time step the algebraic equations can be solved with complexity $\mathcal{O}(\mathcal{N})$ in the best case using an iterative solver. Solving the detailed problem with homogeneous initial condition, the total

computational complexity is determined by $\mathcal{O}(K\mathcal{N})$. For an inhomogeneous initial condition, the right hand side of (2.13b) becomes non-zero. Therefore, it entails also a system of equations that has to be solved and hence the total complexity of Problem 2.11 increases to $\mathcal{O}((K+1)\mathcal{N})$.

The solution coefficients, resulting from the algebraic equations, uniquely represent the detailed solution, for $k = 0, \ldots, K$ and $\xi \in \Gamma$, such that

$$u_h^k(\xi) = \sum_{i=1}^{\mathcal{N}} u_{h,i}^k(\xi)\phi_i. \tag{2.14}$$

Problem 2.11 is also referred to as the detailed model and (2.14) as the detailed solution.

Definition 2.12 (detailed primal residual)**.** For any $\xi \in \Gamma$, the detailed primal residual regarding the detailed primal problem (2.13) is defined by, for $k = 1, \ldots, K$ and $v \in X$,

$$r_h^k(v;\xi) := b(v;\xi) - \frac{1}{\Delta t}(u_h^k(\xi) - u_h^{k-1}(\xi), v)_{L^2(\Omega)} - a(u_h^k(\xi), v;\xi). \tag{2.15}$$

Furthermore, the detailed residual for the initial condition is determined by, for $k = 0$ and $v \in X$,

$$r_h^k(v;\xi) := -(u_h^k(\xi), v)_{L^2(\Omega)}. \tag{2.16}$$

Remark 2.13. The detailed primal residual is zero for each function being an element of the high dimensional discretization space, i.e., for $k = 0, \ldots, K$,

$$X_h \subset \ker\left(r_h^k(\cdot;\xi)\right). \tag{2.17}$$

Definition 2.14 (detailed primal solution error)**.** For any $\xi \in \Gamma$, the detailed primal solution error is denoted by, for $k = 0, \ldots, K$,

$$e_h^k(\xi) := u^k(\xi) - u_h^k(\xi). \tag{2.18}$$

Proposition 2.15. For any $\xi \in \Gamma$, it holds that

$$e_h^k(\xi) = 0, \quad \text{for } k = 0. \tag{2.19}$$

Proof. The initial condition $(u^0(\xi), v)_{L^2(\Omega)} = 0$ has to hold for all $v \in X$ and hence the solution at the inital point in time is zero, i.e. $u^0(\xi) = 0$. By analogy, the initial condition of the detailed problem $(u_h^0(\xi), v)_{L^2(\Omega)} = 0$ has to hold for all $v \in X_h$ and hence the detailed solution at the initial point in time is zero, i.e. $u_h^0(\xi) = 0$. It follows, $e_h^0(\xi) = u^0(\xi) - u_h^0(\xi) = 0$. □

Proposition 2.16. For any $\xi \in \Gamma$, $k = 1, \ldots, K$ and $v \in X$, the relation

$$r_h^k(v;\xi) = \frac{1}{\Delta t}(e_h^k(\xi) - e_h^{k-1}(\xi), v)_{L^2(\Omega)} + a(e_h^k(\xi), v;\xi), \tag{2.20}$$

holds. Further, it holds that, for $k = 0$ and $v \in X$,

$$r_h^k(v;\xi) = 0. \tag{2.21}$$

Proof. Starting from the right hand side of (2.20) it follows

$$a(e_h^k(\xi), v; \xi) + \frac{1}{\Delta t}(e_h^k(\xi) - e_h^{k-1}(\xi), v)_{L^2(\Omega)} \overset{(2.18)}{=} a(u^k(\xi), v; \xi) - a(u_h^k(\xi), v; \xi)$$

$$+ \frac{1}{\Delta t}(u^k(\xi) - u^{k-1}(\xi), v)_{L^2(\Omega)} - \frac{1}{\Delta t}(u_h^k(\xi) - u_h^{k-1}(\xi), v)_{L^2(\Omega)}$$

$$\overset{(2.12a)}{=} b(v; \xi) - a(u_h^k(\xi), v; \xi) - \frac{1}{\Delta t}(u_h^k(\xi) - u_h^{k-1}(\xi), v)_{L^2(\Omega)},$$

which equals the definition of the residual (2.15). Equation (2.21) simply follows from (2.13b) and (2.16). □

2.2.3 Algebraic equations for detailed model

In this section Problem 2.11 is reformulated to a system of linear algebraic equations. The solutions of the algebraic equations determine the representation of the detailed solution (2.14). The detailed model problem tested for all basis functions $v = \phi_j \in X_h$, $j = 1, \ldots, \mathcal{N}$, yields

$$\sum_{i=1}^{\mathcal{N}} u_{h,i}^k(\xi)\Big[(\phi_i, \phi_j)_{L^2(\Omega)} + \Delta t\, a(\phi_i, \phi_j; \xi)\Big]$$

$$= \Delta t\, b(\phi_j; \xi) + \sum_{i=1}^{\mathcal{N}} u_{h,i}^{k-1}(\xi)(\phi_i, \phi_j)_{L^2(\Omega)}, \ k = 1, \ldots, K,$$

$$\sum_{i=1}^{\mathcal{N}} u_{h,i}^k(\xi)(\phi_i, \phi_j)_{L^2(\Omega)} = 0, \qquad\qquad\qquad k = 0,$$

and evaluate the output

$$s_h(\xi) = \sum_{i=1}^{\mathcal{N}} u_{h,i}^K(\xi) l(\phi_i; \xi).$$

The following matrices and vectors are defined

$$M := \big((\phi_i, \phi_j)_{L^2(\Omega)}\big)_{j,i=1}^{\mathcal{N}} \in \mathbb{R}^{\mathcal{N} \times \mathcal{N}}, \qquad (2.23)$$

$$A(\xi) := (a(\phi_i, \phi_j; \xi))_{j,i=1}^{\mathcal{N}} \quad \in \mathbb{R}^{\mathcal{N} \times \mathcal{N}}, \qquad (2.24)$$

$$\underline{b}(\xi) := (b(\phi_j; \xi))_{j=1}^{\mathcal{N}} \qquad \in \mathbb{R}^{\mathcal{N}}, \qquad (2.25)$$

$$\underline{l}(\xi) := (l(\phi_j; \xi))_{j=1}^{\mathcal{N}} \qquad \in \mathbb{R}^{\mathcal{N}}. \qquad (2.26)$$

Then, the solution vectors $\underline{u}_h^k(\xi) = (u_{h,i}^k(\xi))_{i=1}^{\mathcal{N}}$, $k = 0, \ldots, K$ can be computed from the $\mathcal{N}$-dimensional systems of linear algebraic equations

$$(M + \Delta t\, A(\xi))\, \underline{u}_h^k(\xi) = \Delta t\, \underline{b}(\xi) + M\underline{u}_h^{k-1}(\xi), \ k = 1, \ldots, K$$

$$M\underline{u}_h^k(\xi) = 0, \qquad\qquad k = 0,$$

which determines (2.14). Utilizing the solution vector at the end point in time, the output is computed by

$$\underline{l}(\xi)^T \underline{u}_h^K(\xi).$$

2.3   Dual problem

A dual approach is a standard approach for a posteriori error estimation in finite element theory in order to control the output computation or estimate the output error, see, e.g., (Ainsworth and Oden, 2000, chapter 8). The dual problem accomplishes a relation between the primal residual and the error that arises from the output approximation, see (Oden and Prud'homme, 2001, section 3.1). By means of the solution of the dual problem, called dual solution, higher accuracy for the output computation can be achieved and sharper error bounds for the error can be derived.

2.3.1   Derivation for general output functional

In the following the dual problem regarding the primal problem (2.7a) and (2.7b) for a general output functional is derived. The solution of the dual problem allows to derive better error bounds for the output. A general quantity of interest is considered by

$$\int_0^T g(u(t;\xi);\xi)\mathrm{d}t + l(u(T;\xi);\xi), \tag{2.27}$$

where $g\colon X \times \Gamma \to \mathbb{R}$ is a functional and $g(\cdot;\xi) \in X'$ for all $\xi \in \Gamma$. The functional $l\colon X \times \Gamma \to \mathbb{R}$ uses the solution at the end point in time, cf. (2.7c). The choice of such a functional is motivated from optimal control theory, e.g. (Meidner and Vexler, 2012, page 323). Linearity for (2.27) holds. The dual approach is not limited to linear functionals. However, in case of non-linear functionals a different dual problem is obtained, see, e.g., (Ern and Guermond, 2004, section 10.3.2). More details on non-linear functionals and a broad overview on a posteriori error estimation for finite element methods can be found in Becker and Rannacher (2001). The time continuous solution error is denoted by

$$e_h(t;\xi) := u(t;\xi) - u_h(t;\xi), \tag{2.28}$$

where $u_h(t;\xi)$ solves Problem 2.7 on X_h. Since the functionals g and l are linear in X, the error for the quantity of interest can be estimated by (2.5), such that

$$\left| \int_0^T g(e_h(t;\xi);\xi)\mathrm{d}t + l(e_h(T;\xi);\xi) \right|$$
$$\tag{2.29}$$
$$\leq \int_0^T \|g(\cdot;\xi)\|_{X'} \|e_h(t;\xi)\|_X \, \mathrm{d}t + \|l(\cdot;\xi)\|_{X'} \|e_h(T;\xi)\|_{L^2(\Omega)}.$$

The dual norm $\|\cdot\|_{X'}$ is determined by (2.4). However, the objective is to improve the convergence of the estimation for the output error in (2.29).

Definition 2.17 (time continuous primal residual)**.** For any $\xi \in \Gamma$, the time continuous primal residual is defined by, for $t \in (0,T]$ and $v \in X$,

$$r_h(v;\xi) := b(v;\xi) - (\partial_t u_h(t;\xi), v)_{L^2(\Omega)} - a(u_h(t;\xi), v;\xi). \tag{2.30}$$

Furthermore, the time continuous residual for the homogeneous initial condition is determined by, for $t = 0$ and $v \in X$,

$$r_h(v;\xi) := -(u_h(t;\xi), v)_{L^2(\Omega)}. \tag{2.31}$$

Proposition 2.18. For any $\xi \in \Gamma$, $t \in (0, T]$ and $v \in X$, the relation

$$r_h(v; \xi) = \langle \partial_t e_h(t; \xi), v \rangle + a(e_h(t; \xi), v; \xi), \tag{2.32}$$

holds. Further, it holds that, for $t = 0$ and $v \in X$,

$$r_h(v; \xi) = 0. \tag{2.33}$$

Proof. Starting from the right hand side of (2.32) it follows

$$\langle \partial_t e_h(t; \xi), v \rangle + a(e_h(t; \xi), v; \xi) \stackrel{(2.28)}{=} \langle \partial_t u(t; \xi), v \rangle + a(u(t; \xi), v; \xi)$$
$$- \langle \partial_t u_h(t; \xi), v \rangle - a(u_h(t; \xi), v; \xi)$$
$$\stackrel{(2.7a)}{=} b(v; \xi) - \langle \partial_t u_h(t; \xi), v \rangle - a(u_h(t; \xi), v; \xi)$$

which equals the definition of the residual (2.30). Equation (2.33) simply follows from (2.31) and $u_h(0; \xi) = 0$. $\square$

For the derivation of the dual problem a function $\psi(t; \xi) \in X$, for $t \in I$ and $\xi \in \Gamma$ is sought. It relates the time continuous primal residual (2.30) and (2.31) and the quantity of interest for the time continuous error (2.28), such that

$$r_h(\psi(0; \xi); \xi) + \int_0^T r_h(\psi(t; \xi); \xi)\, \mathrm{d}t = \int_0^T g(e_h(t; \xi); \xi)\, \mathrm{d}t + l(e_h(T; \xi); \xi). \tag{2.34}$$

The first term on the left hand vanishes due to (2.33), whereas the second term is rewritten by (2.32). Integration by parts for time shifts the time derivative to the unknown function $\psi(t; \xi)$, i.e.

$$\begin{aligned}
(e_h(T; \xi), &\psi(T; \xi))_{L^2(\Omega)} - (e_h(0; \xi), \psi(0; \xi))_{L^2(\Omega)} \\
&+ \int_0^T -\langle e_h(t; \xi), \partial_t \psi(t; \xi) \rangle + a(e_h(t; \xi), \psi(t; \xi); \xi)\, \mathrm{d}t \\
&= \int_0^T g(e_h(t; \xi); \xi)\, \mathrm{d}t + l(e_h(T; \xi); \xi).
\end{aligned} \tag{2.35}$$

Due to the homogeneous initial condition, (2.28) is zero for $t = 0$, hence $(e_h(0; \xi), \psi(0; \xi))_{L^2(\Omega)} = 0$. Equation (2.35) has to hold for all errors $e_h(t; \xi)$ in the infinite dimensional space X. Then, solving the equation pointwise for each point in time, the continuous dual problem can be stated.

Problem 2.19 (continuous dual problem)**.** Find the dual solution $\psi(t; \xi) \in X$, such that

$$-\langle v, \partial_t \psi(t; \xi) \rangle + a(v, \psi(t; \xi); \xi) = g(v; \xi), \quad \forall v \in X, \tag{2.36a}$$
$$(v, \psi(T; \xi))_{L^2(\Omega)} = l(v; \xi), \quad \forall v \in X. \tag{2.36b}$$

Instead of the initial condition for the primal problem, the dual problem uses a final condition (2.36b). The dual problem evolves backwards in time, denoted by the minus sign in (2.36a).

Remark 2.20. The quantity of interest can either be computed by the primal solution inserted in the output functional, see (2.27), or by the dual solution inserted in the right hand side of the primal problem, cf. (Pierce and Giles, 2000, chapter 2). For further details see appendix A.3.

Analogously to the discretization of the primal problem, the dual problem continuous in time and discrete in space is stated.

Problem 2.21 (time continuous dual problem)**.** Find the detailed dual solution $\psi_h(t;\xi) \in X_h$, such that

$$-\langle v, \partial_t \psi_h(t;\xi)\rangle + a(v, \psi_h(t;\xi); \xi) = g(v;\xi), \quad \forall v \in X_h, \tag{2.37a}$$

$$(v, \psi_h(T;\xi))_{L^2(\Omega)} = l(v;\xi), \quad \forall v \in X_h. \tag{2.37b}$$

The time continuous dual solution error is denoted by

$$\tilde{e}_h(t;\xi) := \psi(t;\xi) - \psi_h(t;\xi). \tag{2.38}$$

The output error computation (2.29) is expanded by a "correction term"

$$-\int_0^T r_h(\psi_h(t;\xi);\xi) = 0, \tag{2.39}$$

cf. (2.17), such that

$$|\int_0^T g(e_h(t;\xi);\xi)\mathrm{d}t + l(e_h(T;\xi);\xi) - \int_0^T r_h(\psi_h(t;\xi);\xi)\,\mathrm{d}t|$$

$$\overset{(2.34)}{=} |\int_0^T r_h(\psi(t;\xi);\xi)\mathrm{d}t - \int_0^T r_h(\psi_h(t;\xi);\xi)\,\mathrm{d}t|$$

$$\overset{(2.38)}{=} |\int_0^T r_h(\tilde{e}_h(t;\xi);\xi)\mathrm{d}t|$$

$$\overset{(2.32)}{=} |\int_0^T \langle \partial_t e_h(t;\xi), \tilde{e}_h(t;\xi)\rangle + a(e_h(t;\xi), \tilde{e}_h(t;\xi);\xi)\mathrm{d}t|.$$

Compared to (2.29), this expression does not only contain the primal solution error (2.28), but also the dual solution error (2.38). Assume that the dual solution error is of the same order of magnitude as the primal solution error, i.e. $e_h \sim \tilde{e}_h$, as $h \to 0$. Then, the last expression asymptotically behaves like

$$\int_0^T \langle \partial_t e_h(t;\xi), e_h(t;\xi)\rangle + a(e_h(t;\xi), e_h(t;\xi);\xi)\mathrm{d}t$$

$$= \frac{1}{2}\|e_h(T;\xi)\|_X^2 + \int_0^T a(e_h(t;\xi), e_h(t;\xi);\xi)\mathrm{d}t \tag{2.40}$$

$$\overset{(2.8)}{\leq} \frac{1}{2}\|e_h(T;\xi)\|_X^2 + \gamma_a(\xi)\int_0^T \|e_h(t;\xi)\|_X^2\,\mathrm{d}t.$$

The first identity utilizes $\langle \partial_t v, v\rangle = \frac{1}{2}\partial_t \|v\|^2$ and $e_h(0;\xi) = 0$. Compared to (2.29), the convergence rate in (2.40) is doubled since the solution error e_h converges to zero for h tending to zero.

2.3.2   Semi-discretized dual problem

Utilizing the previous ideas, the dual problem for the semi-discretized problem (2.12) can be derived. For the problem (2.7), the quantity of interest (2.27)

simplifies to the second term $l(u(T;\xi);\xi)$. Then, the following relation has to hold

$$\Delta t \sum_{k=1}^{K} r_h^k(\psi^{k-1}(\xi);\xi) = l(e_h^K(\xi);\xi), \qquad (2.41)$$

where the discrete residual and the discrete solution error are defined in (2.15) and (2.18), respectively. The function $\psi^k(\xi) \approx \psi(t^k;\xi)$ denotes the discretized dual solution at point in time t^k, $k = 0, \ldots, K$. The abbreviations $e_h^k(\xi) = e_h^k$, $\psi^k(\xi) = \psi^k$ and the identity (2.20) give

$$\sum_{k=1}^{K} (e_h^k - e_h^{k-1}, \psi^{k-1})_{L^2(\Omega)} + \Delta t\, a(e_h^k, \psi^{k-1};\xi) = l(e_h^K;\xi).$$

Using (2.19), the time indices for the first summand on the left hand side can be reordered, such that

$$(e_h^K, \psi^K)_{L^2(\Omega)} + \sum_{k=1}^{K} (e_h^k, \psi^{k-1} - \psi^k)_{L^2(\Omega)} + \Delta t\, a(e_h^k, \psi^{k-1};\xi) = l(e_h^K;\xi).$$

The equation is satisfied if the first term on the left hand side equals the right hand side and the summands are zero for all time steps k. As for the time continuous case, the equation needs to hold for all e_h^k. Then the time discretized dual problem can be stated.

Problem 2.22 (semi-discretized dual problem)**.** For given realization $\xi \in \Gamma$, find $\{\psi^k(\xi)\}_{k=0}^{K} \in X^{K+1}$, such that

$$(v, \psi^k(\xi))_{L^2(\Omega)} + \Delta t\, a(v, \psi^k(\xi);\xi)$$
$$= (v, \psi^{k+1}(\xi))_{L^2(\Omega)}, \ \forall v \in X,\, k = 0, \ldots, K-1, \qquad (2.42a)$$
$$(v, \psi^k(\xi))_{L^2(\Omega)} = l(v;\xi), \qquad\qquad \forall v \in X,\, k = K. \qquad (2.42b)$$

As for the time continuous case, the dual problem evolves backward in time. Hence, Problem 2.22 is solved iteratively where the time index is decreasing, starting with $k = K$.

2.3.3 Fully discretized dual problem

As for the primal problem, the dual problem (2.42) is spatially discretized by a standard Galerkin method, cf. section 2.2.2.

Problem 2.23 (fully discretized dual problem)**.** For given realization $\xi \in \Gamma$, find $\{\psi_h^k(\xi)\}_{k=0}^{K} \in X_h^{K+1}$, such that

$$(v, \psi_h^k(\xi))_{L^2(\Omega)} + \Delta t\, a(v, \psi_h^k(\xi);\xi)$$
$$= (v, \psi_h^{k+1}(\xi))_{L^2(\Omega)}, \ \forall v \in X_h,\, k = 0, \ldots, K-1, \qquad (2.43a)$$
$$(v, \psi_h^k(\xi))_{L^2(\Omega)} = l(v;\xi), \qquad\qquad \forall v \in X_h,\, k = K. \qquad (2.43b)$$

As in section 2.2.2, the discretized dual problem entails an $\mathcal{N}$-dimensional system of linear algebraic equations which for large $\mathcal{N}$ are computationally expensive to solve. The computational complexity over all time steps is determined

by $\mathcal{O}((K + 1)\mathcal{N})$ in the best case, cf. the complexity of the forward problem (2.13). The solution coefficients, coming out of the algebraic equations, uniquely represent the discretized dual solution, for $k = 0, \ldots, K$ and $\xi \in \Gamma$, such that

$$\psi_h^k(\xi) = \sum_{i=1}^{\mathcal{N}} \psi_{h,i}^k(\xi)\phi_i. \tag{2.44}$$

Problem 2.23 is also referred to as the detailed dual problem and (2.44) as the detailed dual solution. Existence and uniqueness of the detailed dual problem follow from Assumption 2.8.

Remark 2.24. On the one hand the discretized dual problem can be derived from the time discretized formulation, see (2.41) to (2.42). On the other hand the discretized dual problem can be derived from the time continuous formulation (2.37), followed by discretization in time. It is emphasized that both ways of the derivation yield the same dual problem (2.43). Since the space discretization does not change the equations of the weak formulation, cf. Problems 2.19 and 2.21, it has no influence on the derivation of the dual problem.

Definition 2.25 (detailed dual residual)**.** For any $\xi \in \Gamma$, the detailed residual regarding detailed dual problem (2.43) is defined by, for $k = 0, \ldots, K - 1$ and $v \in X$,

$$\tilde{r}_h^k(v; \xi) := -\frac{1}{\Delta t}(\psi_h^k(\xi) - \psi_h^{k+1}(\xi), v)_{L^2(\Omega)} - a(\psi_h^k(\xi), v; \xi). \tag{2.45}$$

Furthermore, the detailed residual for the final condition is determined by, for $k = K$ and $v \in X$,

$$\tilde{r}_h^k(v; \xi) := l(v; \xi) - (v, \psi_h^k)_{L^2(\Omega)}. \tag{2.46}$$

Remark 2.26. The detailed dual residual is zero for each function being an element of the high dimensional discretization space, i.e., for $k = 0, \ldots, K$,

$$X_h \subset \ker(\tilde{r}_h^k(\cdot; \xi)).$$

Definition 2.27 (detailed dual solution error)**.** For any $\xi \in \Gamma$, the detailed dual solution error is denoted by, for $k = 0, \ldots, K$,

$$\tilde{e}_h^k(\xi) := \psi^k(\xi) - \psi_h^k(\xi). \tag{2.47}$$

Proposition 2.28. For any $\xi \in \Gamma$ and $k = 0, \ldots, K - 1$ and $v \in X$, the relation

$$\tilde{r}_h^k(v; \xi) = \frac{1}{\Delta t}(\tilde{e}_h^k(\xi) - \tilde{e}_h^{k+1}(\xi), v)_{L^2(\Omega)} + a(v, \tilde{e}_h^k(\xi); \xi), \tag{2.48}$$

holds. Further, it holds that, for $k = K$ and $v \in X$,

$$\tilde{r}_h^k(v; \xi) = (v, \tilde{e}_h^k(\xi))_{L^2(\Omega)}. \tag{2.49}$$

Proof. Starting from the right hand side of (2.48) it follows

$$a(\tilde{e}_h^k(\xi), v; \xi) + \frac{1}{\Delta t}(\tilde{e}_h^k(\xi) - \tilde{e}_h^{k+1}(\xi), v)_{L^2(\Omega)} \overset{(2.47)}{=} a(\psi^k(\xi), v; \xi) - a(\psi_h^k(\xi), v; \xi)$$

$$+ \frac{1}{\Delta t}(\psi^k(\xi) - \psi^{k+1}(\xi), v)_{L^2(\Omega)} - \frac{1}{\Delta t}(\psi_h^k(\xi) - \psi_h^{k+1}(\xi), v)_{L^2(\Omega)}$$

$$\overset{(2.42a)}{=} -a(\psi_h^k(\xi), v; \xi) - \frac{1}{\Delta t}(\psi_h^k(\xi) - \psi_h^{k+1}(\xi), v)_{L^2(\Omega)},$$

which equals the definition of the residual (2.45). Equation (2.49) simply follows from

$$(v, \tilde{e}_h^k(\xi))_{L^2(\Omega)} \overset{(2.47)}{=} (v, \psi^k(\xi))_{L^2(\Omega)} - (v, \psi_h^k(\xi))_{L^2(\Omega)} \overset{(2.42b)}{=} l(v; \xi) - (v, \psi_h^k(\xi))_{L^2(\Omega)},$$

which equals (2.46). □

Remark 2.29 (compliant case)**.** Let the bilinear form be symmetric and the right hand side of the forward problem equals the right hand side of the backward problem, i.e., for example for a general quantity of interest (2.27) that $b \equiv g$. Then the dual solution coincides with the primal solution. Hence, for the time continuous case the solution satisfies $u(t; \xi) = \psi(T - t; \xi)$, where for the time discretized case it holds that $u^k(\xi) = \psi^{K-k}(\xi)$. For further details see appendix A.4.

2.3.4 Algebraic equations for detailed dual model

In this section Problem 2.23 is reformulated to a system of linear algebraic equations. The solutions of the algebraic equations determine the representation of the detailed dual solution (2.44). The detailed dual model problem tested for all basis functions $v = \phi_j \in X_h$, $j = 1, \ldots, \mathcal{N}$, yields

$$\sum_{i=1}^{\mathcal{N}} \psi_{h,i}^k(\xi) \Big[(\phi_j, \phi_i)_{L^2(\Omega)} + \Delta t \, a(\phi_j, \phi_i; \xi) \Big]$$
$$= \sum_{i=1}^{\mathcal{N}} \psi_{h,i}^{k+1}(\xi)(\phi_j, \phi_i)_{L^2(\Omega)}, \, k = 0, \ldots, K - 1,$$
$$\sum_{i=1}^{\mathcal{N}} \psi_{h,i}^k(\xi)(\phi_j, \phi_i)_{L^2(\Omega)} = l(\phi_j; \xi), \qquad\qquad k = K.$$

Using the definitions (2.23), (2.24), and (2.26), the solution vectors of the dual problem $\underline{\psi}_h^k(\xi) = (\psi_{h,i}^k(\xi))_{i=1}^{\mathcal{N}}$, $k = 0, \ldots, K$ can be computed from the $\mathcal{N}$-dimensional systems of linear algebraic equations

$$\left(M + \Delta t \, A(\xi)^T \right) \underline{\psi}_h^k(\xi) = M \underline{\psi}_h^{k+1}(\xi), \, k = 0, \ldots, K - 1 \qquad (2.51a)$$
$$M \underline{\psi}_h^k(\xi) = \underline{l}(\xi), \qquad k = K, \qquad (2.51b)$$

which determines (2.44). If Assumption 2.9 is fulfilled, the stiffness matrix in (2.51a) is symmetric, i.e. $A(\xi) = A(\xi)^T$. Here, A^T denotes the transpose of the matrix A.

Chapter 3

A weighted reduced basis method for parabolic PDEs

The reduced basis method (RBM) is a technique in the field of model order reduction for PPDEs and applies if a PPDE needs to be solved for many different parameters, solutions are required in real time or if the available memory is limited, for instance. The objective is the approximation of the solution manifold, containing the detailed solution for all parameters by a low dimensional reduced space. The RBM has been developed extensively in the last decades. A recent overview can be found in Quarteroni et al. (2016); Hesthaven et al. (2016); Haasdonk (2017). Application of the RBM to parabolic PPDEs was considered in Grepl (2005).

This work considers the RBM for a linear parabolic PPDE with parameter uncertainties. A review for the RBM concerning PPDEs with random input data can be found in Chen et al. (2017). Dealing with data uncertainties, a weighted RBM equips more likely parameters with higher priority. The weighted approach was introduced in Chen et al. (2013) for elliptic PDEs. A recent work on weighted RBM for elliptic PDEs can be found in Venturi et al. (2018). It allows to build up more efficient reduced spaces regarding an approximation of statistical quantities. In this chapter, this idea is transferred to the parabolic case. The primal reduced model and the dual reduced model is set up. By means of the solution of the reduced dual problem, cf. section 2.3, the accuracy for the output computation is increased. Non-weighted and weighted rigorous a posteriori error estimators are stated and utilized for the reduced space construction.

3.1   Reduced model problem

In this section, the reduced order model (ROM) of the detailed model (2.13) using the RBM is stated. The RBM is a Galerkin projection onto a reduced space $X_N := \text{span}\{\varphi_1, \ldots, \varphi_N\} \subset X_h$, where $\Phi_N := \{\varphi_1, \ldots, \varphi_N\}$ is called the reduced basis. The reduced basis is an orthonormal basis w.r.t. $\|\cdot\|_X$, such that $(\varphi_n, \varphi_m)_X = \delta_{nm}$, where δ_{mn} denotes the Kronecker delta. The reduced dimension is denoted by $\dim(X_N) = N$. Analogue to the detailed problem, the $(K+1)$th power of the reduced space is defined by $X_N^{K+1} := X_N \times \cdots \times X_N$. Then, the reduced forward problem can be stated.

Problem 3.1 (reduced primal problem)**.** For given realization $\xi \in \Gamma$, find the reduced solutions $\{u_N^k(\xi)\}_{k=0}^K \in X_N^{K+1}$, such that

$$(u_N^k(\xi), v)_{L^2(\Omega)} + \Delta t\, a(u_N^k(\xi), v; \xi)$$
$$= (u_N^{k-1}(\xi), v)_{L^2(\Omega)} + \Delta t\, b(v; \xi), \forall v \in X_N, k = 1, \ldots, K, \quad (3.1\text{a})$$
$$(u_N^k(\xi), v)_{L^2(\Omega)} = 0, \qquad\qquad\qquad \forall v \in X_N, k = 0. \qquad (3.1\text{b})$$

The solution of the reduced model approximates the detailed solution within the time interval and parameter domain, i.e. $u_N^k(\xi) \approx u_h^k(\xi)$ for $k = 0, \ldots, K$ and $\xi \in \Gamma$.

In order to obtain higher accuracy for the reduced output computation and an improved reduced output error bound, the reduced dual problem is introduced, cf. section 2.3. The corresponding reduced space $\tilde{X}_{\tilde{N}} := \text{span}\{\zeta_1, \ldots, \zeta_{\tilde{N}}\} \subset X_h$ is spanned by an orthonormal basis w.r.t. $\|\cdot\|_X$, such that $(\zeta_n, \zeta_m)_X = \delta_{nm}$. The reduced dimension is denoted by $\dim(\tilde{X}_{\tilde{N}}) = \tilde{N}$. The $(K+1)$th power of the reduced space regarding the reduced dual problem is defined by $\tilde{X}_{\tilde{N}}^{K+1} := \tilde{X}_{\tilde{N}} \times \cdots \times \tilde{X}_{\tilde{N}}$. Then, the reduced backward problem can be stated.

Problem 3.2 (reduced dual problem)**.** For given realization $\xi \in \Gamma$, find the reduced solutions $\{\psi_{\tilde{N}}^k(\xi)\}_{k=0}^K \in \tilde{X}_{\tilde{N}}^{K+1}$, such that

$$(v, \psi_{\tilde{N}}^k(\xi))_{L^2(\Omega)} + \Delta t\, a(v, \psi_{\tilde{N}}^k(\xi); \xi)$$
$$= (v, \psi_{\tilde{N}}^{k+1}(\xi))_{L^2(\Omega)}, \forall v \in \tilde{X}_{\tilde{N}}, k = 0, \ldots, K-1, \qquad (3.2\text{a})$$
$$(v, \psi_{\tilde{N}}^k(\xi))_{L^2(\Omega)} = l(v; \xi), \qquad\qquad \forall v \in \tilde{X}_{\tilde{N}}, k = K. \qquad (3.2\text{b})$$

The reduced spaces X_N and $\tilde{X}_{\tilde{N}}$ are spanned by a different basis and, in general, they can have different dimensions, i.e. $N \neq \tilde{N}$. The reduced primal problem and the reduced dual problem yield a system of linear equations with dimensions N and $\tilde{N}$, respectively. In contrast to the detailed space, the reduced spaces are spanned by global basis functions. Hence, the system matrices for the reduced problems are full. Therefore the total computational complexity for the reduced primal problem with homogeneous initial condition and the reduced dual problem are $\mathcal{O}(KN^3)$ and $\mathcal{O}((K+1)\tilde{N}^3)$, respectively. In order to obtain the desired computational speed up by the RBM, it is required that $N, \tilde{N} \ll \mathcal{N}$.

For each time step and each parameter, the solutions of the algebraic equations yield the primal solution coefficients $\{u_{N,n}^k(\xi)\}_{n=1}^N$ and the dual solution coefficients $\{\psi_{\tilde{N},n}^k(\xi)\}_{n=1}^{\tilde{N}}$. They determine a unique representation of the reduced solutions, for $k = 0, \ldots, K$ and $\xi \in \Gamma$, such that

$$u_N^k(\xi) = \sum_{n=1}^N u_{N,n}^k(\xi)\varphi_n, \qquad\qquad (3.3)$$

$$\psi_{\tilde{N}}^k(\xi) = \sum_{n=1}^{\tilde{N}} \psi_{\tilde{N},n}^k(\xi)\zeta_n. \qquad\qquad (3.4)$$

In the following, the residuals for the primal problem and the dual problem are introduced. The definitions of the residuals are taken from (Grepl and Patera, 2005, equations (21) and (34)) .

Definition 3.3 (reduced primal residual)**.** For any $\xi \in \Gamma$, the reduced primal residual regarding the reduced primal problem (3.1) is defined by, for $k = 1, \ldots, K$,

$$r_N^k(v; \xi) := b(v; \xi) - \frac{1}{\Delta t}(u_N^k(\xi) - u_N^{k-1}(\xi), v)_{L^2(\Omega)} - a(u_N^k(\xi), v; \xi), \ \forall v \in X_h.$$
$$(3.5)$$

Additionally, for $k = 0$, the reduced residual for the homogeneous initial condition is determined by

$$r_N^k(v; \xi) := -(u_N^k(\xi), v)_{L^2(\Omega)}, \ \forall v \in X_h. \tag{3.6}$$

Definition 3.4 (reduced dual residual)**.** For any $\xi \in \Gamma$, the reduced dual residual regarding the reduced dual problem (3.2) is defined by, for $k = 0, \ldots, K-1$,

$$\tilde{r}_{\tilde{N}}^k(v; \xi) := -\frac{1}{\Delta t}(v, \psi_{\tilde{N}}^k(\xi) - \psi_{\tilde{N}}^{k+1}(\xi))_{L^2(\Omega)} - a(v, \psi_{\tilde{N}}^k(\xi); \xi), \ \forall v \in X_h. \quad (3.7)$$

Additionally, the reduced residual for the final condition is determined by, for $k = K$,

$$\tilde{r}_{\tilde{N}}^k(v; \xi) := l(v; \xi) - (v, \psi_{\tilde{N}}^k(\xi))_{L^2(\Omega)}, \ \forall v \in X_h. \tag{3.8}$$

Remark 3.5. The reduced primal residual and the reduced dual residual are orthogonal onto their reduced spaces, i.e., for $k = 0, \ldots, K$, $X_N \subset \ker(r_N^k(\cdot; \xi))$ and $\tilde{X}_{\tilde{N}} \subset \ker(\tilde{r}_{\tilde{N}}^k(\cdot; \xi))$.

Definition 3.6 (reduced solution error)**.** For any $\xi \in \Gamma$, the reduced primal solution error and the reduced dual solution error is denoted by, for $k = 0, \ldots, K$,

$$e_N^k(\xi) := u_h^k(\xi) - u_N^k(\xi), \tag{3.9}$$
$$\tilde{e}_{\tilde{N}}^k(\xi) := \psi_h^k(\xi) - \psi_{\tilde{N}}^k(\xi), \tag{3.10}$$

respectively.

Proposition 3.7. For any $\xi \in \Gamma$, it holds that

$$e_N^k(\xi) = 0, \quad \text{for } k = 0. \tag{3.11}$$

Proof. It is shown analogue to the proof of Proposition 2.15. $\qquad \square$

Proposition 3.8. Let $\xi \in \Gamma$. For the primal residual, the following relation holds, for $k = 1, \ldots, K$,

$$r_N^k(v; \xi) = \frac{1}{\Delta t}(e_N^k(\xi) - e_N^{k-1}(\xi), v)_{L^2(\Omega)} + a(e_N^k(\xi), v; \xi), \ \forall v \in X_h. \quad (3.12)$$

Further, the residual for the initial condition fulfills, for $k = 0$,

$$r_N^k(v; \xi) = 0. \tag{3.13}$$

For the dual residual it holds, $k = 0, \ldots, K-1$,

$$\tilde{r}_{\tilde{N}}^k(v; \xi) = \frac{1}{\Delta t}(\tilde{e}_{\tilde{N}}^k(\xi) - \tilde{e}_{\tilde{N}}^{k+1}(\xi), v)_{L^2(\Omega)} + a(v, \tilde{e}_{\tilde{N}}^k(\xi); \xi), \ \forall v \in X_h. \quad (3.14)$$

Further, the residual for the final condition fulfills, for $k = K$,

$$\tilde{r}_{\tilde{N}}^k(v; \xi) = (v, \tilde{e}_{\tilde{N}}^k(\xi))_{L^2(\Omega)}, \ \forall v \in X_h. \tag{3.15}$$

Proof. The proof is analogue to Proposition 2.16 and Proposition 2.28.   □

As it was motivated in sections 2.3 and 2.3.1, the reduced output computation is expanded by a "correction", cf. (2.39), such that

$$s_{N,\tilde{N}}(\xi) = l(u_N^K(\xi);\xi) + \Delta t \sum_{k=1}^{K} r_N^k(\psi_{\tilde{N}}^{k-1}(\xi);\xi). \qquad (3.16)$$

For the reduced framework the "correction" is not zero compared to the detailed "correction" (2.39). This is due to the fact that the detailed primal problem and the detailed dual problem are solved on the same discretization space X_h. This is not the case for the reduced spaces, i.e. $X_N \neq \tilde{X}_{\tilde{N}}$. The "correction" uses the reduced dual solutions $\{\psi_{\tilde{N}}^k\}_{k=0}^{K-1}$ in order to achieve higher accuracy for the output computation.

For computational efficiency, the computation is split into an offline phase and an online phase, see, e.g., Prud'homme et al. (2001). The former is expensive to compute and depends on the large dimension $\mathcal{N}$, and it is related to the reduced model construction. Once the reduced model exists, solutions are obtained very fast in the online phase by calculations depending only on the reduced dimension N. For such a splitting, the bilinear form $a(\cdot,\cdot;\xi)$ and the functionals $b(\cdot;\xi)$, $l(\cdot;\xi)$ need to be affine with respect to ξ (also known as parameter separable).

Assumption 3.9 (parameter separability)**.**

$$a(v,w;\xi) = \sum_{q=1}^{Q_a} \theta_q^a(\xi)a_q(v,w), \quad \forall v,w \in X, \forall \xi \in \Gamma,$$

$$b(v;\xi) = \sum_{q=1}^{Q_b} \theta_q^b(\xi)b_q(v), \qquad \forall v \in X, \forall \xi \in \Gamma,$$

$$l(v;\xi) = \sum_{q=1}^{Q_l} \theta_q^l(\xi)l_q(v), \qquad \forall v \in X, \forall \xi \in \Gamma.$$

By means of the assumption, the bilinear form and the functionals are computed by a linear combination of a parameter independent and a parameter dependent part. It allows rapid evaluations for different parameters, since the parameter independent quantities, which are computationally expensive, need to be computed only once. If the assumption does not hold, an empirical interpolation method (EIM), see Barrault et al. (2004), can be used instead.

3.1.1   Algebraic equations for reduced model

In this section, Problems 3.1 and 3.2 are reformulated to a system of linear algebraic equations. The solutions of the algebraic equations determine the representation of the reduced solution (3.3) and the reduced dual solution (3.4).

The reduced primal problem tested for all basis functions $v = \varphi_m \in X_N$,

$m = 1, \ldots, N$, yields

$$\sum_{n=1}^{N} u_{N,n}^{k}(\xi) \Big[(\varphi_n, \varphi_m)_{L^2(\Omega)} + \Delta t\, a(\varphi_n, \varphi_m; \xi) \Big] = \Delta t\, b(\varphi_m; \xi)$$

$$+ \sum_{n=1}^{N} u_{N,n}^{k-1}(\xi)(\varphi_n, \varphi_m)_{L^2(\Omega)}, \qquad k = 1, \ldots, K,$$

$$\sum_{n=1}^{N} u_{N,n}^{k}(\xi)(\varphi_n, \varphi_m)_{L^2(\Omega)} = 0, \qquad\qquad\qquad k = 0.$$

The following matrices and vectors are defined,

$$M_N := \big((\varphi_n, \varphi_m)_{L^2(\Omega)}\big)_{m,n=1}^{N} \in \mathbb{R}^{N \times N},$$
$$A_N(\xi) := (a(\varphi_n, \varphi_m; \xi))_{m,n=1}^{N} \in \mathbb{R}^{N \times N},$$
$$\underline{b}_N(\xi) := (b(\varphi_m; \xi))_{m=1}^{N} \in \mathbb{R}^{N}.$$

Then, the solution vectors $\underline{u}_N^k(\xi) = (u_{N,n}^k(\xi))_{n=1}^{N}$, $k = 0, \ldots, K$, can be computed from the N-dimensional systems of linear algebraic equations

$$(M_N + \Delta t\, A_N(\xi))\, \underline{u}_N^k(\xi) = \Delta t\, \underline{b}_N(\xi) + M_N \underline{u}_h^{k-1}(\xi), \ k = 1, \ldots, K, \qquad (3.18\text{a})$$
$$M_N \underline{u}_N^k(\xi) = 0, \qquad\qquad\qquad k = 0, \qquad (3.18\text{b})$$

which determines (3.3).

The reduced dual problem tested for all basis functions $v = \zeta_m \in \tilde{X}_{\tilde{N}}$, $m = 1, \ldots, \tilde{N}$, yield

$$\sum_{n=1}^{\tilde{N}} \psi_{\tilde{N},n}^{k}(\xi) \Big[(\zeta_m, \zeta_n)_{L^2(\Omega)} + \Delta t\, a(\zeta_m, \zeta_n; \xi) \Big]$$

$$= \sum_{n=1}^{\tilde{N}} \psi_{\tilde{N},n}^{k+1}(\xi)(\zeta_m, \zeta_n)_{L^2(\Omega)}, \ k = 0, \ldots, K-1,$$

$$\sum_{n=1}^{\tilde{N}} \psi_{\tilde{N},n}^{k}(\xi)(\zeta_m, \zeta_n)_{L^2(\Omega)} = l(\zeta_m; \xi), \qquad\qquad k = K.$$

The following matrices and vectors are defined

$$M_{\tilde{N}} := \big((\zeta_n, \zeta_m)_{L^2(\Omega)}\big)_{m,n=1}^{N} \in \mathbb{R}^{\tilde{N} \times \tilde{N}},$$
$$A_{\tilde{N}}(\xi) := (a(\zeta_n, \zeta_m; \xi))_{m,n=1}^{N} \in \mathbb{R}^{\tilde{N} \times \tilde{N}},$$
$$\underline{l}_{\tilde{N}}(\xi) := (l(\zeta_m; \xi))_{m=1}^{\tilde{N}} \in \mathbb{R}^{\tilde{N}}.$$

Then, the solution vectors $\underline{\psi}_{\tilde{N}}^k(\xi) = (\psi_{\tilde{N},n}^k(\xi))_{n=1}^{\tilde{N}}$, $k = 0, \ldots, K$, can be computed from the $\tilde{N}$-dimensional systems of linear algebraic equations

$$\big(M_{\tilde{N}} + \Delta t\, A_{\tilde{N}}(\xi)^T\big)\, \underline{\psi}_{\tilde{N}}^k(\xi) = M_{\tilde{N}} \underline{\psi}_{\tilde{N}}^{k+1}(\xi), \ k = 0, \ldots, K-1, \qquad (3.20\text{a})$$
$$M_{\tilde{N}} \underline{\psi}_{\tilde{N}}^k(\xi) = \underline{l}_{\tilde{N}}(\xi), \qquad k = K, \qquad (3.20\text{b})$$

which determines (3.4). If Assumption 2.9 is fulfilled, the stiffness matrix in (3.20a) is symmetric, i.e. $A_{\tilde{N}}(\xi) = A_{\tilde{N}}(\xi)^T$.

The reduced output (3.16) is evaluated by

$$
\begin{aligned}
s_{N,\tilde{N}}(\xi) &= \sum_{n=1}^{N} u_{N,n}^{K}(\xi) l(\varphi_n; \xi) + \Delta t \sum_{k=1}^{K} \sum_{m=1}^{\tilde{N}} \psi_{\tilde{N},m}^{k-1}(\xi) r_N^k(\zeta_m; \xi) \\
&\stackrel{(3.5)}{=} \sum_{n=1}^{N} u_{N,n}^{K}(\xi) l(\varphi_n; \xi) + \Delta t \sum_{k=1}^{K} \sum_{m=1}^{\tilde{N}} \psi_{\tilde{N},m}^{k-1}(\xi) \Big[b(\zeta_m; \xi) \\
&\quad - \frac{1}{\Delta t} \sum_{n=1}^{N} \left(u_{N,n}^{k}(\xi) - u_{N,n}^{k-1}(\xi) \right) (\varphi_n, \zeta_m)_{L^2(\Omega)} \\
&\quad - \sum_{n=1}^{N} u_{N,n}^{k}(\xi) a(\varphi_n, \zeta_m; \xi) \Big].
\end{aligned}
\tag{3.21}
$$

The following matrices and vectors are defined

$$
\begin{aligned}
\underline{l}_N(\xi) &:= (l(\varphi_n; \xi))_{n=1}^{N} &&\in \mathbb{R}^N, \\
\underline{b}_{\tilde{N}}(\xi) &:= (b(\zeta_m; \xi))_{m=1}^{\tilde{N}} &&\in \mathbb{R}^{\tilde{N}}, \\
M_{N,\tilde{N}} &:= \left((\varphi_n, \zeta_m)_{L^2(\Omega)} \right)_{m,n=1}^{\tilde{N},N} &&\in \mathbb{R}^{\tilde{N} \times N}, \\
A_{N,\tilde{N}}(\xi) &:= (a(\varphi_n, \zeta_m; \xi))_{m,n=1}^{\tilde{N},N} &&\in \mathbb{R}^{\tilde{N} \times N}.
\end{aligned}
$$

Utilizing the solution vectors of the reduced primal problem (3.18) and the reduced dual problem (3.20), the reduced output in (3.21) is approximated by

$$
\begin{aligned}
\underline{l}_N(\xi)^T \underline{u}_N^K(\xi) + \Delta t \sum_{k=1}^{K} \Big[&\underline{b}_{\tilde{N}}(\xi)^T \underline{\psi}_{\tilde{N}}^{k-1}(\xi) \\
&- \frac{1}{\Delta t} \left(\underline{\psi}_{\tilde{N}}^{k-1}(\xi) \right)^T M_{N,\tilde{N}} \left(\underline{u}_N^k(\xi) - \underline{u}_N^{k-1}(\xi) \right) \\
&- \left(\underline{\psi}_{\tilde{N}}^{k-1}(\xi) \right)^T A_{N,\tilde{N}}(\xi) \underline{u}_N^k(\xi) \Big].
\end{aligned}
$$

Definition 3.10 (Gramian matrix). The matrix induced by the inner product is defined as

$$
H := ((\phi_i, \phi_j)_X)_{j,i=1}^{\mathcal{N}} \in \mathbb{R}^{\mathcal{N} \times \mathcal{N}}.
\tag{3.22}
$$

In the following, the discrete reduced spaces are introduced.

Definition 3.11 (discrete primal reduced basis space). Let $\varphi_n = \sum_{i=1}^{\mathcal{N}} \varphi_{n,i} \phi_i \in X_h$, $n = 1, \ldots, N$, be the orthonormal basis functions w.r.t. $\|\cdot\|_X$, which span the reduced space $X_N = \operatorname{span}\{\varphi_1, \ldots, \varphi_N\}$. Then the discrete orthonormal reduced basis space V_N is defined by

$$
V_N := (\varphi_{n,i})_{i,n=1}^{\mathcal{N},N} = \left(\underline{\varphi}_1, \ldots, \underline{\varphi}_N \right) \in \mathbb{R}^{\mathcal{N} \times N}, \quad \underline{\varphi}_n^T H \underline{\varphi}_m = \delta_{nm},
\tag{3.23}
$$

where the inner product matrix is determined by (3.22).

Definition 3.12 (discrete dual reduced basis space). Let $\zeta_n = \sum_{i=1}^{\mathcal{N}} \zeta_{n,i}\phi_i \in X_h$, $n = 1, \ldots, \tilde{N}$, be the orthonormal basis functions w.r.t. $\|\cdot\|_X$ which span the reduced space $\tilde{X}_{\tilde{N}} = \text{span}\{\zeta_1, \ldots, \zeta_{\tilde{N}}\}$. Then the discrete orthonormal reduced basis space $\tilde{V}_{\tilde{N}}$ for the dual problem is defined by

$$\tilde{V}_{\tilde{N}} := (\zeta_{n,i})_{i,n=1}^{\mathcal{N},\tilde{N}} = \left(\underline{\zeta}_1, \ldots, \underline{\zeta}_N\right) \in \mathbb{R}^{\mathcal{N} \times \tilde{N}}, \quad \underline{\zeta}_n^T H \underline{\zeta}_m = \delta_{nm}. \qquad (3.24)$$

Remark 3.13. It may occur that the discrete primal reduced basis space V_N and the discrete dual reduced basis space $\tilde{V}_{\tilde{N}}$ contain basis functions which are almost linearly dependent of each other. Hence, the condition number of the reduced matrices becomes large and possibly yields numerical instabilities. In order to obtain algebraic stability, the primal reduced basis V_N and the dual reduced spaces $\tilde{V}_{\tilde{N}}$ are orthonormalized w.r.t. to the discrete inner product induced by the Hilbert space X. An orthonormalization can be achieved by a Gram–Schmidt process (Quarteroni et al., 2007, section 3.4.3), for instance.

The discrete reduced basis space projects a reduced solution onto the high dimensional space, which approximates the discrete high dimensional solution

$$V_N \underline{u}_N^k(\xi) \approx \underline{u}_h^k(\xi) \in \mathbb{R}^{\mathcal{N}}, \quad k = 0, \ldots, K,$$
$$\tilde{V}_{\tilde{N}} \underline{\psi}_{\tilde{N}}^k(\xi) \approx \underline{\psi}_h^k(\xi) \in \mathbb{R}^{\mathcal{N}}, \quad k = 0, \ldots, K.$$

The discrete reduced matrices and reduced vectors can be expressed as

$$\begin{aligned}
M_N &= V_N^T M V_N &&\in \mathbb{R}^{N \times N}, \\
A_N(\xi) &= V_N^T A(\xi) V_N &&\in \mathbb{R}^{N \times N}, \\
\underline{b}_N(\xi) &= V_N^T \underline{b}(\xi) &&\in \mathbb{R}^{N}, \\
\underline{l}_N(\xi) &= V_N^T \underline{l}(\xi) &&\in \mathbb{R}^{N}.
\end{aligned}$$

It is desired that the high dimensional quantities can be efficiently computed for different parameter values. Therefore, it needs to be possible to separate the parameter dependence from the space dependence. This is achieved by Assumption 3.9. With this assumption, the high dimensional matrix and the high dimensional vectors defined in (2.24)–(2.26) are determined by

$$A(\xi) = \sum_{q=1}^{Q_a} \theta_q^a(\xi) A_q, \quad A_q := (a_q(\phi_i, \phi_j))_{j,i=1}^{\mathcal{N}} \in \mathbb{R}^{\mathcal{N} \times \mathcal{N}}, \qquad (3.25)$$

$$\underline{b}(\xi) = \sum_{q=1}^{Q_b} \theta_q^b(\xi) \underline{b}_q, \quad \underline{b}_q := (b_q(\phi_j))_{j=1}^{\mathcal{N}} \qquad \in \mathbb{R}^{\mathcal{N}}, \qquad (3.26)$$

$$\underline{l}(\xi) = \sum_{q=1}^{Q_l} \theta_q^l(\xi) \underline{l}_q, \quad \underline{l}_q := (l_q(\phi_j))_{j=1}^{\mathcal{N}} \qquad \in \mathbb{R}^{\mathcal{N}}. \qquad (3.27)$$

Thus, the parameter dependent quantities are computed by a linear combination of parameter independent, precomputed matrices $\{A_q\}_{q=1}^{Q_a}$ and vectors $\{\underline{b}_q\}_{q=1}^{Q_b}$, $\{\underline{l}_q\}_{q=1}^{Q_l}$.

The parameter separated computation also applies for the parameter dependent reduced quantities, such that

$$A_N(\xi) = \sum_{q=1}^{Q_a} \theta_q^a(\xi) A_{N,q}, \quad A_{N,q} := (a_q(\varphi_n, \varphi_m))_{m,n=1}^N = V_N^T A_q V_N \in \mathbb{R}^{N \times N},$$

$$\underline{b}_N(\xi) = \sum_{q=1}^{Q_b} \theta_q^b(\xi) \underline{b}_{N,q}, \quad \underline{b}_{N,q} := (b_q(\varphi_m))_{m=1}^N \qquad = V_N^T \underline{b}_q \qquad \in \mathbb{R}^N,$$

$$\underline{l}_N(\xi) = \sum_{q=1}^{Q_l} \theta_q^l(\xi) \underline{l}_{N,q}, \quad \underline{l}_{N,q} := (l_q(\varphi_m))_{m=1}^N \qquad = V_N^T \underline{l}_q \qquad \in \mathbb{R}^N.$$

Here, $\{A_{N,q}\}_{q=1}^{Q_a}$, $\{\underline{b}_{N,q}\}_{q=1}^{Q_b}$, $\{\underline{l}_{N,q}\}_{q=1}^{Q_l}$ are precomputed quantities.

3.2 Error estimation

The objective in this section is the a posteriori error estimation in order to assess the accuracy of the reduced models. This work utilizes the error estimators for the primal solution, the dual solution and the output from Grepl and Patera (2005). In an RB-context the error is measured with respect to a high-fidelity discretization. The detailed discretization can be arbitrarily accurate, hence the error between the exact solution and the detailed solution is neglected $\|u - u_h\| \approx 0$, such that

$$\|u - u_N\| \leq \|u - u_h\| + \|u_h - u_N\| \approx \|u_h - u_N\|.$$

In consequence and due to the linearity of the output functional, the same holds for the output

$$|s - s_{N,\tilde{N}}| \leq |s - s_h| + |s_h - s_{N,\tilde{N}}| = |l(u - u_h)| + |s_h - s_{N,\tilde{N}}| \approx |s_h - s_{N,\tilde{N}}|.$$

Reduced basis error estimation is related to a priori residual based error analysis, meaning the error estimates depend on the unknown solution u. In the framework of RBM, the reduced quantities u_N and $s_{N,\tilde{N}}$ approximate the detailed quantities u_h and s_h, which are computable quantities. Hence, the a priori analysis converts to a posteriori error estimation. The error bounds for the solution error and the output error are rigorous, meaning they are provable upper bounds over the parameter domain. By Assumption 3.9, an offline-online decomposition allows to evaluate the error bounds computationally inexpensive, compared to the exact error computation $\|u_h - u_N\|$ and $|s_h - s_{N,\tilde{N}}|$. These error bounds are used as an optimality criterion in order to build up the reduced space. It is shown that the error bounds can be extended to a time continuous framework. The computation of the error bounds is based on the dual norm of the residuals and the coercivity constant. The following error estimators do not require symmetry of the bilinear form $a(\cdot, \cdot; \xi)$.

3.2.1 Non-weighted error estimators

In this section, non-weighted error estimators are stated, which are rigorous upper bounds for the primal solution error, the dual solution error and the output

error for any parameter in the parameter domain. The results for the error bounds are taken from (Grepl and Patera, 2005, section 4.1). Here, however, the parameter ξ is interpreted as a stochastic quantity.

The solution errors of the primal problem and the dual problem are estimated in parameter-dependent energy norms.

Definition 3.14 (parameter-dependent energy norm)**.** The primal parameter-dependent energy norm and the dual parameter-dependent energy norm are defined by

$$\|v\|_{\xi}^{\mathrm{pr}} := \left(\left\| v^K \right\|_{L^2(\Omega)}^2 + \Delta t \sum_{k=1}^{K} a(v^k, v^k; \xi) \right)^{1/2}, \quad \forall v \in X_h^K, \qquad (3.28)$$

$$\|v\|_{\xi}^{\mathrm{du}} := \left(\left\| v^0 \right\|_{L^2(\Omega)}^2 + \Delta t \sum_{k=0}^{K-1} a(v^k, v^k; \xi) \right)^{1/2}, \quad \forall v \in X_h^K. \qquad (3.29)$$

Remark 3.15. The parameter dependence of the norms (3.28) and (3.29) is induced by the parameter dependent bilinear form $a(\cdot, \cdot; \xi)$. Even though error bounds can be derived for parameter independent norms, cf. (Haasdonk, 2017, Proposition 2.80) or appendix A.5, the choice of these parameter dependent norms yield better constants for the error bounds in the following.

Proposition 3.16 (primal solution error estimator)**.** Let $\xi \in \Gamma$. Then the error for the primal solution $e_N(\xi) = u_h(\xi) - u_N(\xi) \in X_h^K$ can be estimated by

$$\|e_N(\xi)\|_{\xi}^{\mathrm{pr}} \le \Delta_N^u(\xi) := \left(\sum_{k=0}^{K} \Delta_N^{u,k}(\xi) \right)^{1/2},$$

$$\text{with } \Delta_N^{u,k}(\xi) := \begin{cases} 0, & k = 0, \\ \frac{\Delta t}{\alpha(\xi)} \left\| r_N^k(\cdot; \xi) \right\|_{X'}^2, & k = 1, \dots, K. \end{cases} \qquad (3.30)$$

The error is measured in the primal parameter-dependent energy norm (3.28). The coercivity constant $\alpha(\xi)$ is determined by (2.8) and the primal residual $r_N^k(\cdot; \xi)$ is defined in (3.5) and (3.6).

Proof. For the sake of notational convenience, the primal solution error (3.9) is written without the parameter dependence, i.e. $e_N^k(\xi) = e_N^k$. Multiplying the identity (3.12) for $v = e_N^k$ with Δt and estimating the residual with (2.5) gives

$$(e_N^k - e_N^{k-1}, e_N^k)_{L^2(\Omega)} + \Delta t\, a(e_N^k, e_N^k; \xi) = \Delta t\, r_N^k(e_N^k; \xi)$$
$$\le \Delta t \left\| r_N^k(\cdot; \xi) \right\|_{X'} \left\| e_N^k \right\|_X. \qquad (3.31)$$

Using the Cauchy–Schwarz inequality, Young's inequality $ab \le \frac{1}{2}\left(\frac{1}{c^2}a^2 + c^2 b^2 \right)$, $a, b \in \mathbb{R}$, $c \in \mathbb{R} \setminus \{0\}$, and (2.8) yields

$$(e_N^{k-1}, e_N^k)_{L^2(\Omega)} \le \left\| e_N^{k-1} \right\|_{L^2(\Omega)} \left\| e_N^k \right\|_{L^2(\Omega)}$$
$$\le \frac{1}{2} \left(\left\| e_N^{k-1} \right\|_{L^2(\Omega)}^2 + \left\| e_N^k \right\|_{L^2(\Omega)}^2 \right)$$

and

$$\left\| r_N^k(\cdot;\xi) \right\|_{X'} \left\| e_N^k \right\|_X \leq \frac{1}{2\alpha(\xi)} \left\| r_N^k(\cdot;\xi) \right\|_{X'}^2 + \frac{\alpha}{2} \left\| e_N^k \right\|_X^2$$

$$\leq \frac{1}{2\alpha(\xi)} \left\| r_N^k(\cdot;\xi) \right\|_{X'}^2 + \frac{1}{2} a(e_N^k, e_N^k;\xi).$$

Thus, (3.31) can be estimated by

$$\frac{1}{2} \left(\left\| e_N^k \right\|_{L^2(\Omega)}^2 - \left\| e_N^{k-1} \right\|_{L^2(\Omega)}^2 \right) + \Delta t\, a(e_N^k, e_N^k;\xi)$$

$$\leq \frac{\Delta t}{2\alpha(\xi)} \left\| r_N^k(\cdot;\xi) \right\|_{X'}^2 + \frac{\Delta t}{2} a(e_N^k, e_N^k;\xi).$$

Then, subtracting the bilinear form from the right hand side and multiplying the inequality by the factor 2 yields

$$\left\| e_N^k \right\|_{L^2(\Omega)}^2 - \left\| e_N^{k-1} \right\|_{L^2(\Omega)}^2 + \Delta t\, a(e_N^k, e_N^k;\xi) \leq \frac{\Delta t}{\alpha(\xi)} \left\| r_N^k(\cdot;\xi) \right\|_{X'}^2.$$

Summing up the inequality for $k = 1, \dots, K$ and utilizing (3.11), it results

$$\left\| e_N^K \right\|_{L^2(\Omega)}^2 + \Delta t \sum_{k=1}^K a(e_N^k, e_N^k;\xi) \leq \sum_{k=1}^K \frac{\Delta t}{\alpha(\xi)} \left\| r_N^k(\cdot;\xi) \right\|_{X'}^2 = \sum_{k=1}^K \Delta_N^{u,k}(\xi).$$

Since $\Delta_N^{u,0}$ is zero, the sum can be extended for $k = 0$, which finishes the proof. $\qquad\square$

Remark 3.17. The fact that $\Delta_N^{u,0}=0$ is based on the homogeneous initial condition of the primal problem.

Proposition 3.18 (dual solution error estimator). Let $\xi \in \Gamma$. Then the error for the dual solution $\tilde{e}_{\tilde{N}}(\xi) = \psi_h(\xi) - \psi_{\tilde{N}}(\xi) \in X_h^K$ can be estimated by

$$\left\|\| \tilde{e}_{\tilde{N}}(\xi) \|\right\|_{\xi}^{\mathrm{du}} \leq \Delta_{\tilde{N}}^{\psi}(\xi) := \left(\sum_{k=0}^K \Delta_{\tilde{N}}^{\psi,k}(\xi) \right)^{1/2}$$

$$\text{with } \Delta_{\tilde{N}}^{\psi,k}(\xi) := \begin{cases} \frac{\Delta t}{\alpha(\xi)} \left\| \tilde{r}_{\tilde{N}}^k(\cdot;\xi) \right\|_{X'}^2, & k = 0, \dots, K-1 \\ \sup_{v \in X_h} \left(\frac{|\tilde{r}_{\tilde{N}}^K(v;\xi)|}{\|v\|_{L^2(\Omega)}} \right)^2, & k = K. \end{cases} \tag{3.32}$$

The error is measured in the dual parameter-dependent energy norm (3.29). The coercivity constant $\alpha(\xi)$ is determined by (2.8) and the dual residual is defined in (3.7) and (3.8).

Proof. The proof is similar to the derivation of the primal solution error estimator. Once more, for the sake of notational convenience, the dual solution error (3.10) is written without the parameter dependence, i.e. $\tilde{e}_{\tilde{N}}^k(\xi) = \tilde{e}_{\tilde{N}}^k$. Multiplying the identity (3.14) for $v = \tilde{e}_{\tilde{N}}^k$ with Δt and estimating the residual with (2.5) gives

$$(\tilde{e}_{\tilde{N}}^k - \tilde{e}_{\tilde{N}}^{k+1}, \tilde{e}_{\tilde{N}}^k)_{L^2(\Omega)} + \Delta t\, a(\tilde{e}_{\tilde{N}}^k, \tilde{e}_{\tilde{N}}^k;\xi) = \Delta t\, \tilde{r}_{\tilde{N}}^k(\tilde{e}_{\tilde{N}}^k;\xi)$$

$$\leq \Delta t \left\| \tilde{r}_{\tilde{N}}^k(\cdot;\xi) \right\|_{X'} \left\| \tilde{e}_{\tilde{N}}^k \right\|_X. \tag{3.33}$$

Using the Cauchy–Schwarz inequality, Young's inequality $ab \leq \frac{1}{2}\left(\frac{1}{c^2}a^2 + c^2b^2\right)$, $a, b \in \mathbb{R}$, $c \in \mathbb{R} \setminus \{0\}$, and (2.8) yields

$$(\tilde{e}_{\tilde{N}}^{k+1}, \tilde{e}_{\tilde{N}}^{k})_{L^2(\Omega)} \leq \left\|\tilde{e}_{\tilde{N}}^{k+1}\right\|_{L^2(\Omega)} \left\|\tilde{e}_{\tilde{N}}^{k}\right\|_{L^2(\Omega)}$$

$$\leq \frac{1}{2}\left(\left\|\tilde{e}_{\tilde{N}}^{k+1}\right\|_{L^2(\Omega)}^2 + \left\|\tilde{e}_{\tilde{N}}^{k}\right\|_{L^2(\Omega)}^2\right)$$

and

$$\left\|\tilde{r}_{\tilde{N}}^{k}(\cdot;\xi)\right\|_{X'}\left\|\tilde{e}_{\tilde{N}}^{k}\right\|_{X} \leq \frac{1}{2\alpha(\xi)}\left\|\tilde{r}_{\tilde{N}}^{k}(\cdot;\xi)\right\|_{X'}^2 + \frac{\alpha}{2}\left\|\tilde{e}_{\tilde{N}}^{k}\right\|_{X}^2$$

$$\leq \frac{1}{2\alpha(\xi)}\left\|\tilde{r}_{\tilde{N}}^{k}(\cdot;\xi)\right\|_{X'}^2 + \frac{1}{2}a(\tilde{e}_{\tilde{N}}^{k}, \tilde{e}_{\tilde{N}}^{k};\xi).$$

Thus, (3.33) can be estimated by

$$\frac{1}{2}\left(\left\|\tilde{e}_{\tilde{N}}^{k}\right\|_{L^2(\Omega)}^2 - \left\|\tilde{e}_{\tilde{N}}^{k+1}\right\|_{L^2(\Omega)}^2\right) + \Delta t\, a(\tilde{e}_{\tilde{N}}^{k}, \tilde{e}_{\tilde{N}}^{k};\xi)$$

$$\leq \frac{\Delta t}{2\alpha(\xi)}\left\|\tilde{r}_{\tilde{N}}^{k}(\cdot;\xi)\right\|_{X'}^2 + \frac{\Delta t}{2}a(\tilde{e}_{\tilde{N}}^{k}, \tilde{e}_{\tilde{N}}^{k};\xi).$$

Then, subtracting the bilinear form on the right hand side and multiplying by the factor 2 yields

$$\left\|\tilde{e}_{\tilde{N}}^{k}\right\|_{L^2(\Omega)}^2 - \left\|\tilde{e}_{\tilde{N}}^{k+1}\right\|_{L^2(\Omega)}^2 + \Delta t\, a(\tilde{e}_{\tilde{N}}^{k}, \tilde{e}_{\tilde{N}}^{k};\xi) \leq \frac{\Delta t}{\alpha(\xi)}\left\|\tilde{r}_{\tilde{N}}^{k}(\cdot;\xi)\right\|_{X'}^2.$$

Summing the inequality up for $k = 0, \ldots, K-1$, it results

$$\left\|\tilde{e}_{\tilde{N}}^{0}\right\|_{L^2(\Omega)}^2 - \left\|\tilde{e}_{\tilde{N}}^{K}\right\|_{L^2(\Omega)}^2 + \Delta t \sum_{k=0}^{K-1} a(\tilde{e}_{\tilde{N}}^{k}, \tilde{e}_{\tilde{N}}^{k};\xi) \leq \sum_{k=0}^{K-1} \frac{\Delta t}{\alpha(\xi)}\left\|\tilde{r}_{\tilde{N}}^{k}(\cdot;\xi)\right\|_{X'}^2 = \sum_{k=0}^{K-1} \Delta_{\tilde{N}}^{\psi,k}(\xi).$$

The following inequality remains to be shown

$$\left\|\tilde{e}_{\tilde{N}}^{K}\right\|_{L^2(\Omega)}^2 \leq \sup_{v \in X_h}\left(\frac{|\tilde{r}_{\tilde{N}}^{K}(v;\xi)|}{\|v\|_{L^2(\Omega)}}\right)^2 = \Delta_{\tilde{N}}^{\psi,K}(\xi).$$

Therefore, using (3.15) gives

$$\left\|\tilde{e}_{\tilde{N}}^{K}\right\|_{L^2(\Omega)}^2 = (\tilde{e}_{\tilde{N}}^{K}, \tilde{e}_{\tilde{N}}^{K})_{L^2(\Omega)} = \tilde{r}_{\tilde{N}}^{K}(\tilde{e}_{\tilde{N}}^{K};\xi)$$

and hence

$$\left\|\tilde{e}_{\tilde{N}}^{K}\right\|_{L^2(\Omega)} = \frac{\tilde{r}_{\tilde{N}}^{K}(\tilde{e}_{\tilde{N}}^{K};\xi)}{\left\|\tilde{e}_{\tilde{N}}^{K}\right\|_{L^2(\Omega)}} \leq \sup_{v \in X_h}\frac{|\tilde{r}_{\tilde{N}}^{K}(v;\xi)|}{\|v\|_{L^2(\Omega)}},$$

which verifies the statement (3.32). $\qquad\square$

Remark 3.19. If the output functional is parameter independent, meaning $l(\cdot;\xi) \equiv l(\cdot)$, and the reduced space for the dual problem contains $\psi_h^K \in \tilde{X}_{\tilde{N}}$, then the error estimator of the final condition is zero, i.e. $\Delta_{\tilde{N}}^{\psi,K} = 0$.

The error bounds (3.30) and (3.32) use the coercivity constant $\alpha(\xi)$ of (2.8). If the constant cannot be determined analytically, it can be approximated by a successive constraint method (SCM), see Huynh et al. (2007), for instance.

Proposition 3.20 (output error estimator)**.** Let $\xi \in \Gamma$. Then the error for the output can be estimated by

$$|s_h(\xi) - s_{N,\tilde{N}}(\xi)| \leq \Delta^s_{N,\tilde{N}}(\xi) := \Delta^u_N(\xi)\Delta^{\psi}_{\tilde{N}}(\xi). \tag{3.34}$$

The detailed output and the reduced output are determined by

$$s_h(\xi) = l(u^K_h(\xi); \xi),$$

$$s_{N,\tilde{N}}(\xi) = l(u^K_N(\xi); \xi) + \Delta t \sum_{k=1}^{K} r^k_N(\psi^{k-1}_{\tilde{N}}(\xi); \xi),$$

and the estimators Δ^u_N and $\Delta^{\psi}_{\tilde{N}}$ are stated in (3.30) and (3.32), respectively.

Proof. For the sake of notational convenience, the primal solution error (3.9) and dual solution error (3.10) is written without the parameter dependence, i.e. $e^k_N(\xi) = e^k_N$ and $\tilde{e}^k_{\tilde{N}}(\xi) = \tilde{e}^k_{\tilde{N}}$. From (2.41), it follows that

$$\Delta t \sum_{k=1}^{K} r^k_N(\psi^{k-1}_h(\xi); \xi) = l(e^K_N; \xi). \tag{3.35}$$

Utilizing (3.35), estimating the primal residual with (2.5) and using Cauchy-Schwarz inequality, the output error can be estimated by

$$
\begin{aligned}
|s_h(\xi) - s_{N,\tilde{N}}(\xi)| &= |\Delta t \sum_{k=1}^{K} r^k_N(\tilde{e}^{k-1}_{\tilde{N}}; \xi)| \\
&\leq \Delta t \sum_{k=1}^{K} \left\| r^k_N(\cdot; \xi) \right\|_{X'} \left\| \tilde{e}^{k-1}_{\tilde{N}} \right\|_X \\
&\leq \left(\sum_{k=1}^{K} \frac{\Delta t}{\alpha(\xi)} \left\| r^k_N(\cdot; \xi) \right\|^2_{X'} \right)^{1/2} \left(\sum_{k=1}^{K} \Delta t\, \alpha(\xi) \left\| \tilde{e}^{k-1}_{\tilde{N}} \right\|^2_X \right)^{1/2} \\
&\leq \left(\sum_{k=0}^{K} \frac{\Delta t}{\alpha(\xi)} \left\| r^k_N(\cdot; \xi) \right\|^2_{X'} \right)^{1/2} \left(\sum_{k=1}^{K} \Delta t\, a(\tilde{e}^{k-1}_{\tilde{N}}, \tilde{e}^{k-1}_{\tilde{N}}; \xi) \right)^{1/2},
\end{aligned}
$$

where the last estimate uses (3.13) and (2.8). The first term in the last inequality already coincides with the primal error estimator in Proposition 3.16. The second term in the inequality can be expanded by the L^2-norm of the dual solution error at the initial point in time, such that

$$\left(\sum_{k=0}^{K-1} \Delta t\, a(\tilde{e}^k_{\tilde{N}}, \tilde{e}^k_{\tilde{N}}; \xi) \right)^{1/2} \leq \left(\left\| \tilde{e}^0_{\tilde{N}} \right\|^2_{L^2(\Omega)} + \sum_{k=0}^{K-1} \Delta t\, a(\tilde{e}^k_{\tilde{N}}, \tilde{e}^k_{\tilde{N}}; \xi) \right)^{1/2}.$$

By Proposition 3.18, the right hand side of the inequality can be further estimated by $\Delta^{\psi}_{\tilde{N}}(\xi)$, hence the statement (3.34) follows. $\qquad\square$

Remark 3.21 (uncorrected output error estimation)**.** The fact that the output error estimator is composed of the primal error estimator and the dual error estimator is due to the expansion by the "correction term" in the reduced output (3.16). If the correction for the output computation is omitted, i.e. $s_{N,\tilde{N}}(\xi) = l(u_N^K(\xi); \xi)$, then the following error bound can be stated

$$|s_h(\xi) - s_{N,\tilde{N}}(\xi)| = |l(u_h^K(\xi) - u_N^K(\xi); \xi)| \overset{(2.5)}{\leq} \|l(\cdot; \xi)\|_{X'} \left\|u_h^K(\xi) - u_N^K(\xi)\right\|_X.$$

This inequality yields no benefit because of two aspects. First, once the solution error $\left\|u_h^K(\xi) - u_N^K(\xi)\right\|_X$ is known for the upper bound, there are no extra computational cost to compute the exact output error. This means that this inequality yields no advantage regarding the exact error computation. Second, the error bound (3.34) tends to zero in a quadratic way, since Δ_N^u and $\Delta_{\tilde{N}}^\psi$ tend to zero for increasing N and $\tilde{N}$, respectively. Whereas for the error bound above only the error $\left\|u_h^K(\xi) - u_N^K(\xi)\right\|_X$ tends to zero for increasing N and the dual norm $\|l(\cdot; \xi)\|_{X'}$ is a constant. Hence, the last error bound has a lower error convergence rate compared to (3.34). The same effect has observed in section 2.3, where the uncorrected output error convergence (2.29) and the corrected output error convergence (2.40) for the infinite dimensional framework were compared.

Remark 3.22. The error estimators can be derived for the time continuous case as well. Then, the primal solution error $e_N(t; \xi) = u_h(t; \xi) - u_N(t; \xi) \in X_h$ and the dual solution error $\tilde{e}_{\tilde{N}}(t; \xi) = \psi_h(t; \xi) - \psi_{\tilde{N}}(t; \xi) \in X_h$ can be estimated by

$$\left(\|e_N(T; \xi)\|_{L^2(\Omega)}^2 + \int_0^T a(e_N(t; \xi), e_N(t; \xi); \xi) \mathrm{d}t \right)^{1/2} \leq \Delta_N^{u,[0,T]},$$

$$\left(\|\tilde{e}_{\tilde{N}}(0; \xi)\|_{L^2(\Omega)}^2 + \int_0^T a(\tilde{e}_{\tilde{N}}(t; \xi), \tilde{e}_{\tilde{N}}(t; \xi); \xi) \mathrm{d}t \right)^{1/2} \leq \Delta_{\tilde{N}}^{\psi,[0,T]},$$

where the error estimators are defined as

$$\Delta_N^{u,[0,T]} := \left(\frac{1}{\alpha(\xi)} \int_0^T \|r_N(\cdot; \xi)\|_{X'}^2 \, \mathrm{d}t, \right)^{1/2} \tag{3.36}$$

$$\Delta_{\tilde{N}}^{\psi,[0,T]} := \left(\frac{1}{\alpha(\xi)} \int_0^T \|\tilde{r}_{\tilde{N}}(\cdot; \xi)\|_{X'}^2 \, \mathrm{d}t + \left(\Delta_{\tilde{N}}^{\psi,T}\right)^2 \right)^{1/2}, \tag{3.37}$$

and $\Delta_{\tilde{N}}^{\psi,T} := \sup_{v \in X_h} \frac{|\tilde{r}_{\tilde{N}}^T(v; \xi)|}{\|v\|_{L^2(\Omega)}}$. The proof is similar to the time discretized case, cf. Propositions 3.16 and 3.18. For details see appendices A.6.1 and A.6.2. It is observed that the sum over all time steps in (3.30) and (3.32) is replaced by the integration over the time interval $[0, T]$. The output for the time continuous case is determined by

$$s_h(\xi) = l(u_h(T; \xi); \xi),$$

$$s_{N,\tilde{N}}(\xi) = l(u_N(T; \xi); \xi) + \int_0^T r_N(\psi_{\tilde{N}}(t; \xi); \xi) \mathrm{d}t.$$

The primal and dual solution error estimators (3.36) and (3.37) determine the output error estimator

$$|s_h(\xi) - s_{N,\tilde{N}}(\xi)| \le \Delta_{N,\tilde{N}}^{s,[0,T]} := \Delta_N^{u,[0,T]} \Delta_{\tilde{N}}^{\psi,[0,T]}.$$

The proof can be found in appendix A.6.3.

This section allows us to evaluate computationally inexpensive error bounds for the computationally expensive primal solution error, dual solution error and output error.

3.2.2   Weighted error estimators

In the case of random input parameters, each parameter configuration occurs with a certain probability, hence statistical quantities are of interest. The thesis studies the approximation of the expectation. Other statistical quantities like the variance or higher moments were studied in (Haasdonk et al., 2013, section 4) for example.

For the statistical computations, the probability density function (pdf) $\rho(\cdot)$ appears. Using the results from Grepl and Patera (2005), see section 3.2.1, the expectation of the squared solution error can be further estimated by

$$\mathbb{E}\left[(\|\|u_h - u_N\|\|_\xi^{\mathrm{pr}})^2\right] = \int_\Gamma (\|\|u_h(\xi) - u_N(\xi)\|\|_\xi^{\mathrm{pr}})^2 \rho(\xi)\mathrm{d}\xi \overset{(3.30)}{\le} \int_\Gamma (\Delta_N^u(\xi))^2 \rho(\xi)\mathrm{d}\xi,$$

just as the expectation of the absolute output error

$$\mathbb{E}[|s_h - s_{N,\tilde{N}}|] = \int_\Gamma |s_h(\xi) - s_{N,\tilde{N}}(\xi)|\rho(\xi)\mathrm{d}\xi \overset{(3.34)}{\le} \int_\Gamma \Delta_{N,\tilde{N}}^s(\xi)\rho(\xi)\mathrm{d}\xi.$$

In the following, weighted error estimators are defined. They were introduced in Chen et al. (2013) for elliptic problems.

Definition 3.23 (weighted error estimators). Let $\rho \colon \mathbb{R} \to \mathbb{R}^+$. Then the weighted primal solution error estimator and the weighted output solution error estimator are defined as

$$\Delta_N^{u,\rho}(\xi) := \Delta_N^u(\xi)\sqrt{\rho(\xi)}, \quad \forall \xi \in \Gamma, \tag{3.38}$$

$$\Delta_{N,\tilde{N}}^{s,\rho}(\xi) := \Delta_{N,\tilde{N}}^s(\xi)\rho(\xi), \quad \forall \xi \in \Gamma,, \tag{3.39}$$

respectively. The error estimators $\Delta_N^u, \Delta_{N,\tilde{N}}^s$ are determined by (3.30) and (3.34). Additionally, the weighted dual solution error estimator is defined as

$$\Delta_{\tilde{N}}^{\psi,\rho}(\xi) := \Delta_{\tilde{N}}^\psi(\xi)\sqrt{\rho(\xi)}, \quad \forall \xi \in \Gamma, \tag{3.40}$$

where the error estimator $\Delta_{\tilde{N}}^\psi$ is determined by (3.32).

Remark 3.24. As for the non-weighted output error estimator (3.34), the weighted output error estimator satisfies

$$\Delta_{N,\tilde{N}}^{s,\rho}(\xi) = \Delta_N^{u,\rho}(\xi)\Delta_{\tilde{N}}^{\psi,\rho}(\xi), \quad \forall \xi \in \Gamma.$$

The pdf $\rho(\xi)$ in (3.38) and (3.39) can be seen as a weight and gives higher priority to more likely parameter values. The weighted estimators are still computationally cheap and will be used as an optimality criterion for a weighted reduced space construction.

3.2.3 Dual norm computation

The error estimators in the previous sections are based on the dual norms of the primal residual and the dual residual. The dual norms are computed by means of the Riesz representation theorem, see, e.g., (Brenner and Scott, 2008, Theorem 2.4.2). The theorem states that a linear functional can be represented by a unique function of a Hilbert space. Furthermore, it establishes a relation between the norm and the dual norm of the Hilbert space. The computation of the dual norm of the primal residual and the dual norm of the dual residual are stated in the following sections.

Dual norm of primal residual

The primal residuals are determined by the unique functions, for $k = 0, \ldots, K$,

$$\hat{r}_N^k(\xi) = \sum_{i=1}^{\mathcal{N}} \hat{r}_{N,i}^k(\xi)\phi_i \in X_h,$$

such that

$$r_N^k(v; \xi) = (\hat{r}_N^k(\xi), v)_X, \quad \forall v \in X_h. \tag{3.41}$$

Additionally, the Riesz representation theorem states the following relation between the norm and the dual norm

$$\left\| r_N^k(\cdot; \xi) \right\|_{X'} = \left\| \hat{r}_N^k(\xi) \right\|_X. \tag{3.42}$$

The primal residual for $k = 0$ is zero, hence

$$\hat{r}_N^0(\xi) = 0. \tag{3.43}$$

For $k = 1, \ldots, K$, the primal residual is represented by (3.3) and (3.5) and Assumption 3.9

$$r_N^k(v; \xi) = \sum_{q=1}^{Q_b} \theta_q^b(\xi) b_q(v) - \frac{1}{\Delta t} \sum_{n=1}^{N} \left(u_{N,n}^k(\xi) - u_{N,n}^{k-1}(\xi) \right) (\varphi_n, v)_{L^2(\Omega)}$$
$$- \sum_{q=1}^{Q_a} \sum_{n=1}^{N} \theta_q(\xi) u_{N,n}^k(\xi) a_q(\varphi_n, v). \tag{3.44}$$

The functionals, L^2 products $(\varphi_n, v)_{L^2(\Omega)} =: m_n(v)$ and bilinear forms can be represented by unique functions

$$\hat{b}_q = \sum_{i=1}^{\mathcal{N}} \hat{b}_{q,i}\phi_i \quad \in X_h, \tag{3.45}$$

$$\hat{m}_n = \sum_{i=1}^{\mathcal{N}} \hat{m}_{n,i}\phi_i \in X_h, \tag{3.46}$$

$$\hat{a}_{q,n} = \sum_{i=1}^{\mathcal{N}} \hat{a}_{q,n,i}\phi_i \in X_h, \tag{3.47}$$

such that

$$b_q(v) = (\hat{b}_q, v)_X, \qquad \forall v \in X_h,\, q = 1, \ldots, Q_b, \tag{3.48}$$

$$m_n(v) = (\hat{m}_n, v)_X, \qquad \forall v \in X_h,\, n = 1, \ldots, N, \tag{3.49}$$

$$a_q(\varphi_n, v) = (\hat{a}_{q,n}, v)_X, \qquad \forall v \in X_h,\, q = 1, \ldots, Q_a,\, n = 1, \ldots, N. \tag{3.50}$$

Utilizing these identities for (3.44), then (3.41) gives

$$(\hat{r}_N^k(\xi), v)_X = \sum_{q=1}^{Q_b} \theta_q^b(\xi)(\hat{b}_q, v)_X - \frac{1}{\Delta t} \sum_{n=1}^{N} \left(u_{N,n}^k(\xi) - u_{N,n}^{k-1}(\xi) \right) (\hat{m}_n, v)_X$$
$$- \sum_{q=1}^{Q_a} \sum_{n=1}^{N} \theta_q^a(\xi) u_{N,n}^k(\xi)(\hat{a}_{q,n}, v)_X.$$

Due to linearity of the inner product and since the equation holds for all functions $v \in X_h$, the parameter dependent function of (3.41) is determined by, $k = 1, \ldots, K$,

$$\hat{r}_N^k(\xi) = \sum_{q=1}^{Q_b} \theta_q^b(\xi)\hat{b}_q - \frac{1}{\Delta t} \sum_{n=1}^{N} \left(u_{N,n}^k(\xi) - u_{N,n}^{k-1}(\xi) \right) \hat{m}_n$$
$$- \sum_{q=1}^{Q_a} \sum_{n=1}^{N} \theta_q^a(\xi) u_{N,n}^k(\xi)\hat{a}_{q,n}. \tag{3.51}$$

Finally the dual norm of the primal residual in (3.30) is computed by

$$\left\| r_N^0(\cdot; \xi) \right\|_{X'}^2 \overset{(3.42)}{=} \left\| \hat{r}_N^0(\xi) \right\|_X^2 = (\hat{r}_N^0(\xi), \hat{r}_N^0(\xi))_X \overset{(3.43)}{=} 0$$

and for $k = 1, \ldots, K$,

$$\left\| r_N^k(\cdot; \xi) \right\|_{X'}^2 \overset{(3.42)}{=} \left\| \hat{r}_N^k(\xi) \right\|_X^2 = (\hat{r}_N^k(\xi), \hat{r}_N^k(\xi))_X$$
$$\overset{(3.51)}{=} \sum_{q=1}^{Q_b} \sum_{q'=1}^{Q_b} \theta_q^b(\xi)\theta_{q'}^b(\xi)(\hat{b}_q, \hat{b}_{q'})_X$$
$$+ \sum_{n=1}^{N} \sum_{n'=1}^{N} \frac{1}{(\Delta t)^2} \left(u_{N,n}^k - u_{N,n}^{k-1} \right) \left(u_{N,n'}^k - u_{N,n'}^{k-1} \right) (\hat{m}_n, \hat{m}_{n'})_X$$
$$+ \sum_{q'=1}^{Q_a} \sum_{q'=1}^{Q_a} \sum_{n=1}^{N} \sum_{n'=1}^{N} \theta_q^a(\xi)\theta_{q'}^a(\xi)u_{N,n}^k u_{N,n'}^k(\hat{a}_{q,n}, \hat{a}_{q',n'})_X$$
$$- \frac{2}{\Delta t} \sum_{q=1}^{Q_b} \sum_{n=1}^{N} \theta_q^b(\xi) \left(u_{N,n}^k - u_{N,n}^{k-1} \right) (\hat{b}_q, \hat{m}_n)_X$$
$$- 2 \sum_{q=1}^{Q_b} \sum_{q'=1}^{Q_a} \sum_{n=1}^{N} \theta_q^b(\xi)\theta_{q'}^a(\xi)u_{N,n}^k(\hat{b}_q, \hat{a}_{q',n})_X$$
$$+ \frac{2}{\Delta t} \sum_{q=1}^{Q_a} \sum_{n=1}^{N} \sum_{n'=1}^{N} \theta_q^a(\xi) \left(u_{N,n}^k - u_{N,n}^{k-1} \right) u_{N,n'}^k(\hat{m}_n, \hat{a}_{q,n'})_X,$$

where for notational convenience the parameter dependence of the reduced primal solution is omitted.

In the following, the algebraic equations of the dual norm computation for the primal residual are stated. The vectors resulting from (3.48)–(3.50) are defined as

$$\underline{m}_n := (m_n(\phi_j))_{j=1}^{\mathcal{N}} \in \mathbb{R}^{\mathcal{N}}, \quad n = 1, \dots, N,$$
$$\underline{a}_{q,n} := (a_q(\varphi_n, \phi_j))_{j=1}^{\mathcal{N}} \in \mathbb{R}^{\mathcal{N}}, \quad q = 1, \dots, Q_a, n = 1, \dots, N,$$

whereas $\underline{b}_q = (b_{q,i})_{i=1}^{\mathcal{N}}$ was defined in (3.26). With the inner product matrix defined in (3.22), (3.48)–(3.50) entail the algebraic equations

$$H\underline{\hat{b}}_q = \underline{b}_q, \quad q = 1, \dots, Q_b,$$
$$H\underline{\hat{m}}_n = \underline{m}_n, \ n = 1, \dots, N,$$
$$H\underline{\hat{a}}_{q,n} = \underline{a}_{q,n}, q = 1, \dots, Q_a, \ n = 1, \dots, N,$$

which yield the coefficients $\underline{\hat{b}}_q = (\hat{b}_{q,i})_{i=1}^{\mathcal{N}}$, $\underline{\hat{m}}_n = (\hat{m}_{n,i})_{i=1}^{\mathcal{N}}$, and $\underline{\hat{a}}_{q,n} = (\hat{a}_{q,n,i})_{i=1}^{\mathcal{N}}$ for (3.45)–(3.47). The right hand side of the last system of equations can be evaluated with (3.23) and (3.25), i.e. $\underline{a}_{q,n} = A_q \underline{\varphi}_n$.

The discrete formulation of (3.43) and (3.51) is given by

$$\underline{\hat{r}}_N^k(\xi) = \begin{cases} 0, & k = 0, \\ \displaystyle\sum_{q=1}^{Q_b} \theta_q^b(\xi)\underline{\hat{b}}_q - \frac{1}{\Delta t}\sum_{n=1}^{N} \left(u_{N,n}^k(\xi) - u_{N,n}^{k-1}(\xi) \right) \underline{\hat{m}}_n & \\ \qquad\qquad - \displaystyle\sum_{q=1}^{Q_a}\sum_{n=1}^{N} \theta_q^a(\xi) u_{N,n}^k(\xi)\underline{\hat{a}}_{q,n}, & k = 1, \dots, K. \end{cases}$$

Then, the dual norm of the primal residual in (3.30) is determined by

$$\left\| r_N^0(\cdot;\xi) \right\|_{X'}^2 = \underline{\hat{r}}_N^0(\xi)^T H \underline{\hat{r}}_N^0(\xi) = 0$$

and for $k = 1, \ldots, K$,

$$
\begin{aligned}
\left\| r_N^k(\cdot;\xi) \right\|_{X'}^2 &= \underline{\hat{r}}_N^k(\xi)^T H \underline{\hat{r}}_N^k(\xi) \\
&= \sum_{q=1}^{Q_b} \sum_{q'=1}^{Q_b} \theta_q^b(\xi)\theta_{q'}^b(\xi) \underline{\hat{b}}_q^T H \underline{\hat{b}}_{q'} \\
&\quad + \sum_{n=1}^{N} \sum_{n'=1}^{N} \frac{1}{(\Delta t)^2} \left(u_{N,n}^k - u_{N,n}^{k-1} \right) \left(u_{N,n'}^k - u_{N,n'}^{k-1} \right) \underline{\hat{m}}_n^T H \underline{\hat{m}}_{n'} \\
&\quad + \sum_{q'=1}^{Q_a} \sum_{q'=1}^{Q_a} \sum_{n=1}^{N} \sum_{n'=1}^{N} \theta_q^a(\xi)\theta_{q'}^a(\xi) u_{N,n}^k u_{N,n'}^k \underline{\hat{a}}_{q,n}^T H \underline{\hat{a}}_{q',n'} \\
&\quad - \frac{2}{\Delta t} \sum_{q=1}^{Q_b} \sum_{n=1}^{N} \theta_q^b(\xi) \left(u_{N,n}^k - u_{N,n}^{k-1} \right) \underline{\hat{b}}_q^T H \underline{\hat{m}}_n \\
&\quad - 2 \sum_{q=1}^{Q_b} \sum_{q'=1}^{Q_a} \sum_{n=1}^{N} \theta_q^b(\xi)\theta_{q'}^a(\xi) u_{N,n}^k \underline{\hat{b}}_q^T H \underline{\hat{a}}_{q',n} \\
&\quad + \frac{2}{\Delta t} \sum_{q=1}^{Q_a} \sum_{n=1}^{N} \sum_{n'=1}^{N} \theta_q^a(\xi) \left(u_{N,n}^k - u_{N,n}^{k-1} \right) u_{N,n'}^k \underline{\hat{m}}_n^T H \underline{\hat{a}}_{q,n'},
\end{aligned}
$$

where the parameter dependence of the reduced primal solution is omitted.

Dual norm of dual residual

The dual residuals are determined by the unique functions, for $k = 0, \ldots, K$,

$$\hat{\tilde{r}}_{\tilde{N}}^k(\xi) = \sum_{i=1}^{\mathcal{N}} \hat{\tilde{r}}_{\tilde{N},i}^k(\xi)\phi_i \in X_h,$$

such that

$$\tilde{r}_{\tilde{N}}^k(v;\xi) = (\hat{\tilde{r}}_{\tilde{N}}^k(\xi), v)_X, \quad \forall v \in X_h. \tag{3.52}$$

Additionally, the Riesz representation theorem states the following relation between the norm and the dual norm

$$\left\| \tilde{r}_{\tilde{N}}^k(\cdot;\xi) \right\|_{X'} = \left\| \hat{\tilde{r}}_{\tilde{N}}^k(\xi) \right\|_X. \tag{3.53}$$

For $k = 0, \ldots, K-1$, the dual residual is represented by (3.4) and (3.7) and Assumption 3.9

$$
\begin{aligned}
\tilde{r}_{\tilde{N}}^k(v;\xi) = &-\frac{1}{\Delta t} \sum_{n=1}^{\tilde{N}} \left(\psi_{\tilde{N},n}^k(\xi) - \psi_{\tilde{N},n}^{k+1}(\xi) \right) (v, \zeta_n)_{L^2(\Omega)} \\
&- \sum_{q=1}^{Q_a} \sum_{n=1}^{\tilde{N}} \theta_q^a(\xi)\psi_{\tilde{N},n}^k(\xi) a_q(v, \zeta_n).
\end{aligned}
\tag{3.54}
$$

The L^2 products $(v, \zeta_n)_{L^2(\Omega)} =: \tilde{m}_n(v)$ and bilinear forms can be represented by unique functions

$$\hat{\tilde{m}}_n = \sum_{i=1}^{\mathcal{N}} \hat{\tilde{m}}_{n,i} \phi_i \; \in X_h, \tag{3.55}$$

$$\hat{\tilde{a}}_{q,n} = \sum_{i=1}^{\mathcal{N}} \hat{a}_{q,n,i} \phi_i \in X_h, \tag{3.56}$$

$$\tag{3.57}$$

such that

$$\tilde{m}_n(v) = (\hat{\tilde{m}}_n, v)_X, \quad \forall v \in X_h, \, n = 1, \dots, \tilde{N}, \tag{3.58}$$

$$a_q(v, \zeta_n) = (\hat{\tilde{a}}_{q,n}, v)_X, \quad \forall v \in X_h, \, q = 1, \dots, Q_a, \, n = 1, \dots, \tilde{N}. \tag{3.59}$$

Utilizing these identities for (3.54), then (3.52) gives

$$\begin{aligned} (\hat{\tilde{r}}_{\tilde{N}}^k(\xi), v)_X = &-\frac{1}{\Delta t} \sum_{n=1}^{\tilde{N}} \left(\psi_{\tilde{N},n}^k(\xi) - \psi_{\tilde{N},n}^{k+1}(\xi) \right) (\hat{\tilde{m}}_n, v)_X \\ &- \sum_{q=1}^{Q_a} \sum_{n=1}^{\tilde{N}} \theta_q^a(\xi) \psi_{\tilde{N},n}^k(\xi) (\hat{\tilde{a}}_{q,n}, v)_X. \end{aligned}$$

Due to linearity of the inner product and since the equation holds for all functions $v \in X_h$, the parameter dependent function of (3.52) is determined by, $k = 0, \dots, K-1$,

$$\begin{aligned} \hat{\tilde{r}}_{\tilde{N}}^k(\xi) = &-\frac{1}{\Delta t} \sum_{n=1}^{\tilde{N}} \left(\psi_{\tilde{N},n}^k(\xi) - \psi_{\tilde{N},n}^{k+1}(\xi) \right) \hat{\tilde{m}}_n \\ &- \sum_{q=1}^{Q_a} \sum_{n=1}^{\tilde{N}} \theta_q^a(\xi) \psi_{\tilde{N},n}^k(\xi) \hat{\tilde{a}}_{q,n}. \end{aligned} \tag{3.60}$$

For $k = K$, the dual residual is represented by (3.4) and (3.8) and Assumption 3.9

$$\tilde{r}_{\tilde{N}}^K(v; \xi) = \sum_{q=1}^{Q_l} \theta_q^l(\xi) l_q(v) - \sum_{n=1}^{\tilde{N}} \psi_{\tilde{N},n}^K(\xi)(v, \zeta_n)_{L^2(\Omega)}. \tag{3.61}$$

The functionals can be represented by unique functions

$$\hat{l}_q = \sum_{i=1}^{\mathcal{N}} \hat{l}_{q,i} \phi_i \in X_h, \tag{3.62}$$

such that

$$l_q(v) = (\hat{l}_q, v)_X, \quad \forall v \in X_h, \, q = 1, \dots, Q_l. \tag{3.63}$$

Utilizing this identity and (3.58) for (3.61), then (3.52) gives

$$(\hat{\tilde{r}}_{\tilde{N}}^K(\xi), v)_X = \sum_{q=1}^{Q_l} \theta_q^l(\xi)(\hat{l}_q, v)_X - \sum_{n=1}^{\tilde{N}} \psi_{\tilde{N},n}^K(\xi)(\hat{\tilde{m}}_n, v)_X.$$

Due to linearity of the inner product and since the equation holds for all functions $v \in X_h$, the parameter dependent function of (3.52) is determined by

$$\hat{\tilde{r}}_{\tilde{N}}^K(\xi) = \sum_{q=1}^{Q_l} \theta_q^l(\xi)\hat{l}_q - \sum_{n=1}^{\tilde{N}} \psi_{\tilde{N},n}^K(\xi)\hat{\tilde{m}}_n. \tag{3.64}$$

Finally the dual norm of the dual residual in (3.32) is computed by, for $k = 0, \ldots, K-1$,

$$
\begin{aligned}
\left\|\tilde{r}_{\tilde{N}}^k(\cdot;\xi)\right\|_{X'}^2 &\overset{(3.53)}{=} \left\|\hat{\tilde{r}}_{\tilde{N}}^k(\xi)\right\|_X^2 = (\hat{\tilde{r}}_{\tilde{N}}^k(\xi), \hat{\tilde{r}}_{\tilde{N}}^k(\xi))_X \\
&\overset{(3.60)}{=} \frac{1}{(\Delta t)^2} \sum_{n=1}^{\tilde{N}} \sum_{n'=1}^{\tilde{N}} \left(\psi_{\tilde{N},n}^k - \psi_{\tilde{N},n}^{k+1}\right)\left(\psi_{\tilde{N},n'}^k - \psi_{\tilde{N},n'}^{k+1}\right)(\hat{\tilde{m}}_n, \hat{\tilde{m}}_{n'})_X \\
&\quad + \sum_{q=1}^{Q_a} \sum_{q'=1}^{Q_a} \sum_{n=1}^{\tilde{N}} \sum_{n=1}^{\tilde{N}} \theta_q^a(\xi)\theta_{q'}^a(\xi)\psi_{\tilde{N},n}^k \psi_{\tilde{N},n'}^k (\hat{\tilde{a}}_{q,n}, \hat{\tilde{a}}_{q',n'})_X \\
&\quad + \frac{2}{\Delta t} \sum_{q=1}^{Q_a} \sum_{n,=1}^{N} \sum_{n',=1}^{N} \theta_q^a(\xi)\left(\psi_{\tilde{N},n}^k - \psi_{\tilde{N},n}^{k+1}\right)\psi_{\tilde{N},n'}^k (\hat{\tilde{m}}_n, \hat{\tilde{a}}_{q,n'})_X
\end{aligned}
$$

and

$$
\begin{aligned}
\left\|\tilde{r}_{\tilde{N}}^K(\cdot;\xi)\right\|_{X'}^2 &\overset{(3.53)}{=} \left\|\hat{\tilde{r}}_{\tilde{N}}^K(\xi)\right\|_X^2 = (\hat{\tilde{r}}_{\tilde{N}}^K(\xi), \hat{\tilde{r}}_{\tilde{N}}^K(\xi))_X \\
&\overset{(3.64)}{=} \sum_{q=1}^{Q_l} \sum_{q'=1}^{Q_l} \theta_q^l(\xi)\theta_{q'}^l(\xi)(\hat{l}_q, \hat{l}_{q'})_X + \sum_{n=1}^{\tilde{N}} \sum_{n'=1}^{\tilde{N}} \psi_{\tilde{N},n}^K \psi_{\tilde{N},n'}^K (\hat{\tilde{m}}_n, \hat{\tilde{m}}_{n'})_X \\
&\quad - 2\sum_{q=1}^{Q_l} \sum_{n=1}^{\tilde{N}} \theta_q^l(\xi)\psi_{\tilde{N},n}^K (\hat{l}_q, \hat{\tilde{m}}_n)_X,
\end{aligned}
$$

where for notational convenience the parameter dependence of the reduced dual solution is omitted.

In the following, the algebraic equations of the dual norm computation for the dual residual are stated. The vectors resulting from (3.58), (3.59), and (3.63) are defined as

$$
\begin{aligned}
\underline{\tilde{m}}_n &:= (\tilde{m}_n(\phi_j))_{j=1}^{\mathcal{N}} \quad \in \mathbb{R}^{\mathcal{N}}, n = 1, \ldots, \tilde{N}, \\
\underline{\tilde{a}}_{q,n} &:= (a_q(\phi_j, \zeta_n))_{j=1}^{\mathcal{N}} \in \mathbb{R}^{\mathcal{N}}, q = 1, \ldots, Q_a, n = 1, \ldots, \tilde{N},
\end{aligned}
$$

whereas $\underline{l}_q = (l_{q,i})_{i=1}^{\mathcal{N}}$ was defined in (3.27). With the inner product matrix defined in (3.22), (3.58), (3.59), and (3.63) entail the algebraic equations

$$
\begin{aligned}
H\hat{\tilde{\underline{m}}}_n &= \underline{\tilde{m}}_n, \ n = 1, \ldots, \tilde{N}, \\
H\hat{\tilde{\underline{a}}}_{q,n} &= \underline{\tilde{a}}_{q,n}, q = 1, \ldots, Q_a, n = 1, \ldots, \tilde{N}, \\
H\hat{\underline{l}}_q &= \underline{l}_q, \quad q = 1, \ldots, Q_l,
\end{aligned}
$$

which yield the coefficients $\hat{\tilde{\underline{m}}}_n = (\hat{\tilde{m}}_{n,i})_{i=1}^{\mathcal{N}}$, $\hat{\tilde{\underline{a}}}_{q,n} = (\hat{\tilde{a}}_{q,n,i})_{i=1}^{\mathcal{N}}$, and $\hat{\underline{l}}_q = (\hat{l}_{q,i})_{i=1}^{\mathcal{N}}$ for (3.55), (3.56), and (3.62). The right hand side of the second system of equations can be evaluated with (3.24) and (3.25), i.e. $\underline{\tilde{a}}_{q,n} = A_q^T \underline{\zeta}_n$.

The discrete formulation of (3.60) and (3.64) is given by

$$
\hat{\underline{\tilde{r}}}^k_{\tilde{N}}(\xi) = \begin{cases} -\dfrac{1}{\Delta t}\displaystyle\sum_{n=1}^{\tilde{N}}\left(\psi^k_{\tilde{N},n}(\xi)-\psi^{k+1}_{\tilde{N},n}(\xi)\right)\hat{\underline{\tilde{m}}}_n \\[2mm] -\displaystyle\sum_{q=1}^{Q_a}\sum_{n=1}^{\tilde{N}}\theta^a_q(\xi)\psi^k_{\tilde{N},n}(\xi)\hat{\underline{\tilde{a}}}_{q,n}, & k=0,\dots,K-1, \\[2mm] \displaystyle\sum_{q=1}^{Q_l}\theta^l_q(\xi)\hat{\underline{l}}_q-\sum_{n=1}^{\tilde{N}}\psi^K_{\tilde{N},n}(\xi)\hat{\underline{\tilde{m}}}_n, & k=K. \end{cases}
$$

Then, the dual norm of the dual residual in (3.32) is determined by, for $k=0,\dots,K-1$,

$$
\begin{aligned}
\left\|\tilde{r}^k_{\tilde{N}}(\cdot;\xi)\right\|^2_{X'} &= \hat{\underline{\tilde{r}}}^k_{\tilde{N}}(\xi)^T H\hat{\underline{\tilde{r}}}^k_{\tilde{N}}(\xi) \\
&= \frac{1}{(\Delta t)^2}\sum_{n=1}^{\tilde{N}}\sum_{n'=1}^{\tilde{N}}\left(\psi^k_{\tilde{N},n}-\psi^{k+1}_{\tilde{N},n}\right)\left(\psi^k_{\tilde{N},n'}-\psi^{k+1}_{\tilde{N},n'}\right)\hat{\underline{\tilde{m}}}^T_n H\hat{\underline{\tilde{m}}}_{n'} \\
&\quad+\sum_{q=1}^{Q_a}\sum_{q'=1}^{Q_a}\sum_{n=1}^{\tilde{N}}\sum_{n=1}^{\tilde{N}}\theta^a_q(\xi)\theta^a_{q'}(\xi)\psi^k_{\tilde{N},n}\psi^k_{\tilde{N},n'}\hat{\underline{\tilde{a}}}^T_{q,n}H\hat{\underline{\tilde{a}}}_{q',n'} \\
&\quad+\frac{2}{\Delta t}\sum_{q=1}^{Q_a}\sum_{n,=1}^{N}\sum_{n'=1}^{N}\theta^a_q(\xi)\left(\psi^k_{\tilde{N},n}-\psi^{k+1}_{\tilde{N},n}\right)\psi^k_{\tilde{N},n'}\hat{\underline{\tilde{m}}}^T_n H\hat{\underline{\tilde{a}}}_{q,n'}
\end{aligned}
$$

and

$$
\begin{aligned}
\left\|\tilde{r}^K_{\tilde{N}}(\cdot;\xi)\right\|^2_{X'} &= \hat{\underline{\tilde{r}}}^K_{\tilde{N}}(\xi)^T H\hat{\underline{\tilde{r}}}^K_{\tilde{N}}(\xi) \\
&= \sum_{q=1}^{Q_l}\sum_{q'=1}^{Q_l}\theta^l_q(\xi)\theta^l_{q'}(\xi)\hat{\underline{l}}^T_q H\hat{\underline{l}}_{q'}+\sum_{n=1}^{\tilde{N}}\sum_{n'=1}^{\tilde{N}}\psi^K_{\tilde{N},n}\psi^K_{\tilde{N},n'}\hat{\underline{\tilde{m}}}^T_n H\hat{\underline{\tilde{m}}}_{n'} \\
&\quad-2\sum_{q=1}^{Q_l}\sum_{n=1}^{\tilde{N}}\theta^l_q(\xi)\psi^K_{\tilde{N},n}\hat{\underline{l}}^T_q H\hat{\underline{\tilde{m}}}_n
\end{aligned}
$$

where the parameter dependence of the reduced dual solution is omitted.

This section stated computationally cheap and residual based error estimators in order to assess the accuracy of the reduced solution. The definitions of weighted error estimators aim for an efficient approximation of statistical quantities. Furthermore, the equations for the error estimator computations were stated. The error estimators are an essential ingredient for the reduced space construction.

3.3 Reduced space construction

In this section, the construction of the reduced space is discussed. The parametrization of the PDE entails a solution manifold

$$
\mathcal{M}^K_h = \{\{u^k_h(\xi)\}^K_{k=0}\colon \{u^k_h(\xi)\}^K_{k=0}\text{ solves (2.13)}, \xi\in\Gamma\}\subset X^{K+1}_h,
$$

cf. Fig. 3.1. The objective is to construct a reduced space $X_N\subset X_h$ that
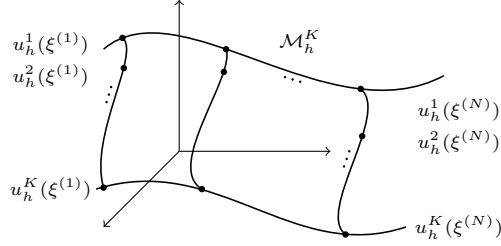
Figure 3.1: Solution manifold

approximates the solution manifold accurately, such that $N \ll \mathcal{N}$. The Kolmogorov N-width is a measure as to how well the solution manifold can be approximated, see, e.g., Pinkus (1985). The reduced space construction is based on the POD-greedy algorithm, introduced in Haasdonk and Ohlberger (2008), which utilizes an error estimator Δ_N over the parameter domain for the basis selection. The procedure is stated in Algorithm 1.

Data: ϵ_{tol}, parameter training set $\Gamma_{\text{train}} \subset \Gamma$
Result: reduced space X_N
$N := 0$, $X_0 := 0$
while $\epsilon_N := \max_{\xi \in \Gamma_{train}} \Delta_N(\xi) > \epsilon_{tol}$ **do**

$\quad \xi^{(N+1)} := \arg \max_{\xi \in \Gamma_{\text{train}}} \Delta_N(\xi)$

$\quad$ compute $u_h^k(\xi^{(N+1)})$, $k = 0, \dots, K$, using (2.13a) and (2.13b)

$\quad e_P^k(\xi^{(N+1)}) := u_h^k(\xi^{(N+1)}) - P_{X_N} u_h^k(\xi^{(N+1)})$, $k = 0, \dots, K$

$\quad \varphi_{N+1} := POD_1(\{e_P^k(\xi^{(N+1)})\}_{k=0}^K)$

$\quad X_{N+1} := X_N \oplus \text{span}\{\varphi_{N+1}\}$

$\quad N := N + 1$

end

Algorithm 1: POD-greedy algorithm

Note, the algorithm is formulated for the primal problem (2.13a), (2.13b), (3.1a), and (3.1b). Analogously the algorithm can be utilized for the dual problem (2.43) and (3.2).

The POD-greedy algorithm combines a greedy algorithm (Haasdonk, 2017, Definition 2.46) for the parameter domain and a POD (Gubisch and Volkwein, 2017, section 1.2) for the time interval. The dimension of the reduced basis N grows iteratively. As a stopping criterion for the iteration, an error estimator of the previous section needs to fall below some given error tolerance $\epsilon_{\text{tol}} > 0$. Alternatively, a predefined reduced dimension can be given as a stopping criterion. The parameter value ξ^{N+1} is determined in each iteration by evaluating an optimality criterion. Maximizing the exact errors over a large parameter domain can be computationally infeasible. Instead, the computationally cheap error estimators are maximized, which is often called weak POD-greedy. The maximum is sought over a training parameter set Γ_{train}, which is a finite and uniformly

sampled approximation set of the parameter domain. The training parameter set is assumed to be large and to represent the infinite parameter domain well. Note, for $N, \tilde{N} = 0$ the reduced solutions $\{u_N^k\}_{k=0}^K, \{\psi_{\tilde{N}}^k\}_{k=0}^K$ are zero. This means that the primal residual (3.5) and (3.6) reduces to the right hand side $b(\cdot; \xi)$ and the dual residual (3.7) and (3.8) reduces to the functional $l(\cdot; \xi)$. Hence, for the first iteration, the optimality criterion maximizes the dual norm of these functionals.

The solutions for the single time steps $\{u_h^k(\xi^{(N+1)})\}_{k=0}^K$, called snapshots, are computed. In order to compress the information of the obtained solution trajectory, the first POD mode of the projection error onto the reduced space is computed and added to the reduced basis. If the eigenvalues obtained from the POD decay slowly, it can be reasonable to choose more than one POD mode in a single POD-greedy iteration, see (Hesthaven et al., 2016, section 6.1.2). The spaces generated by the POD-greedy are hierarchical, i.e. $X_N \subset X_{N+1}$. However, the error convergence of the approximation obtained by the weak POD-greedy is not necessarily monotonically decreasing. This means that, if the dimension of the reduced basis space is increased, the error can possibly increase. If the optimality criterion is replaced by the maximization of the orthogonal projection error, it can be guaranteed that the error convergence of the POD-greedy is monotonically decreasing, see (Haasdonk, 2017, Remark 2.47 (i)).

3.3.1 A non-weighted reduced space construction

A non-weighted reduced space construction is based on Algorithm 1. It is distinguished if the objective is either the approximation of the solution u_h or the approximation of the output s_h. The former uses the primal solution error estimator Δ_N^u in (3.30) for the optimality criterion in the POD-greedy procedure. The latter uses the output error estimator $\Delta_{N,\tilde{N}}^s$ in (3.34) for the optimality criterion in the POD-greedy procedure. The output error estimator consists of a primal error estimator Δ_N^u and dual error estimator $\Delta_{\tilde{N}}^\psi$ in (3.32). Therefore, maximizing the output error estimator yields a reduced space regarding the primal problem and a reduced space regarding the dual problem. A non-weighted reduced space construction weights all parameter values $\xi \in \Gamma$ equally.

3.3.2 A weighted reduced space construction

As in the previous section, a weighted reduced space construction is based on Algorithm 1. However, in this section, the objective is to build up a reduced space that gives better error convergence regarding statistical quantities, compared to the non-weighted approach. Since the input parameters are random, certain parameters are more likely to appear. Highly probable parameters obtain more importance incorporating the pdf. Hence, weighted error estimators of section 3.2.2 are used for the reduced space construction. It is distinguished if the objective is either the approximation of the expected solution $\mathbb{E}[u_h]$ or the approximation of the expected output $\mathbb{E}[s_h]$. The former uses the weighted primal solution error estimator $\Delta_N^{u;\rho}$ in (3.38) for the optimality criterion in the POD-greedy procedure. The latter uses the weighted output error estimator $\Delta_{N,\tilde{N}}^{s;\rho}$ in (3.39) for the optimality criterion in the POD-greedy procedure. The weighted output error estimator is composed of the weighted primal error estimator $\Delta_N^{u;\rho}$ and the weighted dual error estimator $\Delta_{\tilde{N}}^{\psi;\rho}$ in (3.40). Maximizing the weighted

output error estimator yields a weighted reduced space regarding the primal problem and a weighted reduced space regarding the dual problem. Therefore, the primal reduced space construction uses $\Delta_N^u \sqrt{\rho}$, and the dual reduced space construction uses $\Delta_{\tilde{N}}^\psi \sqrt{\rho}$ as an optimality criterion.

The weighted approach uses the same uniformly sampled parameter set Γ_{train} as the non-weighted approach. This means that the weighting comes in only by the optimality criterion that maximizes the weighted error estimators.

3.3.3   Comparison non-weighted and weighted approach

In this section, a few remarks on a non-weighted and weighted reduced space construction and its a priori convergence are given. In principal, the a priori convergence of a greedy algorithm (Haasdonk, 2017, Definition 2.46) is based on the previously mentioned Kolmogorov N-width. If the Kolmogorov N-width converges polynomially $\mathcal{O}(N^{-\alpha})$, the approximation obtained by a greedy algorithm inherits the polynomial convergence rate $\mathcal{O}(N^{-\alpha})$, see (Binev et al., 2011, Theorem 3.1). In case of exponential convergence, the inheritance of the convergence rate does not follow as for the polynomial case. However, if the Kolmogorov N-width converges with $\mathcal{O}(e^{-aN^\alpha})$, the approximation error of a greedy algorithm converges where $\mathcal{O}(e^{-bN^\beta})$, with a, b and α, β are positive constants independent of N, see (Binev et al., 2011, Theorem 3.2). Based on this work, convergence results for the POD-greedy procedure were derived in Haasdonk (2013). In case of polynomial convergence (Haasdonk, 2013, Proposition 4.3), as well as for exponential convergence (Haasdonk, 2013, Proposition 4.4), of the Kolmogorov N-width, the convergence results of the greedy procedure can be carried over to the POD-greedy algorithm. Although the convergence rates of the greedy algorithm and the POD-greedy are the same, the constants of the greedy error bounds differ from the ones for POD-greedy.

The non-weighted approach and the weighted approach were explained in sections 3.3.1 and 3.3.2, respectively. In essence, the methods differ in maximizing a non-weighted error estimator (3.30) and (3.34) compared to a weighted error estimator (3.38) and (3.39). If the parameter follows a uniform distribution, the pdf is parameter independent and hence the non-weighted and the weighted approach coincide. Both reduced space constructions are based on the POD-greedy procedure, see Algorithm 1. The method iteratively constructs a reduced space and terminates if the maximal error estimator falls below a certain error tolerance. Assume the error tolerance is set to zero, i.e. $\epsilon_{\text{tol}} := 0$. Then the POD-greedy algorithm yields a $|\Gamma_{\text{train}}|K$-dimensional reduced basis containing the solutions at each time step, in case they are linearly independent, for all parameters $\xi \in \Gamma_{\text{train}}$. In this case the error between the detailed and the reduced quantities becomes zero on $|\Gamma_{\text{train}}|$, see (Haasdonk, 2017, Proposition 2.78). This means that once the reduced space contains all snapshots, the reduced quantities reconstruct the detailed quantities exactly and the reduced spaces obtained from a non-weighted and a weighted approach coincide. However, maximizing either the non-weighted or the weighted error estimator influences the order for the parameter selection $\xi^{(N+1)}$. Incorporating the weight into the error estimator, it is expected to obtain better error convergence for the approximation of the expectation, but no better rate of error convergence. Still, from an analytical point of view it is not clear how significant is the improvement regarding the

statistical approximation using the weighted approach. A fundamental question is what can be stated about the error convergence utilizing a weighted approach. A priori convergence analysis for the weighted approach applied to elliptic PDEs was studied in (Chen et al., 2013, section 4). The weighted approach for parabolic PDEs were recently also considered in Spannring et al. (2017) and (Torlo et al., 2017, section 4). However, for the weighted parabolic case, there are still no a priori convergence results.

Chapter 4

Model order reduction with a POD projection

In this chapter the objective is to construct a reduced space that gives an approximation which minimizes the expected solution error. Therefore, a pure POD is utilized. This means that, compared to section 3.3, a POD for the parameter domain and the time interval is applied. The POD (Volkwein, 2013) is a MOR technique that extracts the most important information of a set of snapshots. It is based on an eigenvalue problem, where the obtained eigenfunctions span an orthonormal space. If the corresponding eigenvalues decay fast, only a few eigenfunctions are needed in order to represent the snapshot set accurately. The reduced space, obtained by a POD, is optimal in a least squares sense. In the following the expected value is approximated by the Monte Carlo method.

4.1 Monte Carlo approximation

The Monte Carlo (MC) method is a sampling based method that allows to approximate statistical quantities by solving N_{MC} deterministic problems, see, e.g. (Fishman, 1996, section 2.7.3). Here, N_{MC} denotes the number of MC samples. The computational complexity of the MC method is independent of the stochastic dimension p compared to, e.g. a collocation method (Xiu, 2010, chapter 7) or a Galerkin method (Xiu, 2010, chapter 6). However, the convergence rate of the MC method $\mathcal{O}(1/\sqrt{N_{\mathrm{MC}}})$ is rather low. In order to improve the convergence rate, several methods were studied, e.g. Quasi Monte Carlo (QMC) (Niederreiter, 1978, Part I) or Multilevel Monte Carlo (MLMC) (Cliffe et al., 2011, section 2.2). Therefore N_{MC} is chosen to be large, such that the MC error can be neglected,

$$
\begin{aligned}
\mathbb{E}[u_h] - \mathbb{E}_{\mathrm{MC}}[u_N] &= \mathbb{E}[u_h] - \mathbb{E}_{\mathrm{MC}}[u_h] + \mathbb{E}_{\mathrm{MC}}[u_h] - \mathbb{E}_{\mathrm{MC}}[u_N] \\
&\approx \mathbb{E}_{\mathrm{MC}}[u_h - u_N].
\end{aligned} \tag{4.1}
$$

The MC estimator for the expected value is determined by,

$$
\mathbb{E}_{\mathrm{MC}}[u] = \frac{1}{N_{\mathrm{MC}}} \sum_{i=1}^{N_{\mathrm{MC}}} u(\xi^{(i)}), \tag{4.2}
$$

where the realizations $\{\xi^{(i)}\}_{i=1}^{N_{\mathrm{MC}}}$ are independent and sampled by the corresponding pdf. The computations of $\{u(\xi^{(i)})\}_{i=1}^{N_{\mathrm{MC}}}$ are independent, hence the methods allows parallelization techniques for the computation.

Recall, the parameter set Γ_{train} is uniformly sampled. However, the MC estimator can be also approximated by uniformly sampled realization $\xi^{(i)}$. Therefore, denote $\rho_{\mathcal{U}}(\xi)$ as the uniform distribution and $\rho(\xi)$ the actual distribution. Since the parameter $\xi = (\xi_1, \ldots, \xi_p)$ is a p-dimensional random vector, introduced in section 2.2, the uniform distribution is determined by,

$$\rho_{\mathcal{U}}(\xi) = \begin{cases} \prod_{n=1}^{p} \frac{1}{(b_n - a_n)}, & \xi \in \Gamma = [a_1, b_1] \times \cdots \times [a_p, b_p], \\ 0, & else. \end{cases} \tag{4.3}$$

Then, the expected value can be approximated by,

$$\mathbb{E}[u] = \int_{\Gamma} u(\xi)\rho(\xi)\mathrm{d}\xi = \int_{\Gamma} u(\xi) \frac{\rho(\xi)}{\rho_{\mathcal{U}}(\xi)} \rho_{\mathcal{U}}(\xi)\mathrm{d}\xi$$
$$\stackrel{(4.1)}{\approx} \frac{1}{N_{\mathrm{MC}}} \sum_{i=1}^{N_{\mathrm{MC}}} u(\xi^{(i)}) \frac{\rho(\xi^{(i)})}{\rho_{\mathcal{U}}(\xi^{(i)})}, \tag{4.4}$$

with $\xi_n^{(i)} \sim \mathcal{U}(a_n, b_n)$, $n = 1, \ldots, p$. Utilizing (4.3) for the last term in (4.4), the MC estimator for the expected value using uniform samples is defined by,

$$\mathbb{E}_{\mathrm{MC}}^{\mathcal{U}}[u] := \frac{\prod_{n=1}^{p}(b_n - a_n)}{N_{\mathrm{MC}}} \sum_{i=1}^{N_{\mathrm{MC}}} u(\xi^{(i)})\rho(\xi^{(i)}). \tag{4.5}$$

As in (4.1), the number of MC samples is assumed to be large, such that $\mathbb{E}[u_h] - \mathbb{E}_{\mathrm{MC}}^{\mathcal{U}}[u_N] \approx \mathbb{E}_{\mathrm{MC}}^{\mathcal{U}}[u_h - u_N]$.

4.2 Proper orthogonal decomposition

In order to represent a given set of snapshots $\{u_h^k(\xi) : k = 1, \ldots, K, \xi \in \Gamma\}$ optimally, the POD is applied. As a crucial benefit, the POD yields an optimal space regarding the mean square error. Hence, by means of the POD an optimal reduced solution can be found, such that the expected solution error becomes minimal, i.e.

$$\min_{\substack{w_1, \ldots, w_N \in X_h}} \min_{\substack{u_r^1, \ldots, u_r^K \\ \in L^2(\Gamma; \mathrm{span}\{w_1, \ldots, w_N\})}} \mathbb{E}\left[\Delta t \sum_{k=1}^{K} \left\|u_h^k - u_r^k\right\|_X^2\right], \tag{4.6}$$

$$\text{subject to } (w_m, w_n)_X = \delta_{mn}.$$

The snapshots $\{u_h^k(\xi)\}_{k=1}^{K}$ are obtained from Problem 2.11, whereas the reduced solutions $\{u_r^k\}_{k=1}^{K}$ are sought. In order to guarantee that the expectation of the reduced solution exists, the reduced solutions lie in a Bochner space $L^2(\Gamma; \mathrm{span}\{w_1, \ldots, w_N\})$, see definition A.2. The error is measured in the norm induced by the Hilbert space X. An optimal choice for the reduced unknown functions $\{u_r^k\}_{k=1}^{K}$ can be achieved by choosing their orthogonal projection onto the N-dimensional POD space $X_{\mathrm{POD},N} := \mathrm{span}\{w_1, \ldots, w_N\} \subset X_h$, namely

$$u_{\mathrm{POD},N}^k(\xi) := \sum_{n=1}^{N} (u_h^k(\xi), w_n)_X w_n \in X_{\mathrm{POD},N}, \quad k = 1, \ldots K. \tag{4.7}$$

The orthogonal projection (Kunisch and Volkwein, 2002, equation (3.1)) yields an equivalent formulation of the minimization problem (4.6), such that

$$
\min_{w_1,\ldots,w_N \in X_h} \mathbb{E}\left[\Delta t \sum_{k=1}^{K} \left\| u_h^k - \sum_{n=1}^{N} (u_h^k, w_n)_X w_n \right\|_X^2 \right], \tag{4.8}
$$

subject to $(w_m, w_n)_X = \delta_{mn}$.

The expectation in (4.6) and (4.8) can not be determined analytically. Assuming (4.1), the expectation is approximated by the MC method, see section 4.1. Then, the minimization problem in (4.8) is approximated by

$$
\min_{w_1,\ldots,w_N \in X_h} \frac{\Delta t}{N_{\mathrm{MC}}} \sum_{i=1}^{N_{\mathrm{MC}}} \sum_{k=1}^{K} \left\| u_h^k(\xi^{(i)}) - \sum_{n=1}^{N} (u_h^k(\xi^{(i)}), w_n)_X w_n \right\|_X^2, \tag{4.9}
$$

subject to $(w_m, w_n)_X = \delta_{mn}$,

where the realizations $\{\xi^{(i)}\}_{i=1}^{N_{\mathrm{MC}}}$ are sampled by the pdf. However, the MC approximation can be modified such that the statistical quantity is approximated by uniformly sampled realizations, see (4.5). The minimization problem (4.9) can be solved by an eigenvalue problem, see, e.g., (Gubisch and Volkwein, 2017, Theorem 1.8). The resulting eigenfunctions $\{w_n\}_{n=1}^{N}$ are the first $N \in \{1,\ldots,N_{\mathrm{MC}}K\}$ orthogonal POD modes and the eigenvalues $\{\sigma_l\}_{l=1}^{N_{\mathrm{MC}}K}$ determine the error in (4.9), such that

$$
\frac{\Delta t}{N_{\mathrm{MC}}} \sum_{i=1}^{N_{\mathrm{MC}}} \sum_{k=1}^{K} \left\| u_h^k(\xi^{(i)}) - \sum_{n=1}^{N} (u_h^k(\xi^{(i)}), w_n)_X w_n \right\|_X^2 = \sum_{l=N+1}^{N_{\mathrm{MC}}K} \sigma_l. \tag{4.10}
$$

The first N POD modes span the POD space $X_{\mathrm{POD},N} = \mathrm{span}\{w_1,\ldots,w_N\}$.

However, the optimality pays its price. It is emphasized that the reduced space construction using a POD requires the snapshots over the parameter domain differently from the RBM. Hence, for a large parameter set this can be computationally challenging. Compared to the POD-greedy in section 3.3, the evaluation of the error estimator for the parameter values are computationally cheap and eventually only N detailed solutions for the reduced space construction need to be evaluated. Note, the comparison only can be done for the expectation of the squared solution error. For the expected value of the absolute output error $\mathbb{E}[|s_h - s_{N,\tilde{N}}|]$ an optimal reduced space cannot be found with a POD, since the absolute value does not induce an inner product.

In this section optimality for the mean square error measured in the norm $\|\cdot\|_X$ could be stated. Therefore, the POD method determines an optimal reduced POD space based on a finite set of snapshots. Moreover, the optimal representation of the reduced solution is given by the orthogonal projection onto the reduced POD space. The minimal mean square error can be easily computed by the truncated eigenvalues coming out of the POD method.

Chapter 5

Numerical Example

This chapter studies an instationary heat transfer (Grepl and Patera, 2005, section 6) on a rectangular domain with random input parameter. The data uncertainties enter the problem via the boundary conditions. In particular, a random field acts as a stochastic heat inflow on the boundary of the domain. Another random coefficient acts as a cooling parameter on the boundary, which is located inside the spatial domain. The quantity of interest (or output) is determined by the average temperature in the domain. A deterministic finite element solver determines the solution for a randomly sampled parameter in the domain. The solution and the quantity of interest are random variables, hence the expectation of these quantities is determined. The expectation is approximated by a Monte Carlo (MC) method, see section 4.1. Since the MC method requires many finite element solutions, it can be computational infeasible. Hence, the computational costs are reduced by model order reduction. In order to reduce the dimension of the algebraic equations obtained from the finite element method, the reduced basis method from chapter 3 is used. Three different approaches are utilized in order to construct a reduced model: a non-weighted reduced basis approach from section 3.3.1, a weighted reduced basis approach from section 3.3.2 and a POD from section 4.2. The goal is to quantify the expectation of the solution error and the output error among those three approaches. It is expected that the weighted RBM gives better error convergence of the expected value compared to the non-weighted RBM. In order to quantify the quality of the weighted approach, it is numerically verified how close the expected error convergence is compared to the optimum obtained from the POD.

5.1 Mathematical model

This section states the governing equations for the time dependent heat conduction. The heat is considered on a rectangular domain $\Omega \subset \mathbb{R}^2$ where three squares are cut out, see Fig. 5.1. The boundary $\partial\Omega$ contains the left boundary $\partial\Omega_{\text{out}}$ (in blue) and the inner boundary $\partial\Omega_{\text{in}}$ (in red). The end point in time $T > 0$ determines the time interval $I = [0, T]$ and $t \in I$ denotes the time variable. The mathematical model is parametrized by the random parameters ξ^{out} and ξ^{in}, which are acting on the domain boundaries $\partial\Omega_{\text{out}}$ and $\partial\Omega_{\text{in}}$, respectively. The parameter domain Γ is determined by the supports $\Gamma^{\text{out}} \ni \xi^{\text{out}}$ and $\Gamma^{\text{in}} \ni \xi^{\text{in}}$
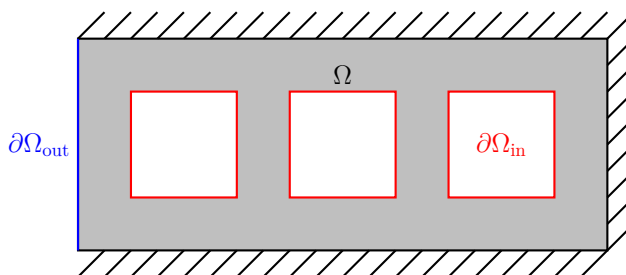
Figure 5.1: Spatial domain Ω

such that $\Gamma = \Gamma^{\text{out}} \times \Gamma^{\text{in}}$.

The two-dimensional model problem is solved for the space, time and parameter dependent temperature field $u\colon \Omega \times I \times \Gamma \to \mathbb{R}$. The temperature field determines the quantity of interest s, which describes the average temperature in the domain at the end point in time. In the following the strong formulation of the heat conduction is stated.

Problem 5.1 (2d heat transfer). For given random realization $\xi = (\xi^{\text{out}}, \xi^{\text{in}}) \in \Gamma$, the solution u satisfies

$$
\begin{aligned}
\partial_t u(\xi) - \Delta u(\xi) &= 0, && \text{in } \Omega \times (0, T], \\
\frac{\partial u(\xi)}{\partial n} &= \begin{cases} \kappa(\xi^{\text{out}})(1 - u(\xi)), & \text{on } \partial\Omega_{\text{out}} \times (0, T], \\ -\xi^{\text{in}} u(\xi), & \text{on } \partial\Omega_{\text{in}} \times (0, T], \\ 0, & \text{on } \partial\Omega \setminus \{\partial\Omega_{\text{out}} \cup \partial\Omega_{\text{in}}\} \times (0, T], \end{cases} \\
u &= 0, && \text{on } \Omega \times \{0\}.
\end{aligned}
$$

There is no external heat force acting in the domain, hence the right hand side is zero. The boundary conditions are composed of a Robin boundary condition on $\partial\Omega_{\text{out}} \cup \partial\Omega_{\text{in}}$ and a Neumann boundary condition on the remaining boundary. The stochastic parameters ξ^{out} and ξ^{in} enter the model problem via the Robin boundary condition. The Robin boundary condition can be seen as a Neumann condition where the heat flux on the boundary in the normal direction also depends on the solution. The heat inflow on $\partial\Omega_{\text{out}}$ is parametrized by a random field $\kappa\colon \partial\Omega_{\text{out}} \times \Gamma^{\text{out}} \to \mathbb{R}$ and $\xi^{\text{in}} \in \Gamma^{\text{in}}$ parametrizes cooling of the domain on $\partial\Omega_{\text{in}}$. A homogeneous Neumann boundary condition governs on the remaining boundary of the domain, which models heat insulation on this boundary. The initial condition, meaning the temperature at point 0 in time, is zero. The solution at final time T determines the quantity of interest $s\colon \Gamma \to \mathbb{R}$

$$
s(\xi) = \frac{1}{|\Omega|} \int_\Omega u(T; \xi).
$$

The random field $\kappa(\xi^{\text{out}})$ is assumed to be a random process of second order and hence can be represented by a Karhunen-Loève expansion (Loève, 1978, section 37.5)

$$
\kappa(x, \xi^{\text{out}}) = \alpha_0(x) + \sum_{l=1}^{\infty} \sqrt{\lambda_l} c_l(x) \xi_l^{\text{out}},
$$

see appendix A.7. Furthermore, the random parameters $\xi^{\text{out}} = (\xi_l^{\text{out}})_{l=1}^{N_{\text{KL}}}$ are assumed to be independent. The KL expansion yields the advantage that the spatial variable and the stochastic variable can be separated and hence fulfills the affine parameter dependence in Assumption 3.9. In the following the random field is approximated by the truncated Karhunen-Loève expansion

$$\kappa(x, \xi^{\text{out}}) \approx \bar{\kappa}(x, \xi^{\text{out}}) = \alpha_0(x) + \sum_{l=1}^{N_{\text{KL}}} \sqrt{\lambda_l} c_l(x) \xi_l^{\text{out}}, \tag{5.1}$$

see (A.11) and (A.12) for a possible choice of N_{KL}. In order to satisfy existence and uniqueness of the model problem, the random field has to be bounded from below and above

$$\kappa_{\min} \leq \bar{\kappa}(x, \xi^{\text{out}}) \leq \kappa_{\max}, \quad \forall x \in \partial\Omega_{\text{out}}, \forall \xi^{\text{out}} \in \Gamma^{\text{out}}, \tag{5.2}$$

with $\kappa_{\min} > 0$ and $\kappa_{\max} < \infty$. The error bounds $\kappa_{\min}, \kappa_{\max}$ are derived in appendix A.7.1.

The random parameters $\xi^{\text{out}} = (\xi_l^{\text{out}})_{l=1}^{N_{\text{KL}}}$ are distributed with uniform distribution $\mathcal{U}(a_{\mathcal{U}}, b_{\mathcal{U}})$, $-\infty < a_{\mathcal{U}} < b_{\mathcal{U}} < \infty$. The random parameters have zero mean and are mutually uncorrelated, see (A.9), hence $a_{\mathcal{U}} = -\sqrt{3}$ and $b_{\mathcal{U}} = \sqrt{3}$. The random parameter ξ^{in} is distributed with beta distribution $\mathcal{B}(p, q, a_{\mathcal{B}}, b_{\mathcal{B}})$ where $p, q \geq 1$ are scaling parameters and $0 < a_{\mathcal{B}} < b_{\mathcal{B}} < \infty$ are the interval bounds of the support. The probability density function (pdf) of the beta distribution is given by

$$\rho_{\mathcal{B}}(z) = \frac{\Gamma(p+q)}{\Gamma(p)\Gamma(q) (b_{\mathcal{B}} - a_{\mathcal{B}})^{p+q-1}} (z - a_{\mathcal{B}})^{p-1} (z - b_{\mathcal{B}})^{q-1}, \quad z \in [a_{\mathcal{B}}, b_{\mathcal{B}}],$$

where $\Gamma(p) = (p-1)!$ is the gamma function. For $p = q = 1$ the pdf of the beta distribution coincides with the uniform distribution and hence the non-weighted and the weighted approach coincides. Therefore, these scaling parameters are chosen such that $p, q > 1$. Furthermore, the parameters ξ^{in} and ξ^{out} are independent as well.

As described in section 2.1, the weak formulation of the parabolic problem is stated. For given realization $\xi = (\xi^{\text{out}}, \xi^{\text{in}}) \in \Gamma$ and for $t \in I$, find the solution $u(t; \xi) \in X = H^1(\Omega)$, such that

$$\int_{\Omega} \partial_t u(t; \xi) v + \int_{\Omega} \nabla u(t; \xi) \cdot \nabla v + \int_{\partial\Omega_{\text{out}}} \kappa(\xi^{\text{out}}) u(t; \xi) v$$

$$+ \xi^{\text{in}} \int_{\partial\Omega_{\text{in}}} u(t; \xi) v = \int_{\partial\Omega_{\text{out}}} \kappa(\xi^{\text{out}}) v, \; \forall v \in X, \, t \in (0, T],$$

$$\int_{\Omega} u(t; \xi) v = 0, \qquad\qquad \forall v \in X, \, t = 0,$$

and evaluate the output

$$s(\xi) = \frac{1}{|\Omega|} \int_{\Omega} u(T; \xi).$$

As in section 2.1, since the space variables are omitted, the integrals are written without the integration variable regarding the space. The weak formulation
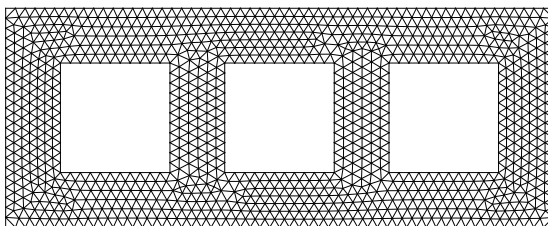
Figure 5.2: Mesh of the spatial domain Ω

determines the bilinear form, right hand side and linear output functional

$$a(w,v;\xi) = \int_\Omega \nabla w \cdot \nabla v + \int_{\partial\Omega_{\mathrm{out}}} \kappa(\xi^{\mathrm{out}})wv + \xi^{\mathrm{in}} \int_{\partial\Omega_{\mathrm{in}}} wv, \quad \forall w,v \in X, \quad (5.3)$$

$$b(v;\xi) = \int_{\partial\Omega_{\mathrm{out}}} \kappa(\xi^{\mathrm{out}})v, \quad l(v) = \frac{1}{|\Omega|}\int_\Omega v, \qquad\qquad \forall v \in X. \qquad (5.4)$$

Regarding existence and uniqueness of the weak formulation, Assumption 2.8 has to hold. Usually coercivity (2.8) of the bilinear form is shown by the Poincaré-inequality (Brenner and Scott, 2008, Proposition 5.3.5). However, the inequality only applies if there is a Dirichlet boundary condition. Since the stated problem has no Dirichlet boundary condition, a modified Poincaré-inequality can show coercivity, see (Brenner and Scott, 2008, Proposition 5.3.2). Using that the random field is positive and bounded (5.2) and that the parameter ξ^{in} is positive, then Assumption 2.8 holds and it exists a unique solution of the weak formulation.

5.2 Finite element simulations

In this section numerical simulations of the heat conduction, see Problem 5.1, are illustrated. A few remarks on the expected solution behavior are given. Since the right hand side in Problem 5.1 is zero, the domain is not heated by an external source. However, the domain is only heated on the left boundary of the domain by a Robin boundary condition. The heat inflow on the left boundary is given by $\kappa(1-u)$. Due to the homogeneous initial condition, the temperature u at initial point in time is zero and hence at initial time the domain is heated by the random field $\kappa > 0$. Evolving in time the temperature u increases by the heat inflow $\kappa(1-u)$. Once the temperature becomes one, there is no more heating and hence the temperature fulfills $0 \le u \le 1$. In consequence the Robin boundary condition on $\partial\Omega_{\mathrm{out}}$ is positive, i.e. $\kappa(1-u) \ge 0$. Since the temperature u and the parameter ξ^{in} is positive, the Robin boundary condition acting on the inner boundary $\partial\Omega_{\mathrm{in}}$ is negative, i.e. $-\xi^{\mathrm{in}}u \le 0$. The minus sign models cooling. Starting at initial time with zero temperature, there is no cooling on $\partial\Omega_{\mathrm{in}}$. Once the temperature increases up to one, the domain is cooled by ξ^{in}.

The heat conduction in Problem 5.1 is solved in the spatial domain $\Omega = \{[0,10] \times [0,4]\} \setminus \{\{(1,3) \times (1,3)\} \cup \{(4,6) \times (1,3)\} \cup \{(7,9) \times (1,3)\}\}$. The domain is meshed by 1980 triangles, see Fig. 5.2. The numerical solutions are obtained by a finite element method using piecewise linear basis functions, see,
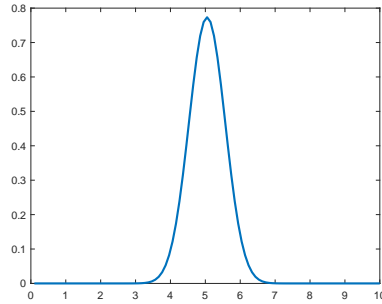
Figure 5.3: Pdf of beta distribution on $[0.1, 10]$ and scaling parameter 50

e.g., (Brenner and Scott, 2008, section 0.4). Further notations regarding the finite element discretization are stated in section 2.2.2. The space discretization uses $\mathcal{N} = 1132$ degrees of freedom. For the time discretization an implicit Euler method is applied with time step size $\Delta t = 0.2$ and $K = 100$. In consequence, the heat conduction is considered up to final time $T = 20$, i.e. the time interval is determined by $I = [0, 20]$.

The eigenpairs $(\lambda_l, c_l)_{l=1}^{N_{\mathrm{KL}}}$ of the random field (5.1) are obtained from the integral equation (A.10) with covariance kernel $C(x, y) = \exp(-|x - y|/a)$ and correlation length $a = 2$. The random field is truncated for a tolerance $\epsilon_{\mathrm{KL}} = 0.1$, see (A.12), which determines the truncation index $N_{\mathrm{KL}} = 9$. In order to fulfill positivity and boundedness (5.2) of the truncated random field, the expectation of the field $\alpha_0 = 10$ is chosen.

The stochastic parameters $\xi^{\mathrm{out}} = (\xi_l^{\mathrm{out}})_{l=1}^{N_{\mathrm{KL}}} \in \Gamma^{\mathrm{out}}$ and $\xi^{\mathrm{in}} \in \Gamma^{\mathrm{in}}$ are elements of $\Gamma^{\mathrm{out}} = [a_{\mathcal{U}}, b_{\mathcal{U}}]^{N_{\mathrm{KL}}}$ and $\Gamma^{\mathrm{in}} = [a_{\mathcal{B}}, b_{\mathcal{B}}]$. Recall, the interval bounds of the uniform distribution are determined by $a_{\mathcal{U}} = -\sqrt{3}$ and $b_{\mathcal{U}} = \sqrt{3}$. The beta distribution $\mathcal{B}(p, q, a_{\mathcal{B}}, b_{\mathcal{B}})$ is determined by the positive interval bounds $a_{\mathcal{B}} = 0.1$, $b_{\mathcal{B}} = 10$ and the scaling parameters $p = q = 50$. The choice of the scaling parameters guarantee that the probability density function (pdf) is far from the uniform distribution and hence the weighted approach is expected to have more impact on a different reduced basis selection compared to the non-weighted approach. The corresponding pdf is shown in Fig. 5.3.

By means of section 2.2.3 the finite element algebraic equations of the weak formulation for Problem 5.1 are derived using the corresponding bilinear form (5.3) and functionals (5.4). The solution of the algebraic equations gives the temperature in each grid point of the mesh. In order to illustrate the behavior of the temperature, the heat conduction is computed for the interval bounds of the cooling parameter ξ^{in} at different time points $t = 1$ and $t = 20$. Therefore, denote $\xi^1 = (\xi^{\mathrm{out},1}, \xi^{\mathrm{in},1})$ and $\xi^2 = (\xi^{\mathrm{out},2}, \xi^{\mathrm{in},2})$, where $\xi^{\mathrm{in},1} = 0.1$ and $\xi^{\mathrm{in},2} = 10$. The parameters $\xi^{\mathrm{out},1} = (\xi_l^{\mathrm{out},1})_{l=1}^{N_{\mathrm{KL}}}$ and $\xi^{\mathrm{out},2} = (\xi_l^{\mathrm{out},2})_{l=1}^{N_{\mathrm{KL}}}$ are two uniformly distributed random samples. The associated results can be seen in Fig. 5.4. Indeed, the figures show that the heat distributes in a larger part of the domain for the parameter ξ^1 containing the smaller cooling parameter (first row) compared to the parameter ξ^2 containing the larger cooling parameter (second row).

5.3   Reduced order modeling

In this section the model order reduction techniques from chapters 3 and 4 are utilized. By means of a non-weighted RBM, a weighted RBM and a POD reduced spaces are constructed. The different reduced spaces yield approximations of the finite element solution. The non-weighted and the weighted RBM constructs the reduced space based on the POD-greedy algorithm, see section 3.3, whereas the POD yields a reduced space obtained by an eigenvalue problem, see section 4.2. However, the differences of the non-weighted and the weighted reduced space construction is explained in sections 3.3.1 and 3.3.2, where section 3.3.3 discusses differences from a theoretical point of view. The objective of this section is the comparison of these MOR methods regarding the expected solution error and the expected output error. The approximation obtained from a weighted RBM should yield better error convergence for the expected value of the solution error and output error compared to the approximation obtained from a non-weighted RBM. In order to assess the accuracy of the weighted approach compared to the best possible approximation, a comparison to the reduced solution obtained by the POD is drawn, which is optimal in a least squares sense, see (4.6).

The reduced spaces obtained from the POD-greedy procedure, see Algorithm 1, uses a finite parameter set Γ_{train}. This parameter set approximates the parameter domain $\Gamma = \left[-\sqrt{3}, \sqrt{3}\right]^{N_{\text{KL}}} \times [0.1, 10]$ with $|\Gamma_{\text{train}}| = 500$ independent uniformly distributed parameter samples. As a stopping criterion a predefined reduced space dimension $N_{max} = 30$ is chosen. Depending on whether the non-weighted or the weighted approach is utilized, non-weighted error estimators (3.30) and (3.34) or weighted error estimators (3.38) and (3.39) are chosen as basis selection criterion in the POD-greedy. Further details regarding the non-weighted and weighted reduced space construction can be found in sections 3.3.1 and 3.3.2. With these reduced spaces, the reduced solutions can be computed by a Galerkin method in section 3.1 with the corresponding bilinear form $a(\cdot, \cdot; \xi)$ (5.3) and functional $b(\cdot; \xi)$ (5.4). By means of section 3.1.1 the reduced algebraic equations of the weak formulation for Problem 5.1 are derived. The solution of the algebraic equations gives the coefficients of a linear combination of the reduced basis which approximates the finite element solution.
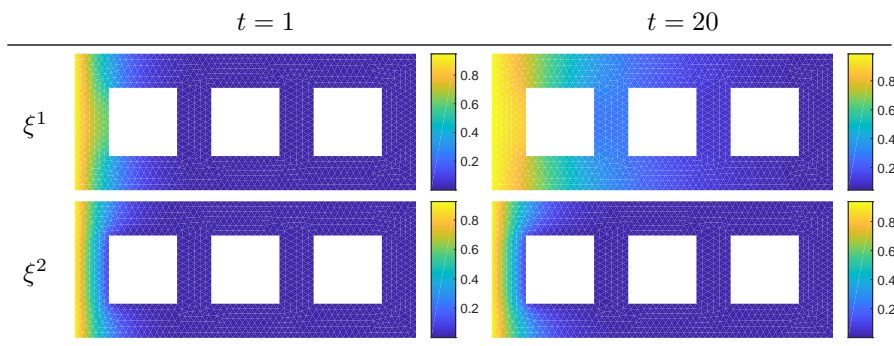

Figure 5.4: 2d heat conduction for different parameters and points in time

(a) Error comparison (5.6)

(c) Error comparison (5.8)

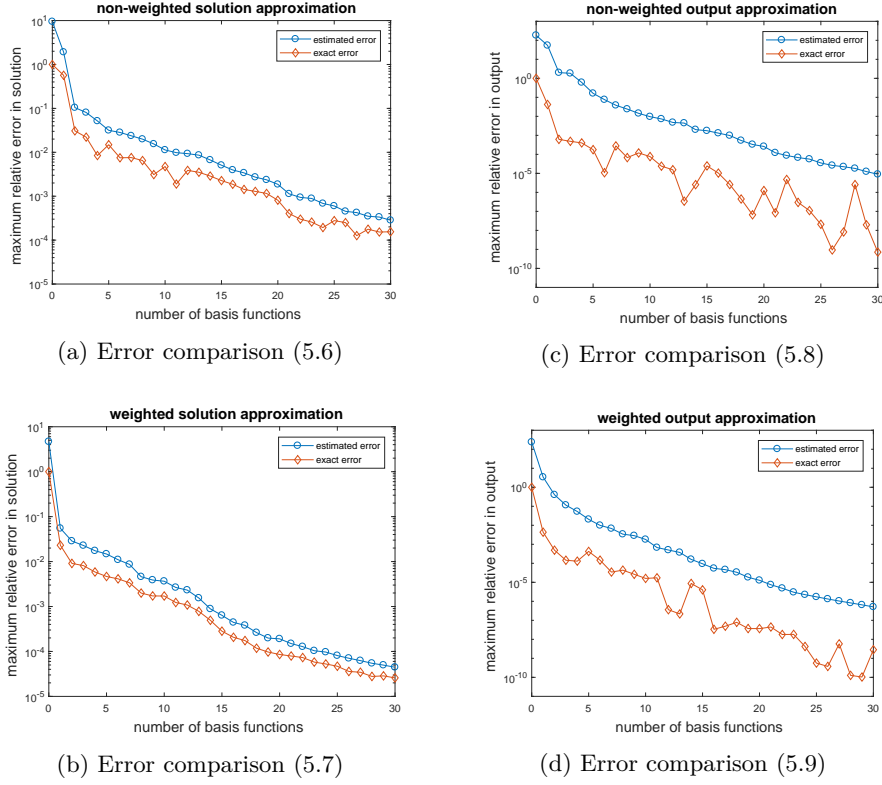(b) Error comparison (5.7)

(d) Error comparison (5.9)

Figure 5.5: Pointwise relative error convergence of true error and error bounds

The reduced space obtained from the POD is based on the snapshots

$$\{u_h^k(\xi)\colon\ k=1,\dots,K,\ \xi\in\Gamma_{\text{train}}\}. \tag{5.5}$$

Since the parameter set Γ_{train} is uniformly distributed, the snapshots are equipped with the pdf. This means that the eigenvalue problem based on (4.9) is solved for the snapshots

$$\{\sqrt{\rho(\xi)}u_h^k(\xi)\colon\ k=1,\dots,K,\ \xi\in\Gamma_{\text{train}}\}.$$

Once the eigenvalue problem is solved and the obtained eigenfunctions span the reduced space, the reduced solution is computed by the orthogonal projection, see (4.7).

In the following the results from section 3.2 are illustrated. The error estimators are based on the coercivity constant and the dual norm of the residuals in each time step. Therefore, the coercivity constant $\alpha(\xi)$ in (2.8) is computed for each $\xi\in\Gamma_{\text{train}}$ by a generalized eigenvalue problem, see, e.g., (Quarteroni et al., 2016, section 2.4.3). The computation of the dual norms of the primal residual and the dual norms of the dual residual are described in section 3.2.3. In Fig. 5.5 a pointwise comparison between the rigorous error estimators Δ_N^u in (3.30), $\Delta_N^{u;\rho}$ in (3.38), $\Delta_{N,\tilde{N}}^s$ in (3.34) and $\Delta_{N,\tilde{N}}^{s,\rho}$ in (3.39) (in blue) and the exact errors (in red) is drawn. The exact error is measured in the

finite element	non-weighted RBM	weighted RBM
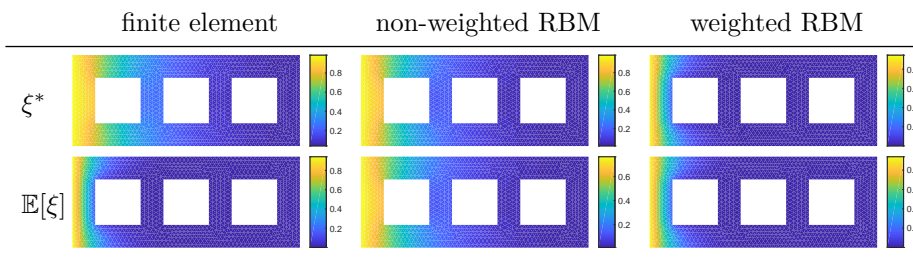
Figure 5.6: Comparison of different solutions at final time $T = 20$

parameter-dependent energy norm $\|\cdot\|_{\xi}^{\mathrm{pr}}$ defined in (3.28). The figures contain eight different errors. The top left figure compares

$$\frac{\max\limits_{\xi\in\Gamma_{\mathrm{train}}} \Delta_N^u(\xi)}{\max\limits_{\xi\in\Gamma_{\mathrm{train}}} \|u_h(\xi)\|_{\xi}^{\mathrm{pr}}} \quad \text{and} \quad \frac{\|u_h(\xi) - u_N(\xi)\|_{\xi}^{\mathrm{pr}}}{\max\limits_{\xi\in\Gamma_{\mathrm{train}}} \|u_h(\xi)\|_{\xi}^{\mathrm{pr}}}, \tag{5.6}$$

whereas the numerator of the second term is determined for the parameter $\xi = \arg\max_{\xi\in\Gamma_{\mathrm{train}}} \Delta_N^u(\xi)$. The bottom left figure compares

$$\frac{\max\limits_{\xi\in\Gamma_{\mathrm{train}}} \Delta_N^{u,\rho}(\xi)}{\max\limits_{\xi\in\Gamma_{\mathrm{train}}} \sqrt{\rho(\xi)}\|u_h(\xi)\|_{\xi}^{\mathrm{pr}}} \quad \text{and} \quad \frac{\|u_h(\xi) - u_N(\xi)\|_{\xi}^{\mathrm{pr}}}{\max\limits_{\xi\in\Gamma_{\mathrm{train}}} \sqrt{\rho(\xi)}\|u_h(\xi)\|_{\xi}^{\mathrm{pr}}}, \tag{5.7}$$

whereas the numerator of the second term is determined for the parameter $\xi = \arg\max_{\xi\in\Gamma_{\mathrm{train}}} \Delta_N^{u,\rho}(\xi)$. The top right figure compares

$$\frac{\max\limits_{\xi\in\Gamma_{\mathrm{train}}} \Delta_{N,\tilde{N}}^s(\xi)}{\max\limits_{\xi\in\Gamma_{\mathrm{train}}} |s_h(\xi)|} \quad \text{and} \quad \frac{|s_h(\xi) - s_{N,\tilde{N}}(\xi)|}{\max\limits_{\xi\in\Gamma_{\mathrm{train}}} |s_h(\xi)|}, \tag{5.8}$$

whereas the numerator of the second term is determined for the parameter $\xi = \arg\max_{\xi\in\Gamma_{\mathrm{train}}} \Delta_{N,\tilde{N}}^s(\xi)$. The bottom right figure compares

$$\frac{\max\limits_{\xi\in\Gamma_{\mathrm{train}}} \Delta_{N,\tilde{N}}^{s,\rho}(\xi)}{\max\limits_{\xi\in\Gamma_{\mathrm{train}}} \rho(\xi)|s_h(\xi)|} \quad \text{and} \quad \frac{|s_h(\xi) - s_{N,\tilde{N}}(\xi)|}{\max\limits_{\xi\in\Gamma_{\mathrm{train}}} \rho(\xi)|s_h(\xi)|}, \tag{5.9}$$

whereas the numerator of the second term is determined for the parameter $\xi = \arg\max_{\xi\in\Gamma_{\mathrm{train}}} \Delta_{N,\tilde{N}}^s(\xi)$. It is observed that the exact error is closer to the error bounds for the solution approximation (Figs. 5.5a and 5.5b) compared to the output approximation (Figs. 5.5c and 5.5d). This coincides with results obtained from elliptic theory, e.g. (Haasdonk, 2017, Proposition 2.21 and Example 6). However, analogue results for the parabolic case are not available. Furthermore, considering the y-axis in Fig. 5.5, double accuracy of the output approximation compared to the solution approximation is observed. This is based on the output correction (3.16). The figures show that the error bounds are reliable. Especially for the solution error, effective bounds are obtained for this example.

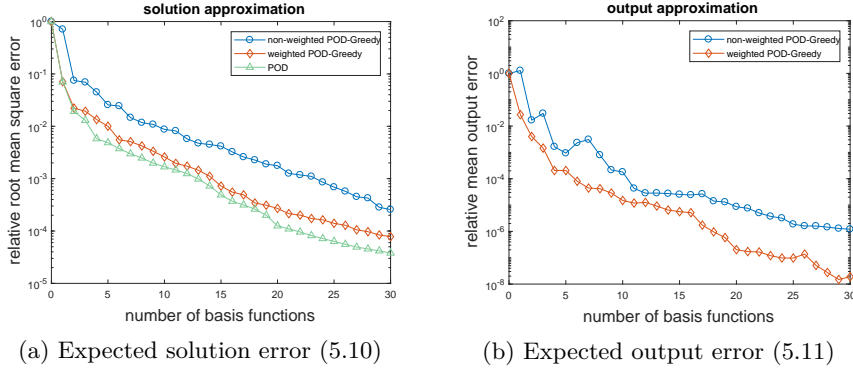In Fig. 5.6 solutions for different parameters are compared. The solutions

(a) Expected solution error (5.10) (b) Expected output error (5.11)

Figure 5.7: Comparing non-weighted, weighted POD-greedy and POD

are evaluated at the end point in time T. The different columns show the solutions obtained from a finite element method, a non-weighted RBM and a weighted RBM, respectively. The RBM in column two and three uses $N = 1$ basis function, albeit the non-weight and weighted basis differs. The first row states the solutions for a sampled parameter $\xi^* = (\xi^{\text{out},*}, \xi^{\text{in},*}) \notin \Gamma_{\text{train}}$ with $\xi^{\text{in},*} = 0.1143 \in [0.1, 10]$ close to the left bound of its support. It is observed that the non-weighted approach approximates the parameter ξ^* better than the weighted approach. However, since the pdf gives $\rho(\xi^{\text{in},*}) = 1.5876 * 10^{-110}$, an accurate representation of the parameter ξ^* is not necessary for the approximation of the expected value. The second row states the solutions for the expectation of the parameter $\mathbb{E}[\xi] = (\mathbb{E}[\xi^{\text{out}}], \mathbb{E}[\xi^{\text{in}}]) \notin \Gamma_{\text{train}}$. Based on the stated probability distributions of ξ^{out} and ξ^{in}, it follows $\mathbb{E}[\xi^{\text{out}}] = (0, \ldots, 0)$ and $\mathbb{E}[\xi^{\text{in}}] = 5.05$, respectively. The plots show that the finite element solution for parameter $\mathbb{E}[\xi]$ is better approximated by the weighted reduced solution compared to the non-weighted reduced solution. This is a first insight that indicates a better approximation of the expected value by a weighted approach.

In the following different ROMs are compared regarding the root mean square solution error and the mean absolute output error. The error convergence of these errors for the first $N_{max} = 30$ basis functions are shown in Fig. 5.7. Fig. 5.7a illustrates the relative root mean square solution error

$$\frac{\mathbb{E}^{\mathcal{U}}_{\text{MC}}\left[\Delta t \sum_{k=1}^{K} \left\| u_h^k - u_N^k \right\|_X^2\right]^{1/2}}{\mathbb{E}^{\mathcal{U}}_{\text{MC}}\left[\Delta t \sum_{k=1}^{K} \left\| u_h^k \right\|_X^2\right]^{1/2}} \tag{5.10}$$

and Fig. 5.7b shows the relative mean absolute output error

$$\frac{\mathbb{E}^{\mathcal{U}}_{\text{MC}}[|s_h - s_{N,\tilde{N}}|]}{\mathbb{E}^{\mathcal{U}}_{\text{MC}}[|s_h|]}. \tag{5.11}$$

The Monte Carlo estimator $\mathbb{E}^{\mathcal{U}}_{\text{MC}}$ is defined in (4.5), which uses the samples from the training parameter set Γ_{train}. The snapshots $u_h^k(\xi)$ in (5.10) are defined in (5.5) and computed by Problem 2.11. They determine the finite element output $s_h(\xi)$, see (2.13c) and (5.4). There are three different reduced solutions $u_N^k(\xi)$: the non-weighted, the weighted and the POD reduced solution. The non-weighted and the weighted RB solutions are determined by Problem 3.1 using
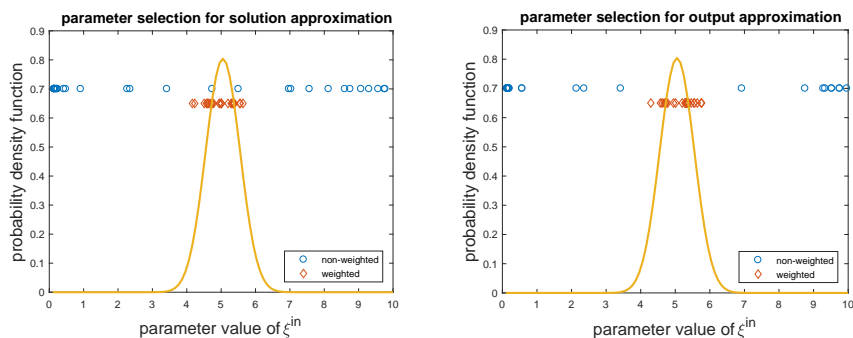
Figure 5.8: Parameter selection for solution and output approximation

the non-weighted reduced space (see section 3.3.1) and the weighted reduced space (see section 3.3.2), respectively. The POD reduced solution is given by (4.7). Recall, the POD cannot construct a reduced solution, which minimizes the expected output error in (5.11). Hence, for the expected output error only the non-weighted and weighted RBM are compared. In Fig. 5.7a the optimal error convergence for the expectation obtained by the POD is observed. The weighted approach yields better error results compared to the non-weighted approach. Furthermore, the plot shows that the expected solution error obtained from the weighted POD-greedy is closer to the optimum than to the expected solution error obtained from the non-weighted POD-greedy. As for the expected solution error, Fig. 5.7b shows that in each iteration of the POD-greedy the weighted approach gives better error results regarding the expected output error compared to the non-weighted approach.

In Fig. 5.8 the parameter selection for the non-weighted and the weighted approach for the first $N_{max} = 30$ parameters are compared. The left figure shows the parameter selection obtained by maximizing the non-weighted and weighted solution error estimator (3.30) and (3.38), respectively. The right figure states the parameter selection obtained by maximizing the non-weighted and weighted output error estimator (3.34) and (3.39), respectively. Both figures clearly show that the weighted approach chooses parameter samples around the peak of the pdf. For the non-weighted case also parameters far from the peak, whose pdf is almost zero, are chosen.

The numerical results in Fig. 5.7 show that the weighted approach gives better error convergence if the objective is the approximation of the expected solution error or the expected output error in this example. This behavior is also illustrated in Fig. 5.6. It has been shown that the error estimators of section 3.2 are upper bounds for the exact errors over a finite dimensional parameter set. By means of the POD, the optimal error convergence of the expected solution is stated. Furthermore, it has been shown that the weighted reduced solution is closer to the optimum than to the non-weighted reduced solution.

Chapter 6

Conclusion

The Focus of this thesis was on parabolic parametrized partial differential equations (PPDEs) with random input data. Reduced order models of the parabolic PPDE were stated applying different model order reduction techniques. The goal of this work was to construct efficient reduced order models regarding statistical quantities of errors, which resulted from model order reduction. To this end, this work extends a weighted reduced basis method (RBM) to parabolic problems with random input data.

In the first part of the thesis the model problem was introduced. The strong formulation of a linear parabolic partial differential equation was stated and the corresponding weak formulation was derived. The random input data were represented by random parameters and the stochastic framework was established. Assumptions for the existence and uniqueness of a solution to the parametrized weak formulation were stated. A quantity of interest (or output) was determined by a linear functional which mapped the solution to a real number. An adjoint correction, obtained by a standard primal-dual approach, was utilized in order to improve error bounds for the output error and increase the accuracy of the output computation. Hence, the dual problem of the model problem was derived. The primal problem and the dual problem were discretized by an implicit Euler method in time and a finite element method in space.

The second part of this work focused on model order reduction techniques for parabolic PPDEs with random input data. In order to replace the high-dimensional finite element model by a low-dimensional surrogate, an RBM was used. The reduced order models were stated for the primal and the dual problem, which provided approximations for the finite element solution and the finite element output for each element of the parameter domain. The solution of the reduced dual problem was used to improve the accuracy of the reduced output computation. Assuming an affine parameter dependence led to an efficient computation of the reduced solution and the reduced output independent of the dimension of the finite element discretization. The reduced space construction was based on a POD-greedy algorithm, introduced in Haasdonk and Ohlberger (2008). In this work the POD-greedy used rigorous a posteriori error bounds for parabolic PPDEs, derived in Grepl and Patera (2005), as a selection criterion for the basis functions. The error estimators assess the accuracy of the approximation obtained by the RBM with respect to the finite element approximation and are computationally cheap compared to the exact error computations. These error

estimators were extended to a time-continuous framework.

Inspired by Chen et al. (2013), where the idea of a weighted RBM was introduced for elliptic problems, the idea of a weighted RBM was transferred to parabolic PPDEs with random input data. Weighted error estimators used the probability density function as a weight function in order to assign higher priority to input data which are more probable. These computationally cheap weighted error estimators were combined with the POD-greedy algorithm, called weighted POD-greedy, in order build a weighted reduced space.

In addition to the non-weighted RBM and the weighted RBM, a POD was utilized in order to obtain an optimal reduced space in a root mean square sense. The expected value was approximated by a Monte Carlo (MC) estimator using uniformly distributed random variables. The reduced POD solution was determined by an orthogonal projection of an MC snapshot onto the reduced POD space, such that the resulting expected squared solution error becomes minimal.

Numerical results for a two dimensional heat conduction with random input data were illustrated. The input data entered the model problem via the boundary conditions and were characterized by a random field and a random model coefficient. The random field was approximated by a truncated Karhunen-Loève (KL) expansion using uniformly distributed random variables. It was shown that for this example a weighted RBM yields better error convergence regarding the expected errors than a non-weighted RBM. It was observed that the convergence of the expected error regarding a weighted RBM was closer to the optimum than to the non-weighted approach.

The aim of this work was to find efficient reduced solutions with respect to the expected value of the solution error and the expectation of the output error. This work showed that a weighted POD-greedy outperforms a POD-greedy in the context of parabolic PPDEs with random input data for a numerical example.

Appendix A

A.1 Spaces

Definition A.1 (Hilbert space)**.** A Hilbert space X is a complete space endowed with an inner product $(\cdot, \cdot)_X \colon X \times X \to \mathbb{R}$, which induces the norm

$$\|f\|_X = \sqrt{(f, f)_X}.$$

Definition A.2 (Bochner space)**.** Let A be a nonempty and compact subset of $\mathbb{R}^p$, $p \in \mathbb{N}$, and X be a Hilbert space. The Bochner space $L^2(A; X)$ is defined by

$$L^2(A; X) = \left\{ f \colon A \to X \quad : f \text{ measurable}, \int_A \|f(a)\|_X^2 \, \mathrm{d}a < \infty \right\}$$

with the inner product

$$(f, g)_{L^2(A;X)} = \int_A (f(a), g(a))_X \mathrm{d}a$$

and the induced norm

$$\|f\|_{L^2(A;X)} = \sqrt{(f, f)_{L^2(A;X)}}.$$

A.2 Derivation of homogeneous initial condition

The linear parabolic PDE in (2.1) with inhomogeneous initial condition is considered. In the following the problem is transformed, such that the initial condition becomes homogeneous. Therefore, let $u_0 \colon \Omega \to \mathbb{R}$. The linear parabolic PDE for an inhomogeneous initial condition reads as follows: Find the solution $u \colon \Omega \times I \to \mathbb{R}$, such that

$$\partial_t u - \Delta u = f, \quad \text{in } \Omega \times I,$$
$$\frac{\partial u}{\partial n} = g, \quad \text{on } \partial\Omega \times I,$$
$$u = u_0, \quad \text{on } \Omega \times \{0\}.$$

The solution u is composed of a homogeneous part $\tilde{u}$ and an inhomogeneous part $\bar{u}_0$, i.e.

$$u = \tilde{u} + \bar{u}_0,$$

with $\bar{u}_0(x,t) = u_0(x)$, $\forall t \in I$. Solving the problem for the homogeneous solution yield: Find the solution $\tilde{u} \colon \Omega \times I \to \mathbb{R}$, such that

$$\partial_t \tilde{u} - \Delta \tilde{u} = \tilde{f}, \quad \text{in } \Omega \times I,$$
$$\frac{\partial \tilde{u}}{\partial n} = \tilde{g}, \quad \text{on } \partial\Omega \times I,$$
$$\tilde{u} = 0, \quad \text{on } \Omega \times \{0\},$$

where $\tilde{f} := f - \partial_t(\bar{u}_0) + \Delta u_0$ and $\tilde{g} := g - \frac{\partial u_0}{\partial n}$.

A.3 Output evaluation

The output can be computed by either using the primal solution $u(t;\xi)$ or the dual solution $\psi(t;\xi)$. This is accomplished by, starting with (2.27),

$$\int_0^T g(u(t;\xi);\xi)\mathrm{d}t + l(u(T;\xi);\xi)$$
$$\overset{(2.37\mathrm{a})}{=} \int_0^T -\langle u(t;\xi), \partial_t \psi(t;\xi)\rangle + a(u(t;\xi), \psi(t;\xi);\xi)\mathrm{d}t + l(u(T;\xi);\xi)$$
$$\overset{(2.37\mathrm{b})}{=} \int_0^T -\langle u(t;\xi), \partial_t \psi(t;\xi)\rangle + a(u(t;\xi), \psi(t;\xi);\xi)\mathrm{d}t + (u(T;\xi), \psi(T;\xi))_{L^2(\Omega)}$$
$$= \int_0^T \langle \partial_t u(t;\xi), \psi(t;\xi)\rangle + a(u(t;\xi), \psi(t;\xi);\xi)\mathrm{d}t$$
$$\overset{(2.7\mathrm{a})}{=} \int_0^T b(\psi(t;\xi);\xi)\mathrm{d}t,$$

where the third equality uses integration by parts and (2.7b). Due to the homogeneous initial condition the output evaluation, utilizing the dual solution, reduces to the computation of the integral.

This equality can be of special interest, if the quantity of interest has to be computed for many different right hand sides b. Without the dual approach the computationally expensive primal problem needs to be solved for each right hand side. Afterwards the corresponding primal solutions are inserted into the functional. However, utilizing the dual approach, the computationally expensive dual solution is computed only once and it is inserted into each single right hand side.

A.4 Compliant case

For the trivial case where the primal problem (2.7) and the dual problem (2.36) satisfy $b \equiv g$. Then, for $t \in (0,T)$, there exists a $t^* \in (0,T)$, such that

$$\langle \partial_t u(t;\xi), v\rangle + a(u(t;\xi), v;\xi) = -\langle v, \partial_t \psi(t^*;\xi)\rangle + a(v, \psi(t^*;\xi);\xi), \quad \forall v \in X.$$

If the bilinear form is symmetric, see (2.10), and since the equation has to hold for all $v \in X$, it holds that

$$u(t;\xi) = \psi(t^*;\xi),$$
$$\partial_t u(t;\xi) = -\partial_t \psi(t^*;\xi).$$

Choosing $t^* := T - t$ fulfills these equations. Hence, the solution of the backward problem coincides with the solution of the forward problem, such that $u(t; \xi) = \psi(T - t; \xi)$, $t \in (0, T)$. Additionally, if the right hand sides of the initial condition and the final condition coincide, then $u(0; \xi) = \psi(T; \xi)$.

A similar relation for the time discretized equations is observed. If the right hand side of the time discretized primal problem and the right hand side of the time discretized dual problem coincides, it holds, for $k = 1, \ldots, K - 1$, there exists a $\tilde{k} = 1, \ldots, K - 1$, such that

$$(u^k(\xi) - u^{k-1}(\xi), v)_{L^2(\Omega)} + \Delta t\, a(u^k(\xi), v; \xi)$$
$$= (v, \psi^{\tilde{k}}(\xi) - \psi^{\tilde{k}+1}(\xi))_{L^2(\Omega)} + \Delta t\, a(v, \psi^{\tilde{k}}(\xi); \xi), \quad \forall v \in X.$$

For a symmetric bilinear form, see (2.10), and since the equation has to hold for all $v \in X$, it holds that

$$u^k(\xi) = \psi^{\tilde{k}}(\xi),$$
$$u^k(\xi) - u^{k-1}(\xi) = \psi^{\tilde{k}}(\xi) - \psi^{\tilde{k}+1}(\xi).$$

Choosing $\tilde{k} := K - k$ fulfills these equations. Hence the solution of the backward problem coincides with the solution of the forward problem, such that $u^k(\xi) = \psi^{K-k}(\xi)$, $k = 1, \ldots, K - 1$. Additionally, if the right hand sides of the initial condition and the final condition coincide, then $u^0(\xi) = \psi^K(\xi)$.

This means that for the compliant case, where the right hand sides of the primal and the dual problem coincide, the dual solution coincides with the primal solution.

A.5 Error bounds for parameter independent norm

In section 3.2 error bounds for parameter dependent norms were derived. Furthermore, error bounds for parameter independent norms can be stated. However, estimating the solution error in a parameter independent norm entails larger constants for the error bounds. This follows from the inequality, see Proposition 3.16,

$$\left(\left\| e_N^K(\xi) \right\|_{L^2(\Omega)}^2 + \Delta t \sum_{k=1}^{K} a(e_N^k(\xi), e_N^k(\xi); \xi) \right)^{1/2} \overset{(3.30)}{\leq} \Delta_N^u(\xi)$$

and using (2.8) for the left hand side gives

$$\left(\left\| e_N^K(\xi) \right\|_{L^2(\Omega)}^2 + \Delta t \sum_{k=1}^{K} \left\| e_N^k(\xi) \right\|_X^2 \right)^{1/2} \leq C \Delta_N^u(\xi),$$

with the constant $C := 1/\min\{1, \sqrt{\alpha(\xi)}\} \geq 1$. Here the left hand side of the inequality does not depend on the parameter dependent norm $\|\cdot\|_\xi$ anymore.

Further, this idea applies for the dual solution error estimation as well. Taking the inequality, see Proposition 3.18,

$$\left(\left\| \tilde{e}_{\tilde{N}}^0(\xi) \right\|_{L^2(\Omega)}^2 + \Delta t \sum_{k=0}^{K-1} a(\tilde{e}_{\tilde{N}}^k(\xi), \tilde{e}_{\tilde{N}}^k(\xi); \xi) \right)^{1/2} \overset{(3.32)}{\leq} \Delta_{\tilde{N}}^{\psi}(\xi)$$

and using (2.8) for the left hand side gives

$$\left(\left\| \tilde{e}_{\tilde{N}}^0(\xi) \right\|_{L^2(\Omega)}^2 + \Delta t \sum_{k=0}^{K-1} \left\| \tilde{e}_{\tilde{N}}^k(\xi) \right\|_X^2 \right)^{1/2} \leq C \Delta_{\tilde{N}}^{\psi}(\xi)$$

with the constant $C = 1/\min\{1, \sqrt{\alpha(\xi)}\} \geq 1$. Again, the left hand side of the inequality does not depend on the parameter dependent norm $\|\cdot\|_\xi$ anymore.

If the solution error for time index k can be estimated by the previous time step, then the coefficient in the error bound obtains the time index as an exponent, cf. (Haasdonk, 2017, Proposition 2.80).

A.6   Time continuous error estimators

As it was done in section 3.2.1, the error estimators can be derived for the time continuous case as well. For the sake of notational convenience the time continuous primal solution error $e_N(t; \xi) = u_h(t; \xi) - u_N(t; \xi) \in X_h$ and the time continuous dual solution error $\tilde{e}_{\tilde{N}}(t; \xi) = \psi_h(t; \xi) - \psi_{\tilde{N}}(t; \xi) \in X_h$ are abbreviated by $e_N(t; \xi) = e_N$ and $\tilde{e}_{\tilde{N}}(t; \xi) = \tilde{e}_{\tilde{N}}$ respectively.

A.6.1   Primal solution error estimator

The time continuous primal error estimator is derived using the time continuous residual

$$\begin{aligned} r_N(v; \xi) &= b(v; \xi) - (\partial_t u_N(t; \xi), v)_{L^2(\Omega)} - a(u_N(t; \xi), v; \xi) \\ &= (\partial_t e_N(t; \xi), v)_{L^2(\Omega)} + a(e_N(t; \xi), v; \xi). \end{aligned} \tag{A.3}$$

Insert $e_N(t; \xi) = e_N$ in (A.3) and integration over time yields

$$\int_0^T r_N(e_N; \xi) \mathrm{d}t = \int_0^T (\partial_t e_N, e_N)_{L^2(\Omega)} + a(e_N, e_N; \xi) \mathrm{d}t.$$

The estimation follows the steps as in the proof of Proposition 3.16. The left hand side is estimated by Proposition 2.4, $ab \leq \frac{1}{2}\left(\frac{1}{c^2}a^2 + c^2 b^2\right)$, $a, b \in \mathbb{R}$, $c \in \mathbb{R} \setminus \{0\}$ and (2.8), such that

$$\int_0^T (\partial_t e_N, e_N)_{L^2(\Omega)} + a(e_N, e_N; \xi) \mathrm{d}t \leq \int_0^T \frac{1}{2\alpha(\xi)} \|r_N(\cdot; \xi)\|_{X'}^2 + \frac{1}{2} a(e_N, e_N; \xi) \mathrm{d}t.$$

Multiplying this inequality by two and using $e_N(0; \xi) = 0$ gives

$$\|e_N(T)\|_{L^2(\Omega)}^2 + \int_0^T a(e_N, e_N; \xi) \mathrm{d}t \leq \frac{1}{\alpha(\xi)} \int_0^T \|r_N(\cdot; \xi)\|_{X'}^2 \, \mathrm{d}t = \left(\Delta_N^{u,[0,T]} \right)^2. \tag{A.4}$$

The left hand side represents the squared primal parameter-dependent energy norm (3.28) for continuity in time.

A.6.2 Dual solution error estimator

The time continuous dual error estimator is derived using the time continuous residual

$$
\begin{aligned}
\tilde{r}_{\tilde{N}}(v;\xi) &= (v, \partial_t \psi_{\tilde{N}}(t;\xi))_{L^2(\Omega)} - a(v, \psi_{\tilde{N}}(t;\xi);\xi) \\
&= -(v, \partial_t \tilde{e}_{\tilde{N}}(t;\xi))_{L^2(\Omega)} + a(v, \tilde{e}_{\tilde{N}}(t;\xi);\xi),
\end{aligned}
\tag{A.5}
$$

Insert $\tilde{e}_{\tilde{N}}(t;\xi) = \tilde{e}_{\tilde{N}}$ in (A.5) and integration over time yields

$$
\int_0^T \tilde{r}_{\tilde{N}}(\tilde{e}_{\tilde{N}};\xi)\mathrm{d}t = \int_0^T -(\tilde{e}_{\tilde{N}}, \partial_t \tilde{e}_{\tilde{N}})_{L^2(\Omega)} + a(\tilde{e}_{\tilde{N}}, \tilde{e}_{\tilde{N}};\xi)\mathrm{d}t.
$$

The estimation follows the steps as in the proof of Proposition 3.18. The left hand side is estimated by Proposition 2.4, $ab \leq \frac{1}{2}\left(\frac{1}{c^2}a^2 + c^2 b^2\right)$, $a, b \in \mathbb{R}$, $c \in \mathbb{R} \setminus \{0\}$ and (2.8), such that

$$
\begin{aligned}
\int_0^T -(\tilde{e}_{\tilde{N}}, \partial_t \tilde{e}_{\tilde{N}})_{L^2(\Omega)} + a(\tilde{e}_{\tilde{N}}, \tilde{e}_{\tilde{N}});\xi)\mathrm{d}t \leq \int_0^T &\frac{1}{2\alpha(\xi)}\|\tilde{r}_{\tilde{N}}(\cdot;\xi)\|_{X'}^2 \\
&+ \frac{1}{2}a(\tilde{e}_{\tilde{N}}, \tilde{e}_{\tilde{N}};\xi)\mathrm{d}t.
\end{aligned}
$$

Multiplying this inequality by two and integrating the L^2-norm on the left hand side gives

$$
\|\tilde{e}_{\tilde{N}}(0)\|_{L^2(\Omega)}^2 + \int_0^T a(\tilde{e}_{\tilde{N}}, \tilde{e}_{\tilde{N}});\xi)\mathrm{d}t \leq \frac{1}{\alpha(\xi)}\int_0^T \|\tilde{r}_{\tilde{N}}(\cdot;\xi)\|_{X'}^2\, \mathrm{d}t + \|\tilde{e}_{\tilde{N}}(T)\|_{L^2(\Omega)}^2.
\tag{A.6}
$$

The left hand side represents the dual parameter-dependent energy norm (3.29) for continuity in time. Furthermore, it is observed that the sum over all time steps in (3.32) is replaced by the integration over the time interval $[0, T]$. The solution error at the end point in time $\|\tilde{e}_{\tilde{N}}(T)\|_{L^2(\Omega)}$ is estimated by the residual

$$
\begin{aligned}
\tilde{r}_{\tilde{N}}^T(v;\xi) &= l(v;\xi) - (v, \psi_{\tilde{N}}(T;\xi))_{L^2(\Omega)} \\
&= (v, \tilde{e}_{\tilde{N}}(T;\xi))_{L^2(\Omega)}.
\end{aligned}
$$

It holds that

$$
\|\tilde{e}_{\tilde{N}}(T)\|_{L^2(\Omega)}^2 = (\tilde{e}_{\tilde{N}}(T), \tilde{e}_{\tilde{N}}(T))_{L^2(\Omega)} = \tilde{r}_{\tilde{N}}^T(\tilde{e}_{\tilde{N}}(T);\xi)
$$

and hence

$$
\|\tilde{e}_{\tilde{N}}(T)\|_{L^2(\Omega)} = \frac{\tilde{r}_{\tilde{N}}^T(\tilde{e}_{\tilde{N}}(T);\xi)}{\|\tilde{e}_{\tilde{N}}(T)\|_{L^2(\Omega)}} \leq \sup_{v \in X_h} \frac{|\tilde{r}_{\tilde{N}}^T(v;\xi)|}{\|v\|_{L^2(\Omega)}} = \Delta_{\tilde{N}}^{\psi, T}.
$$

Using that inequality in (A.6) yields the time continuous dual solution error estimator

$$
\begin{aligned}
\|\tilde{e}_{\tilde{N}}(0)\|_{L^2(\Omega)}^2 + \int_0^T a(\tilde{e}_{\tilde{N}}, \tilde{e}_{\tilde{N}};\xi)\mathrm{d}t \leq &\frac{1}{\alpha(\xi)}\int_0^T \|\tilde{r}_{\tilde{N}}(\cdot;\xi)\|_{X'}^2\, \mathrm{d}t \\
&+ \left(\Delta_{\tilde{N}}^{\psi, T}\right)^2 = \left(\Delta_{\tilde{N}}^{\psi, [0,T]}\right)^2.
\end{aligned}
\tag{A.7}
$$

A.6.3   Output error estimator

The time continuous output error estimator is evaluated by

$$|s_h(\xi) - s_{N,\tilde{N}}(\xi)| = |l(e_N(T;\xi);\xi) - \int_0^T r_N(\psi_{\tilde{N}}(t;\xi);\xi)\mathrm{d}t|$$

$$= |\int_0^T r_N(\psi_h(t;\xi);\xi)\mathrm{d}t - \int_0^T r_N(\psi_{\tilde{N}}(t;\xi);\xi)\mathrm{d}t|$$

$$= |\int_0^T r_N(\tilde{e}_{\tilde{N}}(t;\xi);\xi)\mathrm{d}t|.$$

The expression can be estimated as in Proposition 3.20, hence

$$|s_h(\xi) - s_{N,\tilde{N}}(\xi)| \overset{(2.5)}{\leq} \int_0^T \|r_N(\cdot;\xi)\|_{X'} \|\tilde{e}_{\tilde{N}}\|_X \, \mathrm{d}t$$

$$\leq \left(\int_0^T \frac{\|r_N(\cdot;\xi)\|_{X'}^2}{\alpha(\xi)}\mathrm{d}t\right)^{1/2} \left(\int_0^T \alpha(\xi) \|\tilde{e}_{\tilde{N}}\|_X^2 \, \mathrm{d}t\right)^{1/2}$$

$$\overset{(2.8)}{\leq} \Delta_N^{u,[0,T]} \left(\int_0^T a(\tilde{e}_{\tilde{N}}, \tilde{e}_{\tilde{N}};\xi)\mathrm{d}t\right)^{1/2}$$

$$\leq \Delta_N^{u,[0,T]} \left(\|\tilde{e}_{\tilde{N}}(0)\|_{L^2(\Omega)}^2 + \int_0^T a(\tilde{e}_{\tilde{N}}, \tilde{e}_{\tilde{N}};\xi)\mathrm{d}t\right)^{1/2}$$

$$\overset{(A.7)}{\leq} \Delta_N^{u,[0,T]} \Delta_{\tilde{N}}^{\psi,[0,T]} =: \Delta_{N,\tilde{N}}^{s,[0,T]},$$

where the second inequality uses Cauchy-Schwarz.

A.7   Karhunen-Loève expansion

By means of a Karhunen-Loève (KL) expansion (Ghanem and Spanos, 1991, section 2.3) a second order random process can be represented by an infinite linear combination of orthogonal basis functions. It is strongly related to the POD of section 4.2. In this section a short overview of the KL expansion is given. If a stochastic process is of second order, meaning the second moment is finite, the process can be represented by

$$\kappa(x, Y(\theta)) = \alpha_0(x) + \sum_{l=1}^{\infty} \sqrt{\lambda_l} c_l(x) Y_l(\theta). \tag{A.8}$$

The random process depends on the space variable $x \in \Omega$ and the random outcome $\theta \in \Theta$, which was introduced in section 2.2. The expectation $\alpha_0 \colon \Omega \to \mathbb{R}$ of the random field can depend on the space and the random variables are determined by

$$Y_l(\theta) = \frac{1}{\sqrt{\lambda_l}} \int_\Omega (\kappa(x,\theta) - \alpha_0(x)) \, c_l(x)\mathrm{d}x.$$

They are centered and mutually uncorrelated with unit variance, i.e.

$$\mathbb{E}[Y_l] = 0, \quad \mathbb{E}[Y_l Y_m] = \delta_{lm}. \tag{A.9}$$

For the case that the random field κ is a Gaussian field, and since the random variables are uncorrelated, the random variables are independent. The eigenvalues $\{\lambda_l\}_{l=1}^{\infty}$ are stored in decreasing order $\lambda_1 \geq \lambda_2 \geq \ldots$ and the eigenfunctions $\{c_i\}_{i=1}^{\infty}$ are orthonormal, i.e.

$$\int_{\Omega} c_l(x)c_m(x)\mathrm{d}x = \delta_{lm}.$$

The eigenvalues and eigenfunctions are obtained from a eigenvalue problem which is given by the following integral equation

$$\int_{\Omega} C(x,y)c_l(y)\mathrm{d}y = \lambda_l c_l(x) \tag{A.10}$$

where $C(x,y)$ is the covariance kernel. In case of an exponential covariance kernel $C(x,y) = \exp(-|x-y|/a)$, with correlation length $a > 0$, the eigenvalues and eigenfunctions in (A.10) can be determined analytically, see (Xiu, 2010, example 4.1).

In order to make (A.8) computable the series is truncated (Papadopoulos and Giovanis, 2018, page 31) at $N_{\mathrm{KL}} < \infty$ such that the random field is approximated by

$$\kappa(x, Y(\theta)) \approx \bar{\kappa}(x, Y(\theta)) = \alpha_0(x) + \sum_{l=1}^{N_{\mathrm{KL}}} \sqrt{\lambda_l}c_l(x)Y_l(\theta). \tag{A.11}$$

Similar to (4.10), the error of the truncated expansion can be determined by the decreasing sequence of eigenvalues above the truncation

$$\sum_{l=N_{\mathrm{KL}}+1}^{\infty} \lambda_l.$$

This can be used in order to determine the truncation index. For a given tolerance ϵ_{KL}, the index N_{KL} can be evaluated by

$$\epsilon_{\mathrm{KL}} \leq \frac{\sum_{l=N_{\mathrm{KL}}+1}^{\infty} \lambda_l}{\sum_{l=1}^{\infty} \lambda_l} < 1, \tag{A.12}$$

see (Lord et al., 2014, equation (7.46)). The denominator is computed by a sum that is truncated at $\bar{N}_{\mathrm{KL}} \gg N_{\mathrm{KL}}$, where the decreasing subsequent eigenvalues can be neglected.

A.7.1 Boundedness of Karhunen-Loève expansion

For the numerical example in chapter 5 the truncated Karhunen Loève expansion

$$\bar{\kappa}(x,\xi) = \alpha_0(x) + \sum_{l=1}^{N_{\mathrm{KL}}} \sqrt{\lambda_l}c_l(x)\xi_l$$

is utilized. In order to show that the random field $\bar{\kappa}$ is positive and bounded, it is assumed that $\alpha_0 \in L^{\infty}(\Omega)$ and $\alpha_0(x) > 0$ for all spatial points, the eigenvalues $c_l \in L^{\infty}(\Omega)$ and the random variables $\xi_l \sim \mathcal{U}\left(-\sqrt{3}, \sqrt{3}\right)$ are independent identically distributed random variables for $l = 1, \ldots, N_{\mathrm{KL}}$. In order to satisfy (2.8)

and hence guarantee existence and uniqueness of a weak solution of Problem 5.1, the Karhunen Loève expansion has to satisfy

$$\kappa_{\min} \leq \bar{\kappa}(x,\xi) \leq \kappa_{\max}, \quad \forall x \in \Omega, \, \forall \xi \in \Gamma, \tag{A.13}$$

with $\kappa_{\min} > 0$ and $\kappa_{\max} < \infty$. Finding a lower bound of the KL field it needs to be guaranteed that $\bar{\kappa}(x,\xi) > 0$ and hence

$$\bar{\kappa}(x,\xi) \geq \alpha_0(x) - \sqrt{3} \sum_{l=1}^{N_{\mathrm{KL}}} \sqrt{\lambda_l} \, \|c_l\|_{L^\infty(\Omega)} \tag{A.14}$$

$$\geq \underline{\alpha}_0 - \sqrt{3}\underline{\kappa} > 0$$

with $\underline{\alpha}_0 := \min_{x \in \Omega} \alpha_0(x) > 0$ and $\underline{\kappa} := \sum_{l=1}^{N_{\mathrm{KL}}} \sqrt{\lambda_l} \, \|c_l\|_{L^\infty(\Omega)}$. This inequality is equivalent to

$$\frac{1}{\sqrt{3}} > \frac{1}{\underline{\alpha}_0}\underline{\kappa}.$$

In order to find a lower bound for κ, it holds

$$\frac{1-\epsilon}{\sqrt{3}} \geq \frac{1}{\underline{\alpha}_0}\underline{\kappa} \tag{A.15}$$

for an $\epsilon \in (0,1)$. Bringing (A.14) and (A.15) together, it gives

$$\bar{\kappa}(x,\xi) \geq \epsilon\underline{\alpha}_0$$

and hence the lower bound in (A.13) is defined as $\kappa_{\min} := \epsilon\underline{\alpha}_0$.

The upper bound in (A.13) simply follows by

$$\bar{\kappa}(x,\xi) \leq \|\alpha_0\|_{L^\infty(\Omega)} + \sqrt{3} \sum_{l=1}^{N_{\mathrm{KL}}} \sqrt{\lambda_l} \, \|c_l\|_{L^\infty(\Omega)}.$$

Thus, the upper bound in (A.13) is defined as $\kappa_{\max} := \|\alpha_0\|_{L^\infty(\Omega)} + \sqrt{3}\underline{\kappa}$, with $\underline{\kappa} = \sum_{l=1}^{N_{\mathrm{KL}}} \sqrt{\lambda_l} \, \|c_l\|_{L^\infty(\Omega)}$.

Bibliography

M. Ainsworth and J. T. Oden. *A posteriori error estimation in finite element analysis*. John Wiley & Sons, 2000. doi:10.1002/9781118032824.

B. O. Almroth, P. Stern, and F. A. Brogan. Automatic choice of global shape functions in structural analysis. *AIAA J.*, 16(5):525–528, 1978. doi:10.2514/3.7539.

M. Barrault, Y. Maday, N. C. Nguyen, and A. T. Patera. An 'empirical interpolation' method: application to efficient reduced-basis discretization of partial differential equations. *Comptes Rendus Mathematique*, 339(9):667–672, 2004. doi:10.1016/j.crma.2004.08.006.

R. Becker and R. Rannacher. An optimal control approach to a posteriori error estimation in finite element methods. *Acta Numer.*, 10:1–102, 2001. doi:10.1017/S0962492901000010.

P. Binev, A. Cohen, W. Dahmen, R. DeVore, G. Petrova, and P. Wojtaszczyk. Convergence rates for greedy algorithms in reduced basis methods. *SIAM J. Math. Anal.*, 43(3):1457–1472, 2011. doi:10.1137/100795772.

S. C. Brenner and L. R. Scott. *The mathematical theory of finite element methods*. Springer-Verlag New York, 2008. doi:10.1007/978-0-387-75934-0.

P. Chen, A. Quarteroni, and G. Rozza. A weighted reduced basis method for elliptic partial differential equations with random input data. *SIAM J. on Numer. Anal.*, 51(6):3163–3185, 2013. doi:10.1137/130905253.

P. Chen, A. Quarteroni, and G. Rozza. Reduced basis methods for uncertainty quantification. *SIAM/ASA J. Uncertain. Quantif.*, 5(1):813–869, 2017. doi:10.1137/151004550.

K. A. Cliffe, M. B. Giles, R. Scheil, and A. L. Teckentrup. Multilevel monte carlo methods and applications to elliptic pdes with random coefficients. *Comput. Vis. Sci.*, 14(1):3, 2011. doi:10.1007/s00791-011-0160-x.

A. Ern and J.-L. Guermond. *Theory and practice of finite elements*. Springer-Verlag New York, 2004. doi:10.1007/978-1-4757-4355-5.

G. Fishman. *Monte Carlo concepts algorithms and applications*. Springer-Verlag New York, 1996. doi:10.1007/978-1-4757-2553-7.

R. G. Ghanem and P. D. Spanos. *Stochastic finite elements a spectral approach*. Springer-Verlag New York, 1991. doi:10.1007/978-1-4612-3094-6.

M. A. Grepl. *Reduced-basis approximation and a posteriori error estimation for parabolic partial differential equations*. PhD thesis, Massachusetts Institute of Technology, 2005. http://hdl.handle.net/1721.1/32387.

M. A. Grepl and A. T. Patera. A posteriori error bounds for reduced-basis approximations of parametrized parabolic partial differential equations. *ESAIM: M2AN*, 39(1):157–181, 2005. doi:10.1051/m2an:2005006.

M. Gubisch and S. Volkwein. Proper orthogonal decomposition for linear-quadratic optimal control. In P. Benner, M. Ohlberger, A. Cohen, and K. Willcox, editors, *Model reduction and approximation theory and algorithms*, chapter 1, pages 3–63. SIAM, 2017. doi:10.1137/1.9781611974829.ch1.

M. Gunzburger, C. G. Webster, and G. Zhang. Stochastic finite element methods for partial differential equations with random input data. *Acta Numer.*, 23:521–650, 2014. doi:10.1017/S0962492914000075.

B. Haasdonk. Convergence rates of the POD–greedy method. *ESAIM: M2AN*, 47(3):859–873, 2013. doi:10.1051/m2an/2012045.

B. Haasdonk. Reduced basis methods for parametrized PDEs—a tutorial introduction for stationary and instationary problems. In P. Benner, M. Ohlberger, A. Cohen, and K. Willcox, editors, *Model reduction and approximation theory and algorithms*, chapter 2, pages 65–136. SIAM, 2017. doi:10.1137/1.9781611974829.ch2.

B. Haasdonk and M. Ohlberger. Reduced basis method for finite volume approximations of parametrized linear evolution equations. *ESAIM: M2AN*, 42(2):277–302, 2008. doi:10.1051/m2an:2008001.

B. Haasdonk, K. Urban, and B. Wieland. Reduced basis methods for parametrized partial differential equations with stochastic influences using the Karhunen–Loève expansion. *SIAM/ASA J. Uncertain. Quantif.*, 1(1):79–105, 2013. doi:10.1137/120876745.

J. S. Hesthaven, G. Rozza, and B. Stamm. *Certified reduced basis methods for parametrized partial differential equations*. Springer International Publishing, 2016. doi:10.1007/978-3-319-22470-1.

D. B. P. Huynh, G. Rozza, S. Sen, and A. T. Patera. A successive constraint linear optimization method for lower bounds of parametric coercivity and inf–sup stability constants. *Comptes Rendus Mathematique*, 345(8):473–478, 2007. doi:10.1016/j.crma.2007.09.019.

K. Kunisch and S. Volkwein. Galerkin proper orthogonal decomposition methods for a general equation in fluid dynamics. *SIAM J. Numer. Anal.*, 40(2):492–515, 2002. doi:10.1137/S0036142900382612.

O. P. LeMaître and O. M. Knio. *Spectral methods for uncertainty quantification with applications to computational fluid dynamics*. Springer Netherlands, 2010. doi:10.1007/978-90-481-3520-2.

M. Loève. *Probability Theory II*. Springer-Verlag New York, 1978.

G. J. Lord, C. E. Powell, and T. Shardlow. *An introduction to computational stochastic PDEs.* Cambridge University Press, 2014. doi:10.1017/CBO9781139017329.

D. Meidner and B. Vexler. Adaptive space-time finite element methods for parabolic optimization problems. In G. Leugering, S. Engell, A. Griewank, M. Hinze, R. Rannacher, V. Schulz, M. Ulbrich, and S. Ulbrich, editors, *Constrained optimization and optimal control for partial differential equations*, pages 319–348. Springer Basel, 2012. doi:10.1007/978-3-0348-0133-1_18.

N. C. Nguyen, G. Rozza, and A. T. Patera. Reduced basis approximation and a posteriori error estimation for the time-dependent viscous burgers' equation. *Calcolo*, 46(3):157–185, 2009. doi:10.1007/s10092-009-0005-x.

N. C. Nguyen, G. Rozza, D. B. P. Huynh, and A. T. Patera. Reduced basis approximation and a posteriori error estimation for parametrized parabolic pdes; application to real-time bayesian parameter estimation. In L. Biegler, G. Biros, O. Ghattas, M. Heinkenschloss, D. Keyes, B. Mallick, Y. Marzouk, L. Tenorio, and K. W. B. van Bloemen Waanders, editors, *Large scale inverse problems and quantification of uncertainty*, chapter 8, pages 151–178. John Wiley & Sons, 2010. doi:10.1002/9780470685853.ch8.

H. Niederreiter. Quasi-Monte Carlo methods and pseudo-random numbers. *Bull. Amer. Math. Soc. (N.S.)*, 84(6):957–1041, 1978. doi:10.1090/S0002-9904-1978-14532-7.

A. K. Noor and J. M. Peters. Reduced basis technique for nonlinear analysis of structures. *AIAA J.*, 18(4):455–462, 1980. https://arc.aiaa.org/doi/abs/10.2514/3.50778.

J. T. Oden and S. Prud'homme. Goal-oriented error estimation and adaptivity for the finite element method. *Comput. Math. Appl.*, 41(5):735–756, 2001. doi:10.1016/S0898-1221(00)00317-5.

V. Papadopoulos and D. G. Giovanis. *Stochastic finite element methods an introduction.* Springer International Publishing, 2018. doi:10.1007/978-3-319-64528-5.

N. A. Pierce and M. B. Giles. Adjoint recovery of superconvergent functionals from PDE approximations. *SIAM Rev.*, 42(2):247–264, 2000. doi:10.1137/S0036144598349423.

A. Pinkus. *n-widths in approximation theory.* Springer-Verlag Berlin Heidelberg, 1985. doi:10.1007/978-3-642-69894-1.

C. Prud'homme, D. V. Rovas, K. Veroy, L. Machiels, Y. Maday, A. T. Patera, and G. Turinici. Reliable real-time solution of parametrized partial differential equations: reduced-basis output bound methods. *J. Fluids Eng.*, 124(1):70–80, 2001. doi:10.1115/1.1448332.

A. Quarteroni, R. Sacco, and F. Saleri. *Numerical mathematics.* Springer-Verlag Berlin Heidelberg, 2007. doi:10.1007/b98885.

A. Quarteroni, A. Manzoni, and F. Negri. *Reduced basis methods for partial differential equations: an introduction.* Springer International Publishing, 2016. doi:10.1007/978-3-319-15431-2.

D. V. Rovas, L. Machiels, and Y. Maday. Reduced-basis output bound methods for parabolic problems. *IMA J. Numer. Anal.*, 26(3):423–445, 2006. doi:10.1093/imanum/dri044.

C. Spannring, S. Ullmann, and J. Lang. A weighted reduced basis method for parabolic pdes with random data. arXiv, 2017. https://arxiv.org/abs/1712.07393.

D. Torlo, F. Ballarin, and G. Rozza. Stabilized weighted reduced basis methods for parametrized advection dominated problems with random inputs. arXiv, 2017. https://arxiv.org/abs/1711.11275.

K. Urban and A. T. Patera. An improved error bound for reduced basis approximation of linear parabolic problems. *Math. Comp.*, 83(288):1599–1615, 2014. doi:10.1090/S0025-5718-2013-02782-2.

L. Venturi, F. Ballarin, and G. Rozza. A weighted pod method for elliptic PDEs with random inputs. arXiv, 2018. https://arxiv.org/abs/1802.08724.

K. Veroy, C. Prud'homme, D. Rovas, and A. T. Patera. A posteriori error bounds for reduced-basis approximation of parametrized noncoercive and nonlinear elliptic partial differential equations. *AIAA Computational Fluid Dynamics Conference*, 2003. doi:10.2514/6.2003-3847.

S. Volkwein. Proper orthogonal decomposition: theory and reduced–order modelling. Lecture notes, University of Konstanz, 2013. http://www.math.uni-konstanz.de/numerik/personen/volkwein/teaching/POD-Book.pdf.

D. Xiu. *Numerical methods for stochastic computations a spectral method approach.* Princeton University Press, 2010.

M. Yano. A space-time petrov–galerkin certified reduced basis method: application to the boussinesq equations. *SIAM J. Sci. Comput.*, 36(1):A232–A266, 2014. doi:10.1137/120903300.

Curriculum Vitae

Christopher Spannring
Born: April 30, 1989 in Hartberg, Austria

10/2009–11/2012	Studium Technische Mathematik (B. Sc.), Johannes Kepler Universität Linz
11/2012–11/2014	Industriemathematik (Dipl.-Ing.), Johannes Kepler Universität Linz
02/2015–06/2018	Stipendiat, Graduate School of Excellence Computational Engineering, Technische Universität Darmstadt
06/2018	Promotion, Fachbereich Mathematik, Technische Universität Darmstadt